Study on Ultrasound Technologies Concerning with Nitrogen for Decomposition of Organic Compound and For Soil Washing Application

（窒素が関与する超音波技術による有機物分解と土壌洗浄応用の研究）

Kwedi Nsah Louis-Marly

（クエディ ンサ ルイ マーリー）

Department of Energy and Environmental Science

Nagaoka University of Technology, Nagaoka, Japan

August 2020

Acknowledgements

The work presented in this thesis is the achievement of many years of research conducted in Nagaoka University of Technology, in collaboration with Fukuda cooperation Ltd. Niigata, Japan.
First of all, I would take this opportunity to express my sincere gratitude to The Honjo International Scholarship Foundation, for sponsoring the entire program.

Further, I would like to thank my supervisor Pr. Takaomi Kobayashi, for suggesting the theme and for his insightful guidance throughout this research. His confidence and training gave me the autonomy to attain this level, creating in me a spirit of self-responsibility and leadership.

I am also thankful to Pr. Hisao Uchiki, Professor Emeritus of Nagaoka University of Technology, for his mentorship.

Significant contributions made by Kobayashi laboratory members are gratefully acknowledged, special thanks goes to Ms. Tominaga for her administrative support.

To conclude, I cannot forget to thank my family; Mr & Mrs. Nsah, my siblings; Pharm. E.B. Eko, Dr. F.E. Eko, Dr. E. Niba, Ms. L. Eyambe, Dr. E.M. Nsah, Ms. S. Abong, Mr. D.A. Eko and Ms. N.L. Nsah, not forgetting my brother-in-law Mr. R. Niba. Thank you for all the unconditional support.

Kwedi Nsah Louis-Marly
August 2020

CHAPTER: 1.

GENERAL INTRODUCTION

Recent emphasis on the risks of rapid climate change and global warming is an alert to the ecosystem, as well as the huge impact it has on human life. While, the reality of irrecoverable ecological damage is being emphasized on solutions of sustainable technologies in energy, recycling and pollution reservation are being introduced by the United Nations Organization.

In 2015, the United Nations Member States drafted "The 2030 Agenda for Sustainable Development" with 17 Sustainable Development Goals (SDGs). Most of them, as seen in Figure 1.1, the SDGs on 2, 3, 6, 9, 12 and 15 strongly focus on environmental conservation technologies. But, the category most in line with the present research is number 15, with regards to a prevailing global economic environment, building resilient infrastructure, promoting inclusive and sustainable industrialization, and fostering innovation.

Figure 1.1: Sustainability goals of ultrasound technologies in each SDGs categories.

Ultrasound is an excellent technology for sustainable industrialization and fostering innovation technology. Ultrasound is inaudible sound waves with frequencies in the range of 20 kHz to 500 MHz, which is greater than the upper limit of human hearing. It can be transmitted through any elastic medium such as water, gas-saturated water, and slurry. Ultrasound has been used for diverse purposes in a variety of areas. It is well known for its medical application, in diagnostic sonography (ultrasonography), internal body structure observation including tendons, muscles, joints, vessels and internal organs.

Ultrasound technology offers great potential in industrial applications, such as welding, cutting, punching, thermos-fixing, washing, embossing, sealing and so on. In cleaning technology, ultrasonic cleaners offer perfect cleaning of a wide range of materials in a short time. In daily life, they are used to clean jewelry, lenses, dental and surgical instruments, watches, car fuel injectors, musical instruments, and so on. It has a daily usage in industrial metallurgy and the semiconductor industry. A brief summary of some of the uses of ultrasound is given below.

Above all, ultrasound is employed in processing technology, because of its capacity to mix and improve chemical reactions. Other applications in line with the SDGs include analysis methods and food processing, by eliminating microorganisms and enzymes without destroying nutrients in food, it can be used as an alternative method to thermal treatments in food preservation, contributing to **Goal 2 of No Hunger.** In terms of food security, a variety of treatment methods have been proposed for the removal of organic compounds from contaminated soil in agricultural zones, among them, soil washing has been considered an effective method taking into account its low cost, particularly when dealing with highly contaminated soil, this relates to **Goal 3 for Good health.** The necessity of soil treatment is not limited to food security, but also to protect human health and aquatic life by limiting

contaminants from leaching into groundwater, and consequently rivers and ocean. Therefore, ultrasound technology helps in conserving clean water relating to **GOAL 6**. In addition to **Goal 9**, these soils can be recycled after treatment to fabricate geopolymer, resulting in innovation from waste soils. The material technology produces innovation for the novelty in several industrial fields and for example, provides a cheap source of construction materials for concrete and others. With these numerous applications (Figure 1.2), ultrasound technology is considered an innovative and smart technology contributing to achieve the SDGs, ensuring a sustainable future for developed and developing countries.

Ultrasound technology is now applied in many fields. In recent years, with the great technological advances that have occurred, there has been significant growth in the number and diversity of ultrasound applications. Figure 1.2 summarises the variety of applications today. Although the well-known sector is that of medicine, sonochemical and Industrial applications are fast growing in number and usefulness in many areas.

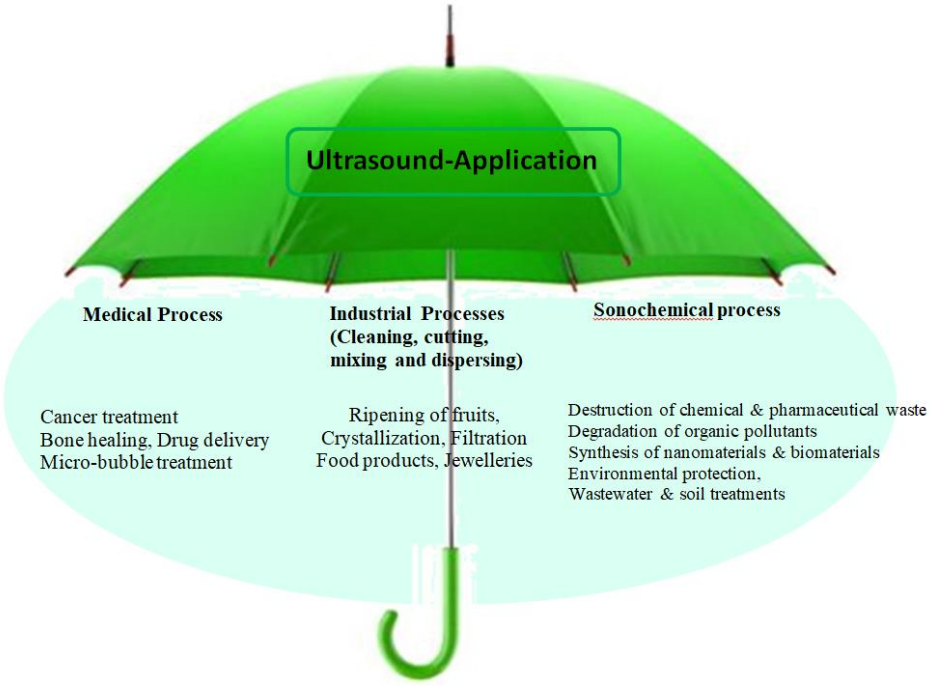

Figure 1.2 Ultrasound application in industrial processes and special ones for medical and sonochemical processes.

1.1. Environmental waste generation

Rapid industrialization in recent decades has caused serious environmental problems, be it through the release of solid waste (contaminated soil) as well as liquid waste (wastewater) to the surrounding. Industrial wastewater which is a by-product of industries is released by most companies on a daily basis. This industrial waste which contains organic, inorganic matter and heavy metals in varying concentrations is usually emptied into the ocean, rivers or sometimes accidentally leaks into the soil and ground water [1-3]. Previously occupied land for mining exploitation (Figure 1.3-1.4) for example, can be a threat and would remain polluted for 50-100 years after the end of mining activities.

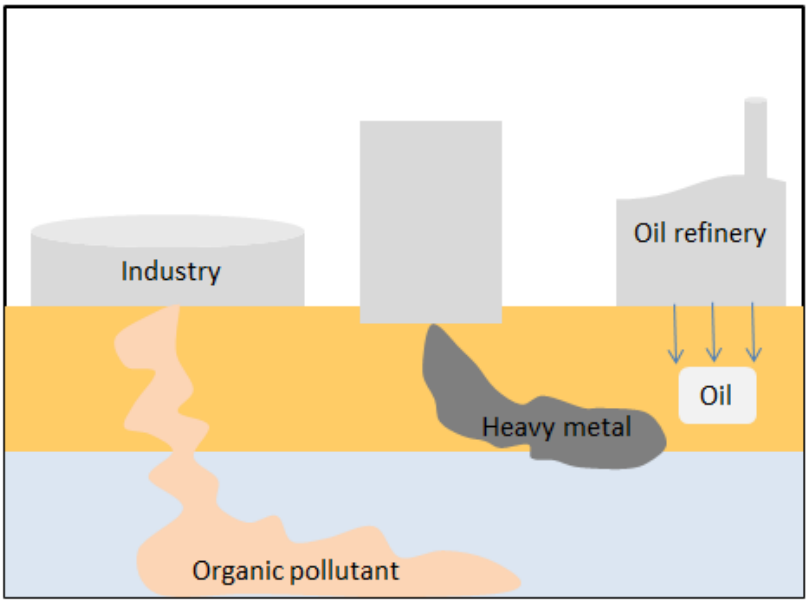

Figure 1.3: Environmental waste generation

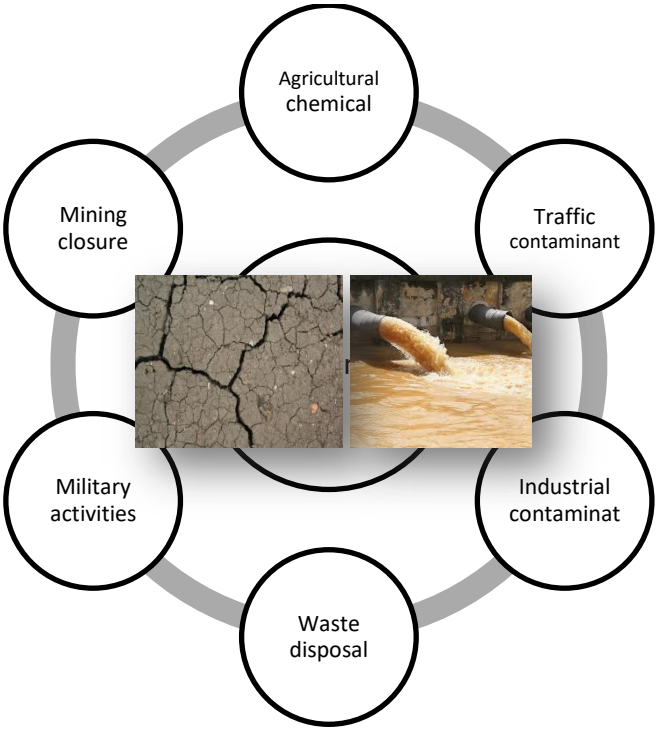

Figure 1.4: Causes of environmental pollution

Industrial Wastewater usually contains synthetic organic colorants used for research purposes, in textile, hair dyeing, paper-making, food industries, etc. [4]. These colorants called Azo dyes, usually become a threat to public health when they get in contact with soil [5]. Soil by nature is known to be man's source of life, regulating plant productivity, and maintaining biogeochemical cycles with the activity of microorganisms, which are capable of degrading organic including xenobiotics [6-7]. Since most pollutants are generally non-biodegradable [8], they would consequently accumulate in edible parts of plants, and get into the human body by way of the food chain as bio-magnification, resulting to cancer, intellectual and possibly developmental disabilities in man [9-14]. The three common routes of human soil contamination are; eating, inhalation, and through the skin. Thus there is an urgent need to effectively treat contaminated water and soil [1]. The grid below shows the chemicals of major public health concern present in wastewater and/or contaminated soil identified by the WHO (Figure 1.5) [15].

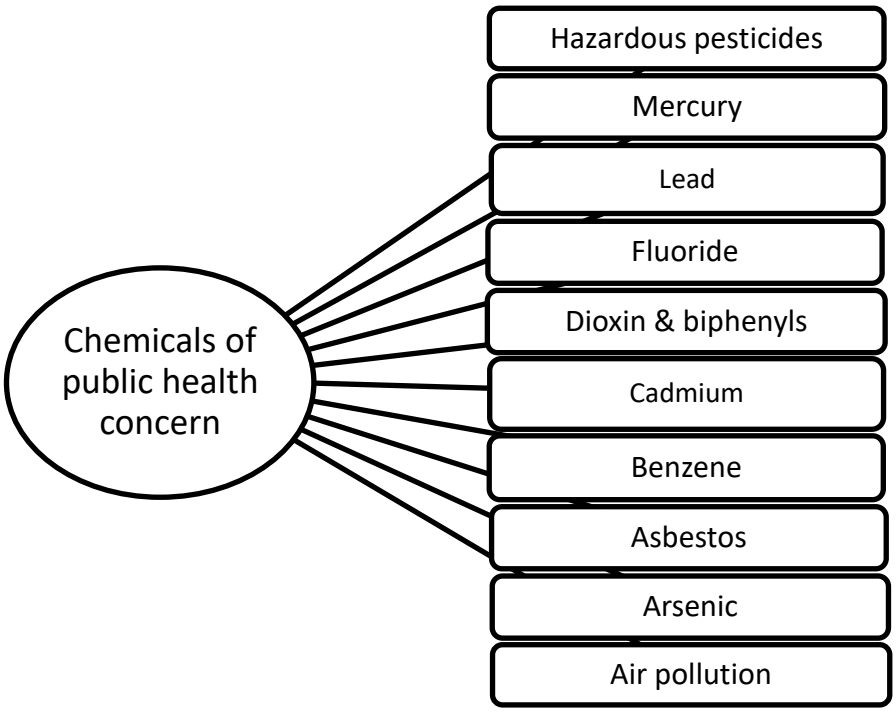

Figure 1.5: Ten chemicals of major public health concern, Source: WHO

1.2. Possible soil and wastewater solutions for sustainability

To comply with environmental protection laws, certain protocols must be followed during waste management. It is very difficult to straight-forwardly claim a certain way on how to efficiently deal with these wastes. In order to mitigate environmental problems, much research has been performed to help prevent the generation of waste, to reduce the volume of waste being disposed of, to turn hazardous waste into non-hazardous waste by an intermediate treatment process, and to recycle/reuse waste materials [16-19].

Waste treatments usually encounter application problems such as high cost, ineffective removal of some pollutants, operation problems, and generation of toxic secondary pollutants [20-21]. For example, fouling encountered during membrane filtration and the disinfection with chlorine products which result in serious problems [22-23]. Many investigations have

been performed to eliminate these limitations by the application of innovative techniques such as semiconductor catalysts, forward osmoses, advances oxidation process, and magnetic purification [24-25]. One of the innovative technologies used for the improvement of the wastewater treatment process is the application of ultrasound (US) waves. Generally, ultrasonic application as a remediation technique for the degradation of toxic organic pollutants relies on two main effects, which are the removal of chemical and biological contaminants from soil and water [26-27]. Although ultrasonic has been found to have a potential application for the remediation of contaminated soil from various contaminants ranging from heavy metals to organic compounds [28], however, research on ultrasonic applications on soil remediation is still limited.

It is not just sufficient to treat this waste but its reuse for "sustainable development" is of major concern. In this study, the utilization of ultrasound for waste treatment and recycling is evaluated as a cheaper and 'green' route solution.

1.3. Ultrasound applications for environmental remediation

1.3.1. Ultrasound application with sonoprocess

Sonoprocess is the application of US to an industrial process for food quality (food technology, material extraction), Nanotechnology (nano-particle synthesis), Polymeric material (Drug delivery, gelation). Applications employing higher powers generally rely on compound vibration-induced phenomena occurring in the object. It can be summarized that the US frequency range is divided into two parts (Figure 1.6). Power US which capable of influencing chemistry and processing mainly in the frequency range between 20 kHz and 100

kHz. On the other hand, diagnostic US does not have enough power to produce cavitation, since their frequency is very high (above 5 MHz).

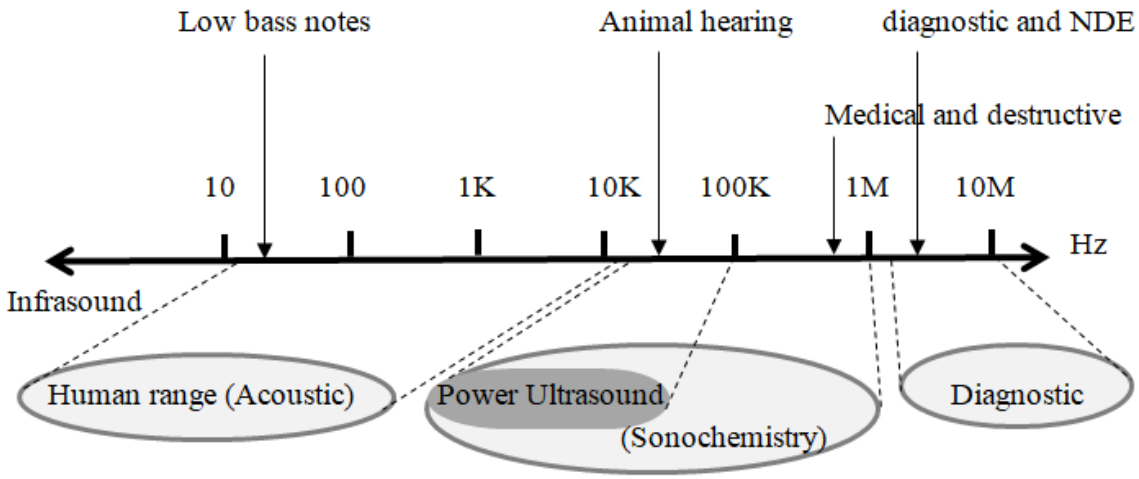

Figure 1.6: Ultrasound applications at various frequencies

Like any sound wave, ultrasound is propagated via a series of compression and rarefaction waves induced in the molecules of the medium through which it passes. Compression cycles push molecules together, while expansion (rarefaction) cycles pull them apart. The US can be transmitted through any elastic medium such as water and slurry. For liquids and gases, particle oscillation takes place in the direction of the wave and produces longitudinal waves (Figure 1.7 (a)) [30-31]. However, in solids, since they possess shear elasticity, supporting tangential stresses gives rise to transverse waves, in which particle movement takes place perpendicular to the direction of the wave (Figure 1.7 (b)) [31].

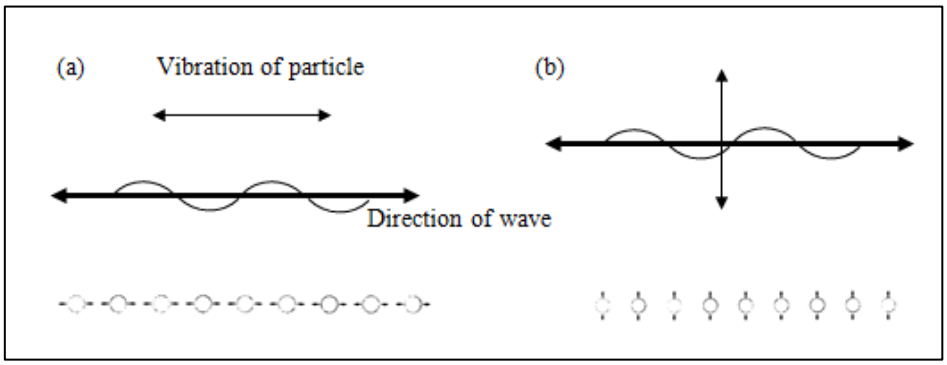

Figure 1.7: Wave and particle movement (a) longitudinal waves and b) transverse waves

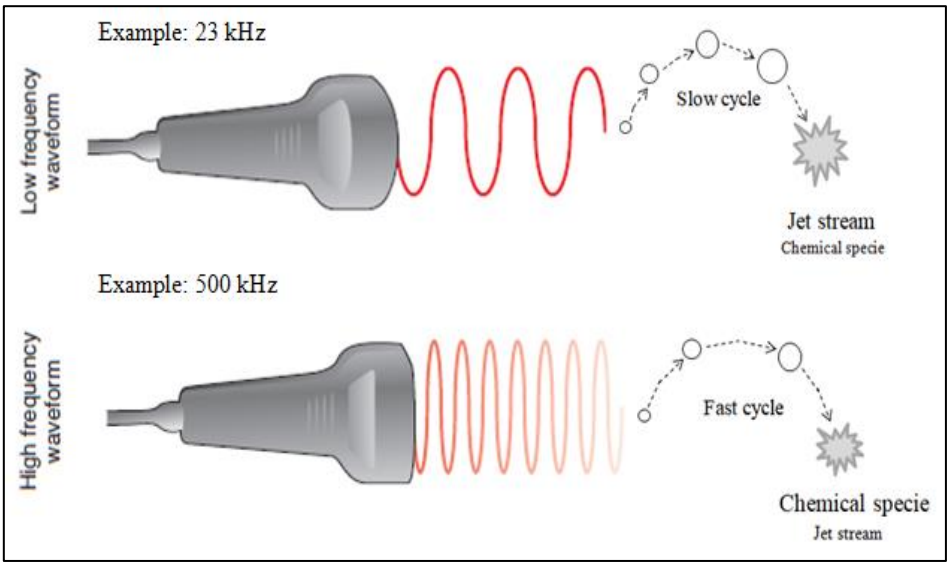

Figure 1.8: Ultrasound frequency and cavitation bubble effect

Depending on the frequency and power, US can be divided into two;

(a) High frequency (5-10 MHz) and low power (<1 W/cm^2) HFLP

(b) Low frequency (20-100 kHz) and high power (>5 W/cm^2) LFHP

As earlier mentioned, HFLP ultrasound is mostly used in diagnostic applications such as thickness measurement, detecting the size and location of extraneous matter, particle size, and for chemical synthesis, since it can lead to HO radical formation in water or slurry phase.

On the other hand, LFHP ultrasound is used for physical effects in applications such as cleaning, drying and degassing, soil washing [32-35]. In addition, ultrasonic humidifier, ultrasound identification, and sonography [36]. By combining the right frequencies, the right amplitude and using the right transducer, different types of US application can be realized.

During ultra-sonication, bubbles are formed which collapses causing the associated release of energy known as cavitation. This cavitation causes physical, chemical, or biological effects during the process. The physical (mechanical) effects of ultrasound are useful in some environmental applications like air purification [37], sludge dewatering [38], and metal leaching [39] (Figure 1.9). The chemical effects (sonochemistry) are useful for applications in environmental remediation, especially in organic decontamination.

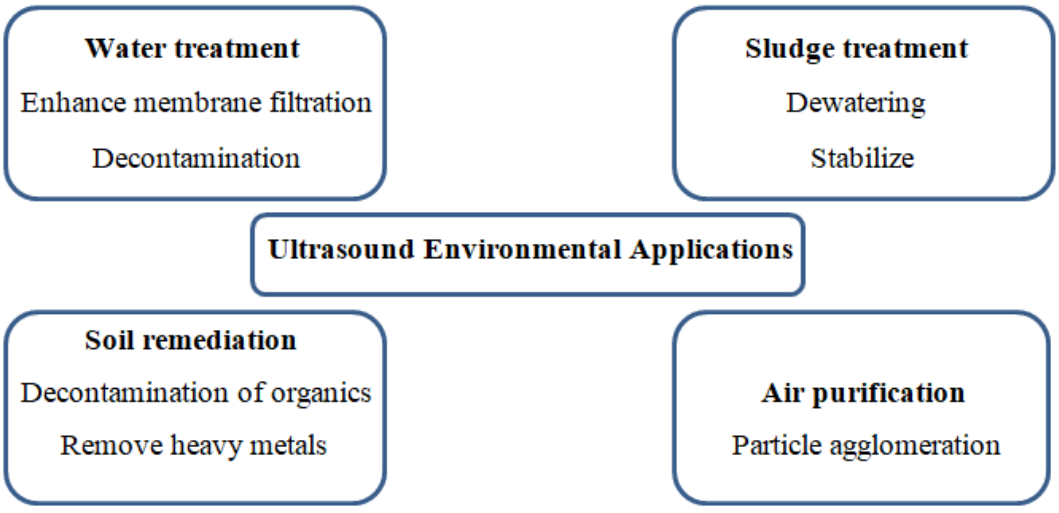

Figure 1.9: Ultrasound environmental applications

At sufficiently high power, the US reactor leads to the acoustic cavitation phenomenon with the formation, growth, and collapse of bubbles (cavitation) (Figure 1.10). This is accompanied by the generation of intense local heating (5000 K) and pressures (>1000 atm) with very short lifetimes, and reactive radical species (^{o}OH, ^{o}OOH) via thermal dissociation

of water and oxygen. Implying the existence of extremely high heating and cooling rates (>109 K/s) [40-44].

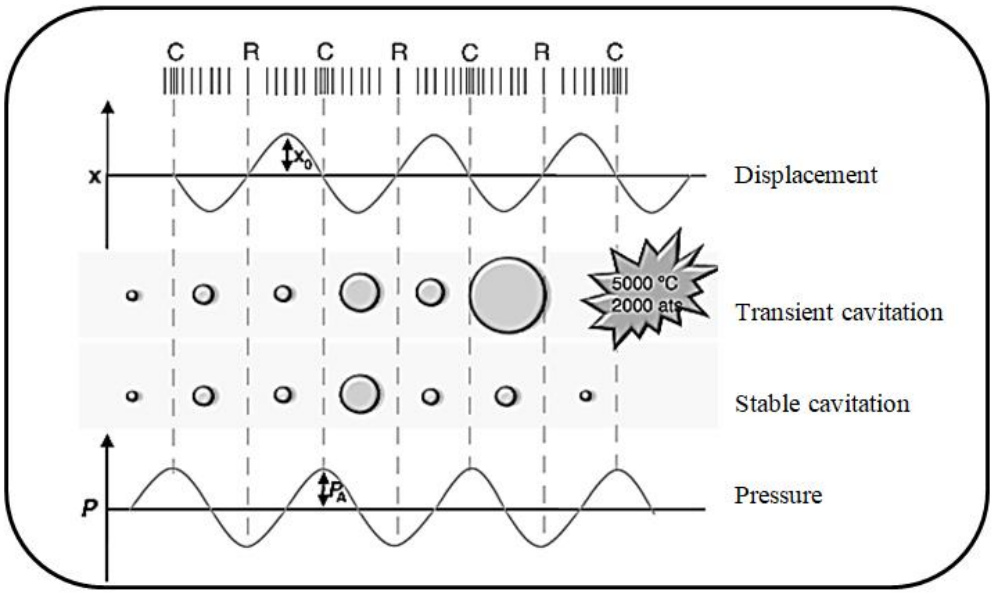

Figure 2.10: Growth and collapse of stable and transient cavitation

Due to the cavitation effect, ultra-sonication remains unique, since no other method of sample treatment can produce such effects [45-46].

Whether these bubbles collapse completely (transient cavitation) with ultrasound intensity in excess of 10W/cm^2 or oscillates and exist for a considerable period of time (stable cavitation) when produced at low intensity (in water 1–3W/cm^2), will depend on many factors, *e.g.* temperature, acoustic amplitude, frequency, external pressure, bubble size, and the gas type and content.

1.3.2. Factors influencing cavitation

It is important to really understand these factors which influence cavitation because reproducibility of ultrasonic experiments is only possible if these parameters are carefully chosen, adjusted, and reported. These parameters may be subdivided into 3 groups [47];

Acoustic	Solvent	External
Frequency	Viscosity	Bubbled gas
Intensity (Power)	Dissolved matter	Temperature
Signal type	Surface tension	Pressure

Frequency

At high sonic frequencies, in the order of the MHz, the production of cavitation bubbles becomes more difficult than at low sonic frequencies, in the order of the kHz. To achieve cavitation, as the sonic frequency increases, the intensity of the applied sound must be increased, to ensure that the cohesive forces of the liquid media are over-come and voids are created. The physical explanation for this lies in the fact that, at very high frequencies, the cycle of compression and decompression caused by the ultrasonic waves becomes so short that the molecules of the liquid cannot be separated to form a void and thus, cavitation is no longer obtained [48]. Ultrasonic cavitation intensity is inversely proportional to the frequency related to the ultrasonic frequency.

Intensity

The word intensity is usually interchangeable with power between researchers, so it is necessary to emphasize that *power is energy per time* while intensity is the *power per area*.

Ultrasonic power is directly related to the bath volume and mostly to the cleaning application and is expressed in *watts per liter* while intensity is expressed in *watts per* m^2. The intensity of cavitation is directly related to the ultrasonic power and frequency choice. High amplitude is not always necessary to obtain the desired results as it can lead to rapid deterioration of the ultrasonic transducer, resulting in liquid agitation instead of cavitation and poor transmission of the US through the media. However, the amplitude should be increased when working with samples of high viscosity. [49-50].

Signal type

Pulsed, sweeping, or bi-modal signals are the different types of ultrasonic signals which can influence cavitation compared to continuous-wave output [51]. Continuous-wave ultrasound is inefficient due to limited spatial distribution and bubble growth beyond the region of active cavitation. Pulsed wave ultrasound consists of a power-on time, P_{ON} and a power-off time, P_{OFF} which tends to increase sonochemistry and reduce bubble growth [52]. The shorter the P_{ON} the shorter the lifetime of the active bubbles once the signal is switched off. That is, if P_{ON} is short enough a bubble may dissolve completely during P_{OFF} before the next P_{ON} pulse, or subsequent P_{ON} pulses may not cause remaining bubbles to become active [53]. Conversely, a longer P_{ON} time can result in the bubbles becoming too large to dissolve to an active size during P_{OFF}. Frequency sweeping has seen both positive and negative effects on sonochemical activity. During the sweep from 250 to 290 kHz there was a reduction in the active bubble population, and frequency sweeping resulted in less violent collapse [54-55].

Another method of frequency utilization is a dual frequency (or bi-modal) signal. This results in a change in the active bubble population and a potential increase in bubble collapse temperature [56]. The sonochemical activity taking place under these conditions can result in

a sonochemical yield greater than the individual sum of the single frequencies that are used. The proposed reason for this is a reduction in the standing wave and thus more distributed cavitation activity coupled with an increase in transferred energy efficiency [57].

Viscosity

As a general rule, most applications are performed in water. However, other less polar liquids, such as some organics, can also be used depending on the intended purpose. Hence, the solvent used to perform sample treatment with ultrasonication must be carefully chosen. The higher the natural cohesive forces acting within a liquid (e.g., high viscosity and high surface tension) the more difficult it is to attain cavitation [58].

Bubbled gas

The presence of gases will determine the physical and chemical reactions that occur during sonication. For noble gases at 20 and 513 kHz (10 W/cm^2 and 1.5 W/cm^2 respectively) the zero-order rate of production of H_2O_2 increases in the order of He < Ar < Kr [59]. If a gas is used to increase the cavitation effect, it must be bubbled continuously into the solvent to maintain the effect. It is important to degas the sample at the start of the experiment before the preferred gas can be bubbled, as ultrasonic energy can convert any gas present to generate cavitation.

Temperature

Solvent temperature is an important parameter of sonochemistry to maximize the intensity of the cavitation, therefore during an experiment, the solvent must be properly chosen. This is because when the temperature of the solvent rises so too does its vapor pressure and so more

solvent vapor fills the cavitation bubbles, which then tend to collapse less violently, that is, the sonication effects are less intense than expected[60]. The table shows different solvents and their cavitation effect (Table 1.1).

Solvent	Boiling point (^{o}C)	Cavitation temperature range (^{o}C)	Temperature for max. cavitation (^{o}C)
Water	100	20-50	35
Ethanol	78	15-27	21
Benzene	80	10-32	19
Ethyleneglycol	197	75-120	93

Table 1.1: Solvent temperature based of cavitation [60]

1.3.3. Ultrasound system and device

Ultrasonication can be applied to the sample through ultrasonic probes, immersed in the sample. These probes perform directly in the solution without any barrier, but this approach has several drawbacks. For instance, metals detaching from the probe can contaminate the sample but modern ultrasonic probes made from glass greatly reduce this problem [61-62]. Another disadvantage arises from the fact that most ultrasonic probes are used in open, that is, the sample container is not sealed during sample treatment. Consequently, some volatile analytes can be lost.

Contrary to the probe, in an ultrasonic bath, the ultrasonic wave needs to cross first the liquid inside the ultrasonic device and then the wall of the sample container. But the ultrasonic cleaning bath is by far the cheapest and very simple. It consists of a stainless-steel tank with one or several transducers (depending on bath size) firmly attached underneath or by the side

of the tank. The smallest baths suitable for sonochemistry are of about 1.5 L capacity and a single transducer is sufficient to drive this with a power rating of around 50 W. A bath of 1 m x 0.6 m x 0.5 m, holding (1 x 0.6 x 0.5 x 1000) 300 liters of water can be driven by up to 1200W power (Figure 1.11). The liquid in the bath will normally be water sometimes with a small quantity of surfactant.

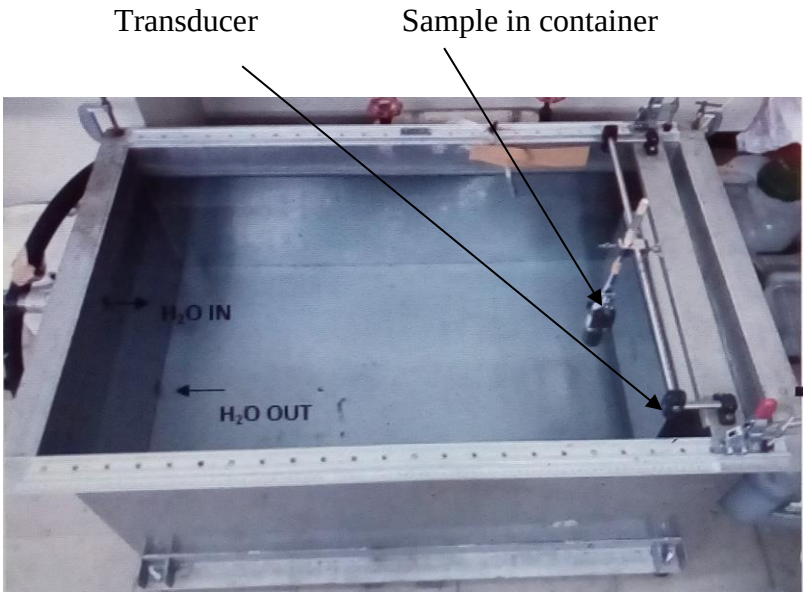

Figure 1.11: Ultrasonic stainless-steel baths
(1200W High power ultrasonic bath in Kobayashi lab-NUT Japan)

Regardless of the type of commercial instrument used, the energy will be generated via an ultrasonic transducer to convert mechanical or electrical energy to sound energy. There are three main types of ultrasonic transducer used in sonochemistry; Liquid-driven, magnetostrictive and piezoelectric transducers [63-64].

1.4. Sonochemistry

Sonochemistry is the term used to describe the effect of ultrasonic sound waves on chemical reactions. For chemical applications, US require only the presence of a liquid that can generate cavitation in order to transmit its power. When water is sonicated, the extreme conditions generated on the collapse of the cavitation bubbles are sufficient to cause rupture of the O-H bond itself [65]. This results in the formation of radical species and the production of oxygen gas and hydrogen peroxide (Scheme 1) [66]. The cavitation implosion leads to the production of solvent radicals, which in the case of water are $H^{\bullet}$ and $OH^{\bullet}$ radical species that can react with each other to give hydrogen and hydrogen peroxide.

$H_2O \rightarrow H^{\bullet} + OH^{\bullet}$
$OH^{\bullet} + OH^{\bullet} \rightarrow H_2O_2$
$OH^{\bullet} + OH^{\bullet} \rightarrow H_2O + O$
$OH^{\bullet} + OH^{\bullet} \rightarrow H_2 + O_2$
$H^{\bullet} + O_2 \rightarrow HO_2^{\bullet}$
$HO_2^{\bullet} + H^{\bullet} \rightarrow H_2O_2$
$HO_2^{\bullet} + HO_2^{\bullet} \rightarrow H_2O_2 + O_2$
$OH^{\bullet} + H_2O \rightarrow H_2O_2 + H^{\bullet}$
$H^{\bullet} + H^{\bullet} \rightarrow H_2$
$H^{\bullet} + OH^{\bullet} \rightarrow H_2O$

Scheme 1.1 – Ultrasonically induced decomposition of water

During sonochemical reactions, a chemical dosimeter monitors the production of a chemical species. Common chemical dosimetry systems are the Fe^{2+}/Fe^{3+} dosimeter (Fricke dosimeter), the terephthalate dosimeter, the iodine dosimeter.

1.4.1. Sonochemical optimization

During sonochemical reactions, the shape of the reaction vessel is critical for the application of ultrasonication with a bath. This is because, just like any other wave, when the ultrasonic wave impinges against any solid surface some energy is reflected. If the base of the container is flat, such as in a conical flask, the ultrasound reflected is minimized. Conversely, when the base of the container is spherical the ultrasonic wave hits the container at an angle, and a huge proportion of the ultrasonic wave is reflected away [19, 67]. The thickness of the wall of the sample container should be kept to a minimum to avoid intense attenuation. This problem must be also borne in mind when the objective is to favor the solid–liquid extraction of analytes from solids deposited on a column: inside the column, the effectiveness of the ultrasonic wave diminishes as it passes through the solid to the inner part of the column. Consequently, large-thin columns are preferred to short-wide ones for in-column ultrasonic bath applications.

The ultrasonic intensity distribution inside an ultrasonic bath is not homogeneous, so the evaluation of sound intensity in the liquid is important. However, apart from calorimetry method, simple, rapid methods have been developed to locate the position that has the highest intensity of sonication, this includes the Aluminum foil test, Luminol test [68], hydrophone method [69]. To concentrate US intensity on the membrane module, a semi-cylindrical reflection plate is placed behind the sample.

1.5. Objective and content of the present study for a doctoral thesis

The objective of this study is to demonstrate the possibility of utilizing ultrasound technology for waste treatment and consequent recycling. During waste treatment or waste

recycling, the addition of other material is usually considered in most instances. From the standpoint of waste utilization, however, the addition of stabilizers or other chemicals influences efficiency and reliable treatment. Therefore, chemical stabilization by using additives is considered essential. However, for human safety, the environmental reuse of such material may have an adverse effect on humans, animals, and the environment in general.

US devices have different effects based on their frequency, as they can generate chemical species in aqueous medium. In this study, waste materials were treated in an ultrasonic aqueous medium under different ultrasonic systems.

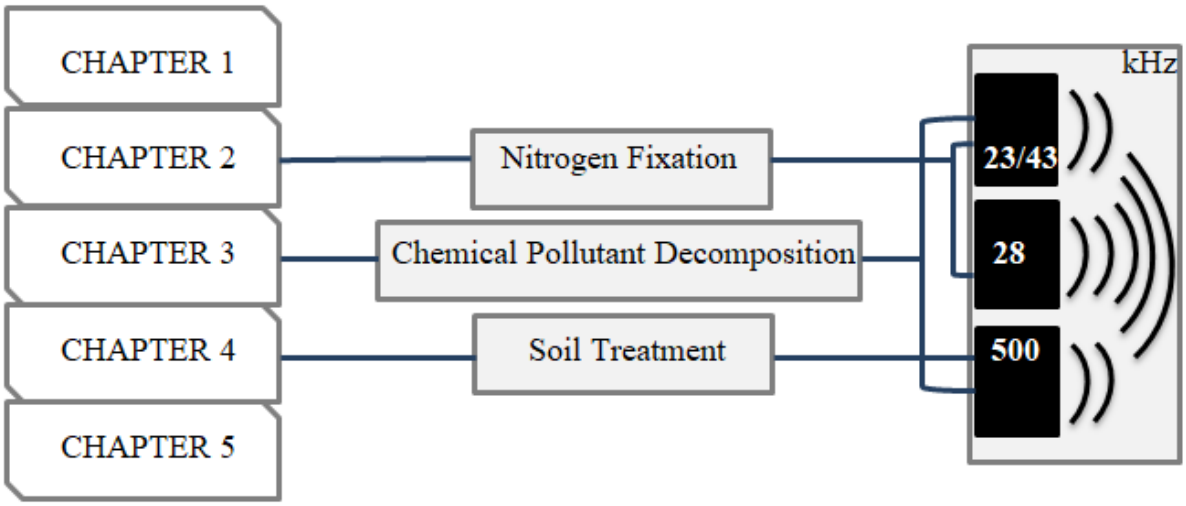

Figure 1.12

Details on this is elaborated in the thesis; divided into 5 chapters. **Chapter 2** which is the next chapter describes the influence of various factors like frequency, power, and time ultrasonic on the generation of chemical species. **Chapter 3** discusses the detection of Nitrous species under different US systems with diaminobenzidine as a probe in the aqueous medium. This technology is an environmentally friendly technology that can be applied for the treatment of laboratory and industrial wastewater containing azo dyes. In **Chapter 4**, soil

washing is introduced and a proposed application for geopolymer synthesis is explained in detail as a means to fight soil disposal or storage due to limited land field. Finally, the entire research work is concluded in **Chapter 5.**

References

1. M. Hutton, C. Symon, The quantities of cadmium, lead, mercury and arsenic entering the U.K. environment from human activities *Sci. Total Environ*, 57(1986)129.
2. M. Nadal, A. Bocio, M. Schuhmacher, J. Domingo, *Arch. Environ. Contam. Toxicol.*, 49(2005)290.
3. K. D. Ladwani., V. S Manik., D. S Ramteke., Impact of industrial effluent discharge on physico-chemical characteristics of agricultural soil, *I. Res. J. Environment Sci* 3 (2012) 32-36
4. U. Meyer, Biodegradation of synthetic organic colorants, *FEMS Symposium*, 12(1981)371.
5. A. Pielesz, I. Baranowska, A. Rybak, A. Wochowicz, *Ecotoxicology and Environmental Safety*, 53 (2002) 42–47.
6. P. Nannipieri, J. Ascher, M.T. Ceccherini, L. Landi, G. Pietramellara, G. Renella, *European Journal of Soil Science* 54 (2003) 655–670.
7. B. Jalili, F. Nourbakhsh, M. Ghiasi, plant soil environ, 56 (9) (2010) 429–433.
8. P.B. Tchounwou, C. G. Yedjou, D. J. Sutton, Heavy metals toxicity and the environment, *EXS*, 101 (2012)133-164.
9. H. I. Abdel-shafy, M. S. M. Mansour, Solid waste issue: Sources, composition, disposal, recycling and valorization, *Egyp. J. Petr* 27 (2018) 1275-1290.
10. I. Savic-Gajic, I. Savic, D. Gajic, The role and health risk of heavy metals in human organism. *Heavy metals and health* (2016) 47–89.
11. B. Sarkar, in *Heavy Metals in the Environment*, CRC Press, New York (2002).

12. C. H Yan, 1994. Arsenic distribution in soils, In Advances in Environmental Science and Technology, Arsenic in the Environment (Nriagu J O, ed.). Part I. Cycling and Characterization. John Wiley and Sons, Inc., New York.
13. M. J Abedin, J. Feldmann, A. A Meharg, 2002. Uptake kinetics of arsenic in rice plants. Plant Physiology, 128(3): 1120–1128.
14. M. R Karagas, T. D Tosteson, J. Blum, J. S Morris, J. A Baron, Klaue B, 1998. Design of an epidemiologic study of drinking water arsenic exposure and skin and bladder cancer risk in a U.S. population. Environmental Health Perspectives, 106(Suppl 4): 1047–1050.
15. WHO (2013) *Ten chemicals of major health concern*. [online]. Retrieved from: www.who.int/ipcs/assessment/public_health/chemicals_phc/en/index.html.
16. S. C. Dogruparmak, M.K. Yenice, E. Durmusoglu, B. Ozbay, H. O. Oz, Pol. J. Environ. Stud., 20 (2) (2011) 479-484.
17. S. Balachandran, S. E Kentish, R. Mawson, M. Ashokkumar, Ultrasonic enhancement of the supercritical extraction from ginger. Ultrason. Sonochem. 2006, 13, 471-479.
18. J. J. Cronin Jr, J. S. Smith, M. R. Gleim, E. Ramirez, & J. D. Martinez, 'Green marketing strategies: an examination of stakeholders and the opportunities they present.' J. Acad. Marketing Sci. [Online]. 39 (2011): 158-174.
19. T. Christensen, Solid Waste Technology and Management (1) [e-book]. (2010) Available from:http://site.ebrary.com.libproxy.aalto.fi/lib/aalto/reader.action?docID=10510413 [Accessed on 1 December 2016].
20. U. I Gaya, A. H Abdullah. Heterogeneous photocatalytic degradation of organic contaminants over titanium dioxide: a review of fundamentals, progress and problems. Journal of Photochemistry and Photobiology C: Photochemistry Reviews, 9(2008)1-12.
21. R. Kumar, N. Yadav, L. Rawat, M. K Goyal, Effect of Two Waves of Ultrasonic on Waste Water Treatment. J Chem Eng Process Technol 5(2014)193. doi: 10.4172/2157-7048.1000193.

22. H. L Liu, Y. R Chiou. Optimal decolorization efficiency of Reactive Red 239 by UV/TiO2 photocatalytic process coupled with response surface methodology. Chemical Engineering Journal, 112(2005)173-179.
23. G. Lunn, E.B. Sansone, The safe disposal of diaminobenzidine. Appl. Occup. Environ. Hyg. 6 (1991) 49-53.
24. M. N Chong, B. Jin, C.W.K. Chow, et al. Recent developments in photocatalytic water treatmenttechnology: A review. Water Research, 44(2010)2997-3027.
25. R. D Ambashta, M. Sillanpaa. Water purification using magnetic assistance: A review. Journal of Hazardous Materials, 180(2010)38-49.
26. J. Wang, Z. Wang, C. L. Z Vieira, J. M. Wolfson, Guiyou Pingtian, Huang Shaodan: Review on the treatment of organic pollutants in water by ultrasonic technology. Ultrason Sonochem, 55(2019)273–278.
27. Y. Yon, J. Cha, M. Lim, M. Ashokkumar, Khim: J. Comparison of ultrasonic and conventional mechanical soil-washing processes for diesel-contaminated sand. Ind Eng Chem Res 2011, 50:2400–2407.
28. R.A. Shrestha, A. Mudhoo, T. D. Pham, Sillanpää M: Ultrasound and sonochemistry in the treatment of contaminated soils by persistent organic pollutants. In Handbook on applications of ultrasound: sonochemistry for sustainability. Edited by Chen D, Sharma SK, Mudhoo A, FL: CRC Press Taylor & Francis Group; 2012:407–418.
29. P. A. Deymier, J. O. Vasseur, A. Khelif, Second-order sound field during megasonic cleaning of patterned silicon wafers: Application to ridges and trenches. Journal of Applied Physics 90 (2004) 4211-4218.
30. Y. Chu. Orbital motion of water particles in oscillatory waves. J. Waterway, Eng. 109 (1983).
31. M.C. Ziskin., Fundamental Physics of Ultrasound and Its propagation in tissues, Philadelphia, 13 (1993) 705-709.

32. Gregorich, E. G., Kachanoski, R. G and voroney, R. P 1988. ultrasonic dispersion of aggregates: distribution of organic matter in size fractions. Can. J. Soil Sci. 68: 395-403.
33. Raine, S. R. and So, H. B. 1994. Ultrasonic dispersion of soil water: the effect of suspension properties on energy dissipation and soil dispersion. Aust. J. Soil Res. 32: 1157-1174.
34. Roscoe, R., Buurman, P. and Velthorst, E. J., Disruption of soil aggregates by varied amount of ultrasound energy in fractionation of organic matter of a clay latosol: carbon, nitrogen and delta 13C distribution in particle size fractions. Eur. J. Soil Sci. 51(2000) 445-454.
35. Bray, R, H., The significance of particle-size within the clay fraction. J. American Cer Soc., 20 (1937) 257- 261.
36. G. Chatel, L. Novikova, P. Sabine: How efficiently combine sonochemistry and clay science? Appl Clay Sci 119(2006)193–201.
37. Mason. T. J 2007, Sonochemistry and the environment-proving a green link between chemistry, physics and engineering. Ultrason. Sonochem, 14(2007) 476-483.
38. Mao. T, Hong. S. Y, Show. K. Y, Tay. J. H, A comparison of ultrasound treatment on primary and secondary sludges. Water. sci techn. 50 (2004) 91-97.
39. Kyllonen. H, Pirkonen. P, Hintikka. V. Ultrasonically aided mineral processing technique for remediation of soil contaminated by heavy metals. Ultrason. Sonochem 11 (2004) 211-216.
40. Jiang Y, Petrier CH, Waite TD. Effect of pH on the ultrasonic degradation of ionic aromatic compounds in aqueos solution. *Ultrason Sonochem*, 9 (2002) 163-68.
41. Laughrey Z, Bear E, Jones R, Tarr MA., Aqueous sonolytic decomposition of polycyclic aromatic hydrocarbons in the presence of additional dissolved species. *Ultrason Sonochem*, 8 (2001) 353-57.
42. Visscher AD, Langenhove HV., Sonochemistry of organic compounds in homogeneous aqueous oxidizing system. *Ultrason Sonochem*, 5(1998)87-92.
43. Suslick, K.S., Cline, R.E. and Hammerton, D.A. (1986) Journal of the American Chemical Society, 108, 5641.

44. S. Abbas, K. Hayat, E. Karangwa, M. Bashari, X. Zhang., An Overview of Ultrasound-Assisted Food-Grade Nanoemulsions, Food Eng Rev DOI 10.1007/s12393-013-9066-3.
45. Wibetoe, G, Takuwa, D.T., Lund, W.D. and Sawula, G. X., Fresenius' Journal of Analytical Chemistry, 363(1999)46. 6.
46. Capelo-Martınez, J.L., Ximenez-Embun, P., Madrid, Y. and Camara, C. Trends in Analytical Chemistry, 23(2004)331.
47. Timothy j. M, Dietmar. P., practical sonochemistry (2002)8-11.
48. Pena-Farfal, C., Moreda-Pineiro, A., Bermejo-Barrera, A. et al. Anal.Chem, 549(2004)3541–3547.
49. Amoedo, L., Capelo, J.L., Lavilla, I. and Bendicho, C., J. Ref. j15 Anal. Atom Spec, 14 (1999)1221–1226.
50. Lima, E.C., Barbosa, F., Krug, F.J. et al. J. Ref. j15 Anal. Atom Spec, 15(2000) 995–1000.
51. A. Henglein, R. Ulrich, J. Lilie, Luminescence and chemical action by pulsed ultrasound, J. Am. Chem. Soc. 111 (1989) 1974–1979.
52. J. Lee, K. Yasui, T. Tuziuti, T. Kozuka, A. Towata, Y. Iida, Spatial distribution enhancement of sonoluminescence activity by altering sonication and solution conditions, J. Phys. Chem. B 112 (2008) 15333–15341.
53. C. Dekerckheer, K. Bartik, J.-P. Lecomte, J. Reisse, Pulsed sonochemistry, J. Phys. Chem. A 102 (1998) 9177–9182.
54. M.R. Bailey, Duel frequency high frequency ultrasound to control bubbles., 2nd International Symposium on Therapeutic Ultrasound, 2002.
55. L. Hallez, J. Lee, F. Touyeras, A. Nevers, M. Ashokkumar, J.-Y. Hihn, Enhancement and quenching of high-intensity focused ultrasound cavitation activity via short frequency sweep gaps, Ultrason. Sonochem. 29 (2016) 194–197.
56. J. Holzfuss, M. Rüggeberg, R. Mettin, Boosting sonoluminescence, Phys. Rev. Lett. 81 (1998) 1961.

57. P.A. Tatake, A.B. Pandit, Modelling and experimental investigation into cavity dynamics and cavitational yield: influence of dual frequency ultrasound sources, Chem. Eng. Sci. 57 (2002) 4987–4995.
58. Mason, T.J., Practical Sonochemistry: User's Guide to Applications in Chemistry and Chemical Engineering, Ellis Horwood Ltd, 1992, New York.
59. F.R. Young, Sonoluminescence from water containing dissolved gases, J. Acoust. Soc. Am. 60 (1976) 100–104.
60. Mason, T.J. Sonochemistry, Oxford Chemistry Primers, (2000)63 Oxford, UK.
61. Wibetoe, G., Takuwa, D.T., Lund, W. and Sawula, G. Fresenius. Journal of Analytical Chemistry, 363(1999) 46–54.
62. Santos, H.M. and Capelo, J.L. Talanta, 73(2007) 795–802.
63. Duck, F.A., Baker, A.C., Starritt, H. C., 1998 ultrasound medicine, CRC press, US.
64. Duck, F. A., Medical and non-medical protection standards for ultrasound and infrasound, project in biophysics and molecular biology 93(2007)176-191.
65. Makino, K., Mossoba, M.M. and Riesz, P. **(1983)** J. Phys. Chem., **87**, 1369.
66. Petrier, C., Jeunet, A., Luche, J.-L., & Reverdy, G. J. Am. Chem. Soc., 1992, 114, 3148.
67. L.M. Kwedi Nsah, T. Kobayashi., Sonochemical nitrogen fixation for the generation of NO_2^- and NO_3^- ions under high-powered ultrasound in aqueous medium, Ultrason. Sonochem, https://doi.org/10.1016/j.ultsonch.2020.105051.
68. K.K. Latt, T. Kobayashi / Ultrason Sonochem 13 (2006) 321–328 Ultrasound-membrane hybrid processes for enhancementof filtration properties.
69. J. Borenius, E. Lampio, K. Peronen, T. Jauhiainen., Akustiikan perusteet isinooritieto Oy. *Finland* 1981.

CHAPTER: 2.

SONOCHEMICAL NITROGEN FIXATION FOR THE GENERATION OF NO_2^- AND NO_3^- IONS UNDER HIGH-POWERED ULTRASOUND IN AQUEOUS MEDIUM

Abstract: Sonochemical species such as nitrite (NO_2^-) and nitrate (NO_3^-) were detected in an ultrapure aqueous medium with 28 kHz low-frequency ultrasound (US) in the range of 200 – 1200 W output power. The concentration of their anionic ions monitored with high-performance liquid chromatography, increased with increasing US power especially under air atmosphere. When the generation of NO_2^- and NO_3^- ions under US exposure was investigated for N_2, O_2 and Ar-bubbled solutions, no trace of NO_2^- was observed while NO_3^- was slightly generated. Under air atmosphere, the concentration of dissolved oxygen in the aqueous medium increased especially when 1200 W power was used. In addition, the bulk pH shifted towards the acidic side with an increase in exposure time, which indicated that NO_2^- was formed. The formation of oxidizing specie under 28 kHz low-frequency ultrasonic treatments was confirmed with an absorption spectrum that was dominated by two maxima peaks at 288 nm and 352 nm representing triiodide I_3^- anion.

2.1. Introduction

Ultrasound (US), is sound wave above 20 kHz used in a wide variety of processes such as cleaning, sterilization, soldering, homogenization and as a stimulus of chemical reaction [1-2]. Its application usually depends on the ultrasonic frequency used. By using US, complicated reactions can be performed with fewer steps as opposed to conventional methods

[3]. This is because the cycled frequency of the US generates cavitation bubbles in an aqueous medium which causes sonochemical processes. For example, water molecules thermally dissociate to active oxygen species, which produces different kinds of reactive species [4]. Such sonolysis is due to the cavitation, the adiabatic compression and rarefaction cycles which causes the collapse of bubbles creating a local hot spot source for reactive chemical species. It is known that, in US aqueous medium, the water molecules thermally decompose to form a hydrogen atom (H) and hydroxyl radical (OH) [5]. These active species can recombine to form hydrogen, hydrogen peroxide, and water [6]. In the presence of air composing of N_2 and O_2, the oxygen present in the air atmosphere being a good scavenger, leads to the formation of a higher concentration of H_2O_2 which oxidizes NO_2^- to NO_3^- [7-9]. As indicated in Ref. [10], this conversion seems to be favored at lower pH values and pH decreases with sonication time.

Using a 540 kHz US, Schultes and Gohr also noted a change in the acidity of water, with increasing nitrite formation [11]. In this case, in liquids under US exposure, free radicals were considered as an important triggering factor to initiate chemical reactions. In addition, ionic species were diagnosed for occurrence by using ion chromatography [12], fluorometry [13], and UV-vis spectroscopy [14]. Ion chromatography was usually preferred because of economic and efficient performance, since it can be used for simultaneous determination of NO_2^- and NO_3^- [15]. On the other hand, as activated chemical species, hydroxyl radicals generated in water was detected by UV-vis spectroscopy, using the KI method [16, 17].

Many advanced studies have reported the formation of chemical species, when multiple ranges of US frequencies were used from 41 kHz to 3217 kHz [18]. In their reports, neither nitrite nor nitrate was generated at lower US frequencies with a BLT transducer, implying that only higher frequencies influenced the sonochemical processes [19]. However, to the best of our knowledge, the formation of radicals under low ultrasonic irradiation is still

unclear. Therefore, nitrite and nitrate formation under low frequency is attractive for the subject of sonochemistry research. So far, in sonochemical reactions, factors such as solvent [20], US frequency [21], temperature [20], dissolved gas [22] and static pressure [23] were studied and found to influence the reaction for nitrite and nitrate. Although Mason et al. found out that ultrasonic power or intensity was another important factor of sonochemical effects [24], however, until now, this variable has not been given proper attention.

In the present report, the investigation of nitrite and nitrate was performed with a point of view for the formation of their species under 28 kHz US operated at different output power of 200,600, 900 and 1200 W. Evidence was described in US nitrogen fixing by the formation of nitrite and nitrate under high power US.

2.2. Materials and Method

The commercially available potassium Iodide reagent, product of Tokyo casei (Tokyo, Japan), Sodium chloride from nacalai tesque (Kyoto, Japan) and hydrochloric acid from Wako (Tokyo, Japan) were all used without further purification. Ultrapure water was used throughout the experiment for sample preparation.

The ultrasonic device used for 23, 43 kHz was HSR-305R and for 28 kHz, Dynashock WD-1200-28 (Honda electronic, Japan). The exposure tank was fabricated with 3 cm thick stainless steel sheets and measured 100 x 65 x 50 cm. At one end of the tank, was a fixed acoustic transducer 40 x 30 x 10 cm, and the other end was the water inlet and outlet, which kept the bath water at 25^{o} C to avoid thermal gradient that might disturb the acoustic exposure.

Ultrapure water was placed in a 200 ml reaction vessel and positioned at a 5 cm distance from the transducer in the US water bath. US with 28 kHz frequency was exposed to the ultrapure water opened to the atmosphere except in certain cases. In argon, oxygen and nitrogen gas systems, each gas was bubbled for 12 hours in the ultrapure water prior to US exposure. 28 kHz US was operated with different US output power (200, 600, 900 and 1200 W). For NO_2^- and NO_3^- determination, HPLC, pH and dissolved oxygen were measured every 30 min US exposure time, for a total duration of 120 min. The dissolved oxygen concentration was measured using an OD meter LT Lutron DO-5509; while HPLC analyses were performed using a Metrohm 861 advanced compact IC equipped with automatic injection having a 10 ml loop volume.

For oxidizing specie determination under US, 0.1 M concentration of KI solution was used for oxidation dosimetry experiment [25]. KI solution pH was adjusted to 2 and 10 by adding HCl and NaOH, respectively. The analyses were carried out by UV-Vis spectroscopy (V-570 JASCO, Japan).

2.3. Results and discussion

2.3.1. Detection of NOx species under 28 kHz US

After the exposure of 28 kHz US to ultrapure water with 200 to 1200 W powers, the water sample was saved for ionic species detection. The sample was analyzed before US exposure, and no peak was identified in the chromatogram of ultrapure water. Figure 2.1 shows the chromatogram observed at each US output power, with each value of ion conductivities of NO_2^- and NO_3^- plotted for different US power after 120 min exposure. The nitrite and nitrate peaks appeared at 5.7 min and 7.1 min, respectively. Although US were exposed for 120 min, under 200 W US irradiation, an extremely weak peak for NO_2^- was detected.

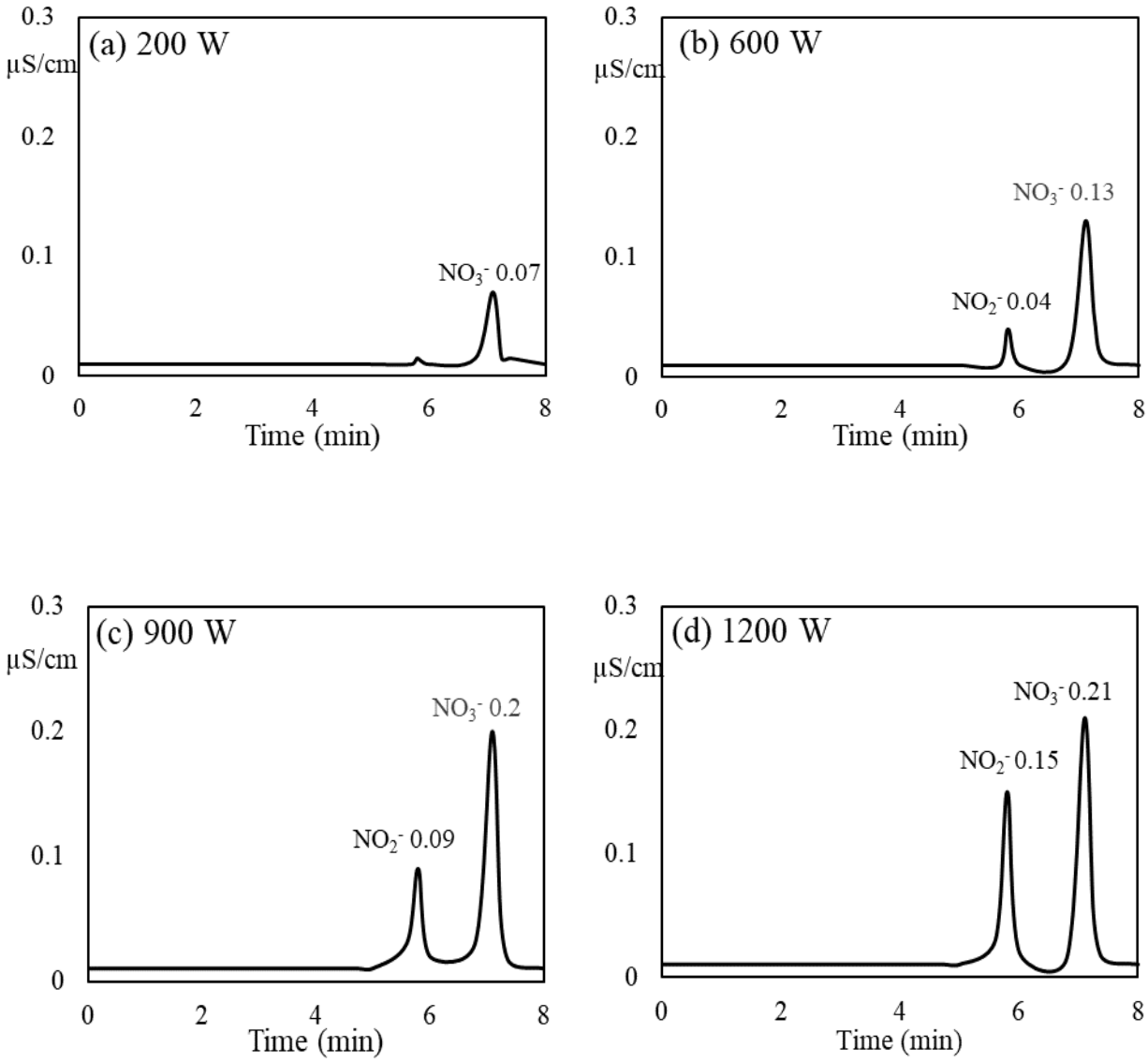

Figure 2.1: Chromatograms of ultrapure H_2O under 28 kHz (a) 200 W (b) 600 W (c) 900 W (d) 1200 W for 120 min.

However, increasing the US output power to 600, 900 and 1200 W, the peak became intense and the US generated clear peaking of both NO_2^- and NO_3^- ions under 900–1200 W. The peak intensity of NO_2^- when 1200 W was used was about fifteen times higher than that under 200 W. This means that higher US intensity is more efficient for NO_2^- and NO_3^- formation.

For the US exposure under 23, 28, and 24 kHz, the time change relating to NO_2^- and NO_3^- ions concentration is shown in Figure 2.2 below.

In figure 2.2(a), 23 and 43 kHz showed no change in concentration, meanwhile due to the effect of high power with 28 kHz (200,600, 900 and 1200 W), NO_2^- and NO_3^- ions were generated. This is related to slight faster generation of bubbles due to 1200W effect compared to 23 and 43 kHz with 75W power.

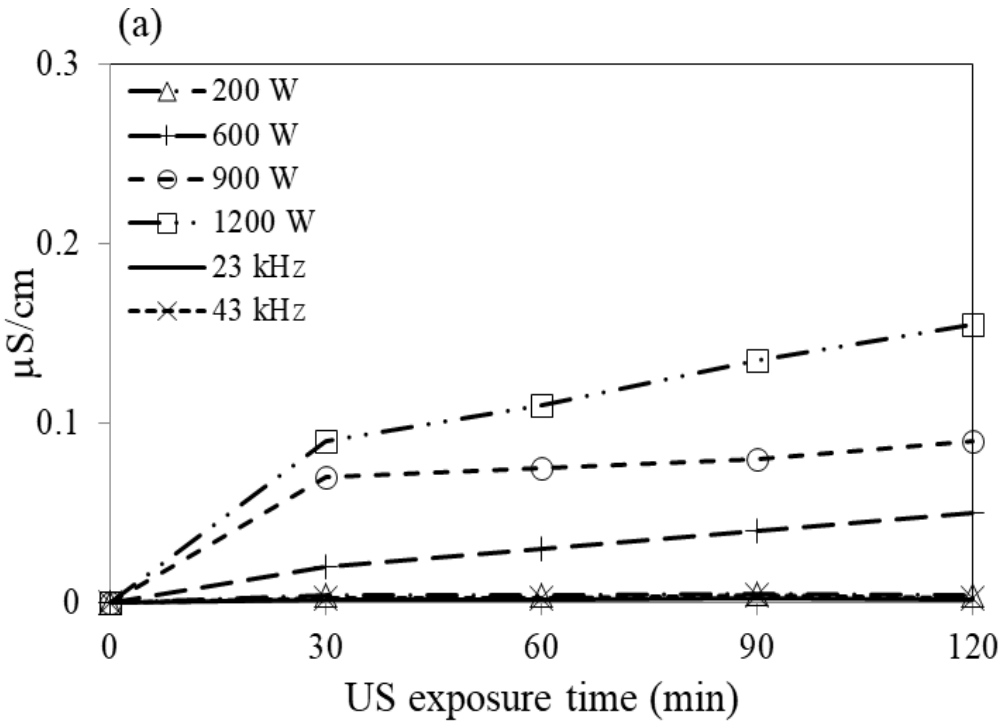

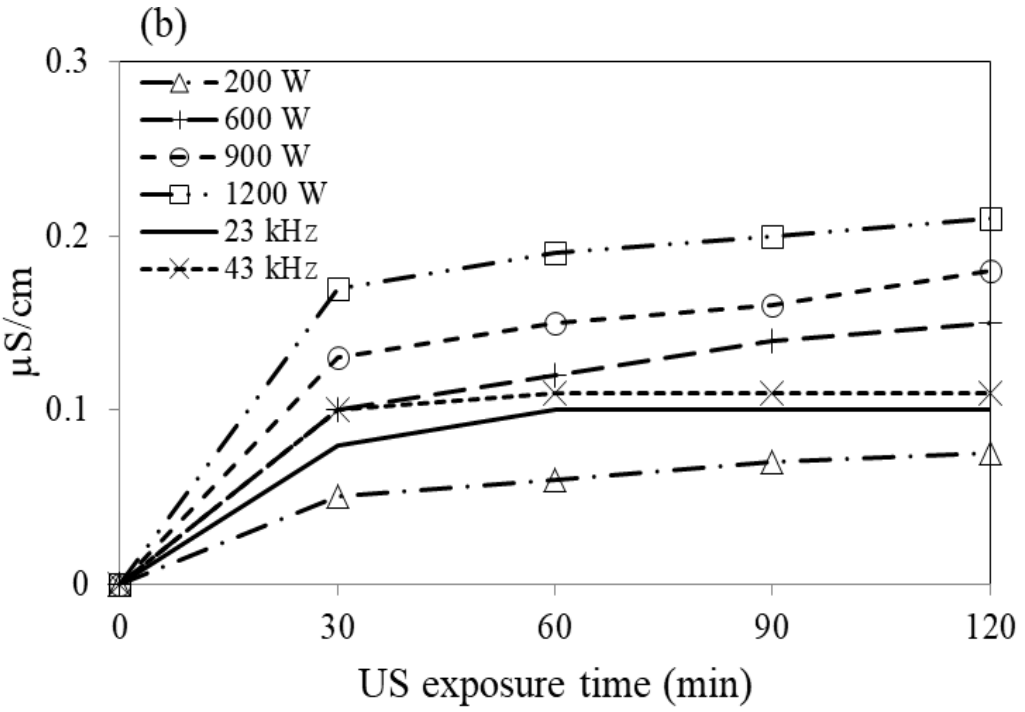

Figure 2.2: Chromatograms of ultrapure H_2O under 23, 43 and 28 kHz US exposure time relative to (a) NO_2^- and (b) NO_3^- ion.

For quantitative information on the formation of NO_2^- and NO_3^- under different US conditions, a standard curve of NO_2^- and NO_3^- was determined. In this case, different concentrations (0 – 100 µM) of $NaNO_2$ and $NaNO_3$ were prepared in ultrapure water and their chromatogram was measured. The linear regression equations of NO_2^- and NO_3^- standard curves were calculated as y = 0.1854x + 1.5808 (R^2 =0.9795) and y = 0.3672x +1.594 (R^2 =0.9937), respectively, showing a good linearity in the calibration. By using this calibration, the resultant conductivity of the chromatogram was converted to NO_2^- and NO_3^- concentrations. Based on the calibration, the formation of NO_2^- and NO_3^- ion under 1200 W after 120 min was deduced to be 72.3 µM and 52.8 µM, respectively as shown in figure 2.3.

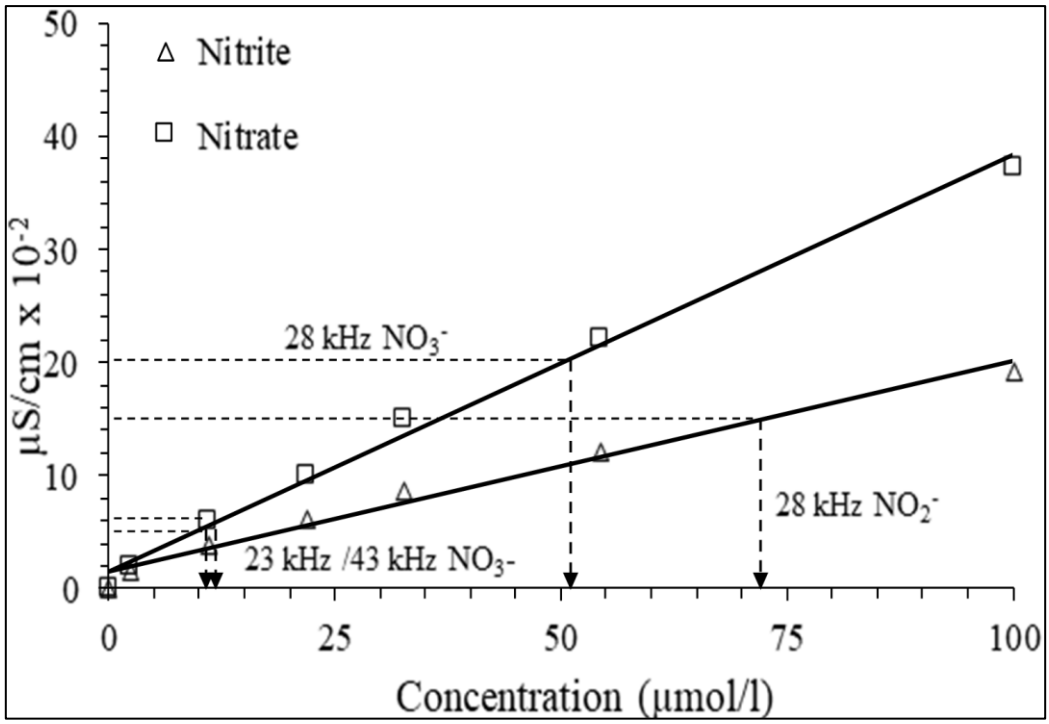

Figure 2.3: Standard curves for determining concentration of nitrite and nitrate.

Prior to US exposure, a gas (O_2, N_2 or Ar) was bubbled in the water medium for 12 hours, afterwards NO_2^- and NO_3^- ions generated were examined. Figure 2.4(a) shows NO_2^- and NO_3^- concentrations at different US exposure for each bubbling case. It was eminent that no specie was detected in the case of Ar bubbling. However, a negligible amount of NO_3^- was detected in the cases of N_2 and O_2 bubbling. As a result, it was concluded that 1200 W enabled generation of NO_2^- and NO_3^-. When the effect of US power was compared in figure 2.4(b), an increase in ion concentration was seen with increasing US power.

In our previous research [26], it was noticed that the nitration of 3, 3-diaminobenzidine ratio increased with ultrasonic power. The suggested reason was that, nitration under US was strengthened by oxygen depletion which caused the reduction of NO_3^- to NO_2^- [27]. During this study, for this to be confirmed, dissolved oxygen in the water medium was therefore investigated as shown in Figure 2.5(a). The dissolved oxygen concentration decreased with

an increase in US exposure time, and US power, which was consistent with the previous study. Under 200 W powers, no change in dissolved oxygen was observed even after the 120 min US exposure. Figure 2.5(b) revealed that the aqueous medium was oxygen free after 12 hours of N_2 or Ar bubbling, under similar conditions.

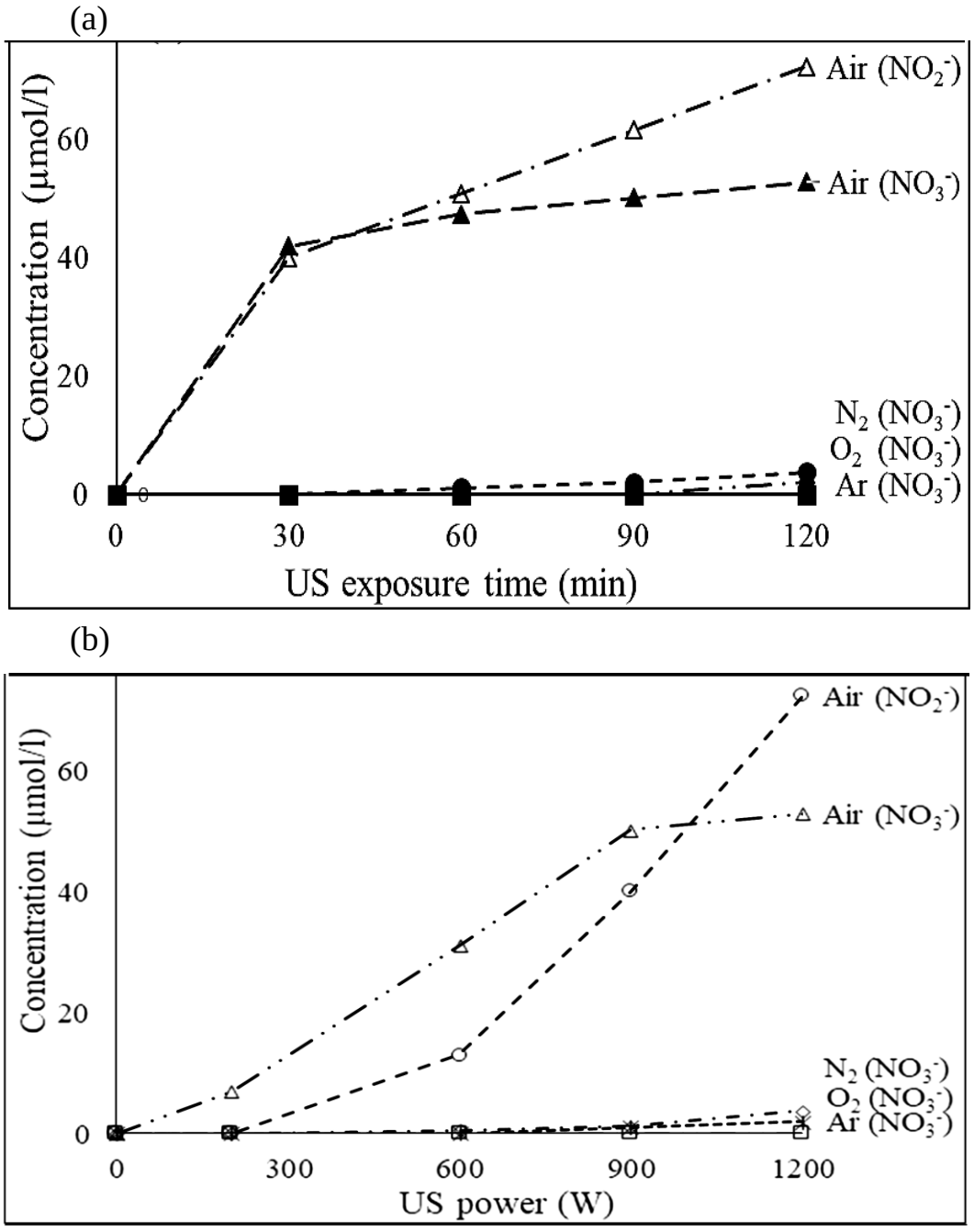

Figure 2.4: (a) Relationship of US exposure time with nitrite and nitrate concentration.

(b) Relationship of US exposure power with nitrite and nitrate concentration.

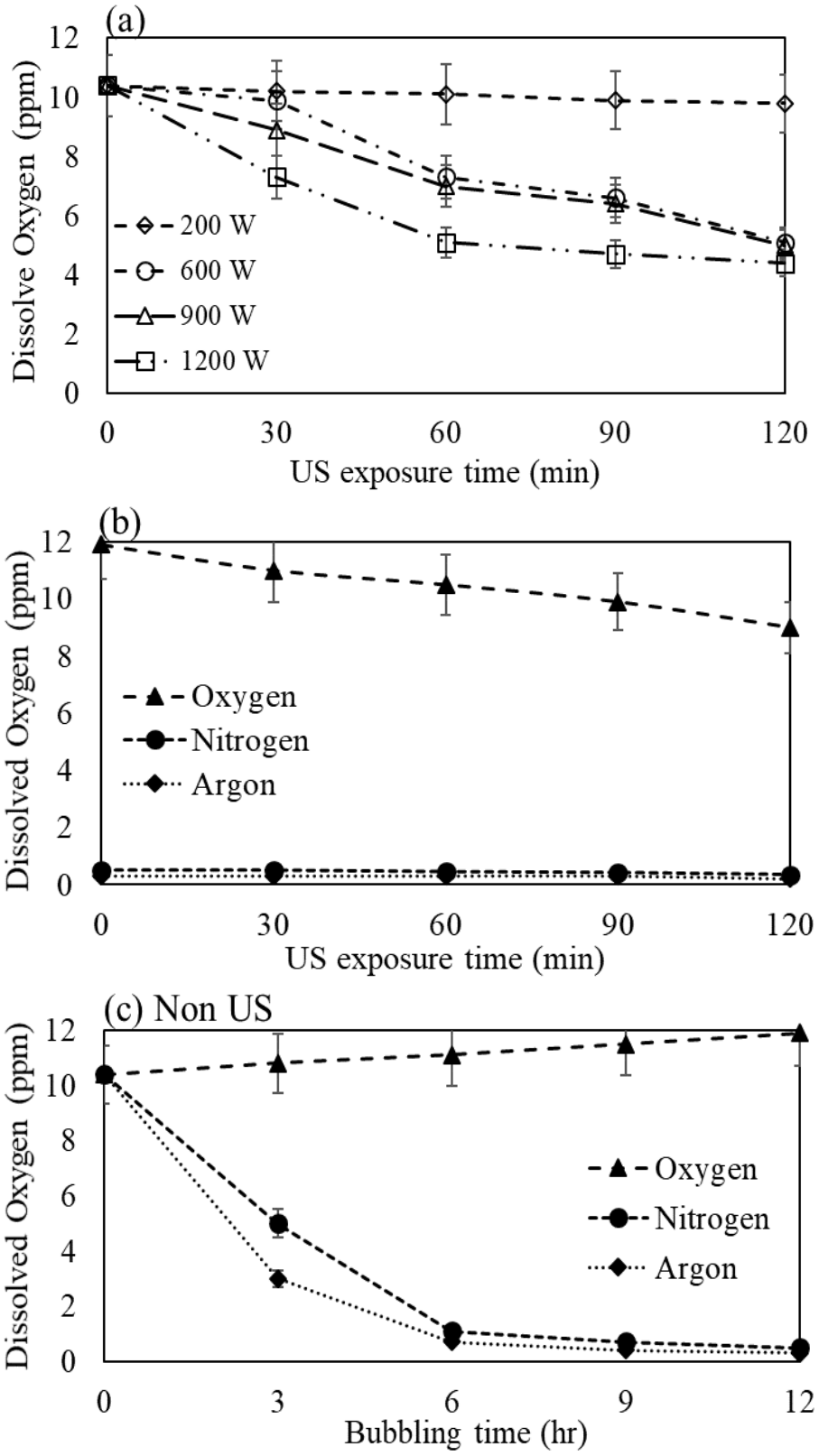

Figure 2.5: (a) Changes of dissolved oxygen concentration under US at different US power in air. (b) Changes of dissolved oxygen concentration after O_2, N_2 and Ar gas bubbling. (c) Changes of dissolved oxygen concentration during O_2, N_2 and Ar gas bubbling.

An investigation was carried out during gas bubbling before US exposure, and it was seen that when the aqueous medium was bubbled with O_2, the concentration of dissolved oxygen had an increment of about 2 ppm as seen in Figure 2.5(c). In contrast, for N_2 or Ar bubbling, 6 hours was enough to reduce the dissolved oxygen concentration to about 1 ppm in the medium.

In another previous work, during the nitration of diaminonaphthalene, [28] the solution pH shifted towards the acidic end. This was influenced by the presence of acidic HNO_2 and HNO_3 species. For this reason, during this study the pH was monitored. Figure 2.6 shows that the acidity of the exposed ultrapure water increased after 120 min of US exposure. This phenomenon was evident with higher powers (600 – 1200 W) were pH changed from 6.3 to 5.4. The pH value on the contrary did not change in mediums which were bubbled with O_2, N_2 or Ar gas prior to US exposure (Figure 2.6(b)). This indicated that the acidic species of HNO_2 and HNO_3 were not produced due to the absence of either O_2 or N_2 or both in each case. For such experiment, the principal oxidation product of NO_2^- and NO_3^- in the US ultrapure water was not produced. Referring to Figure 2.1 earlier, the production of NO_2^- and NO_3^- in the ultrapure water was not concurrent. When NO_2^-/NO_3^- ratio was evaluated in figure 2.7(a), it was seen that US activated the NO to NO_2^- under 600-1200 W after 120 min. NO_2^-/NO_3^- ranged from 0.33 to 0.71, this indicated that there was a tendency to increase NO_2^- produced in the ultrapure water, when high US power was used.

2.3.2. Detection of oxidizing species generated under the US exposure

Iodide has been reported to be oxidised in aqueous medium by means of oxidant radicals and molecules such as hydroxyl radicals (OH), hydroperoxyl radicals (HO_2), hydrogen peroxide (H_2O_2) [29-30] or HNO_2 [31], generated as a result of cavitation.

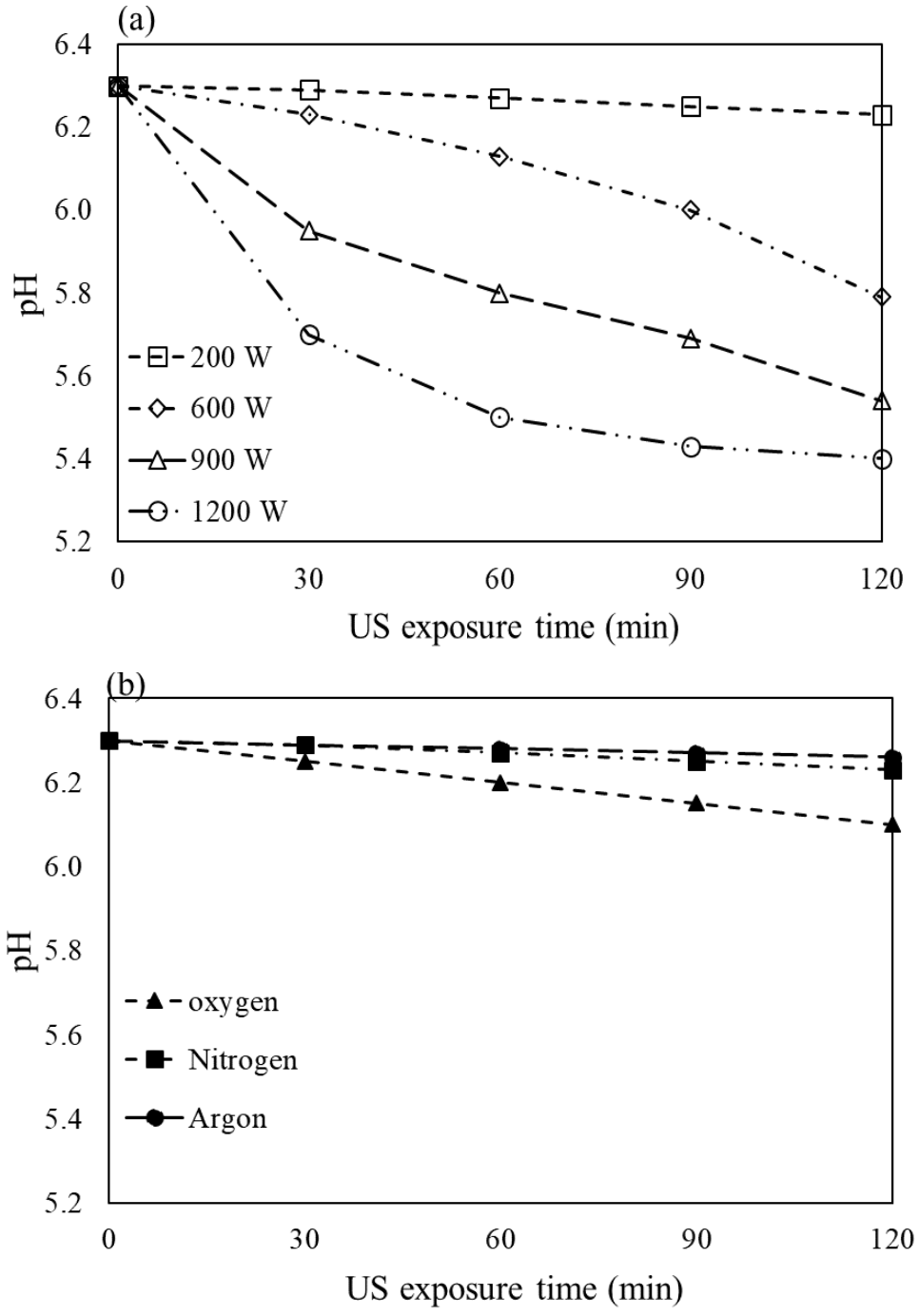

Figure 2.6: (a) Relation of pH value with US exposure time at different US power.
(b) pH of ultrapure water after US exposure under O_2, N_2 and Ar atmosphere.

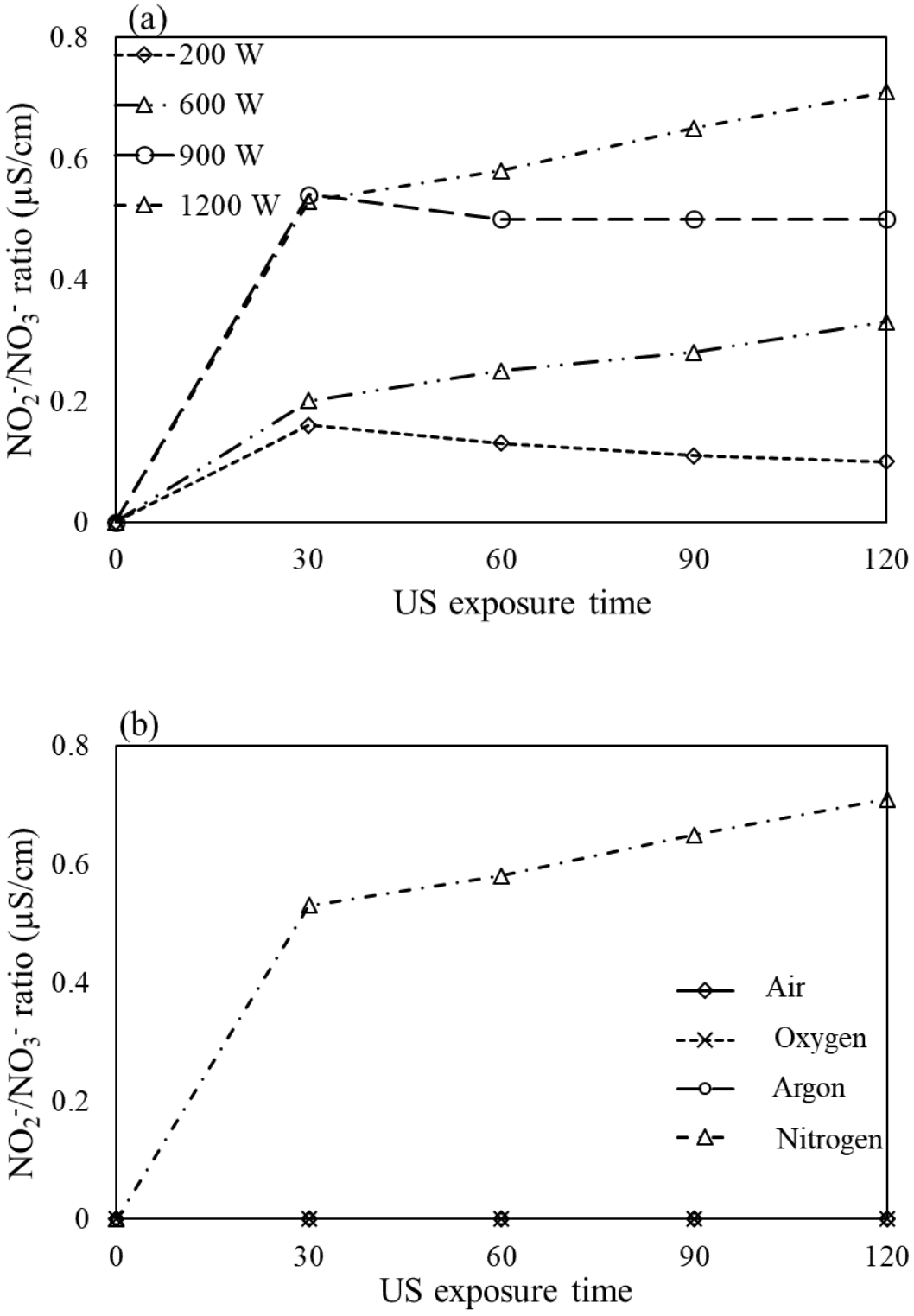

Figure 2.7: (a) NO_2^-/NO_3^- ratio (µS/cm) at different US power.

(b) NO_2^-/NO_3^- ratio (µS/cm) exposed to 1200 W US power for O_2, N_2 and Ar samples.

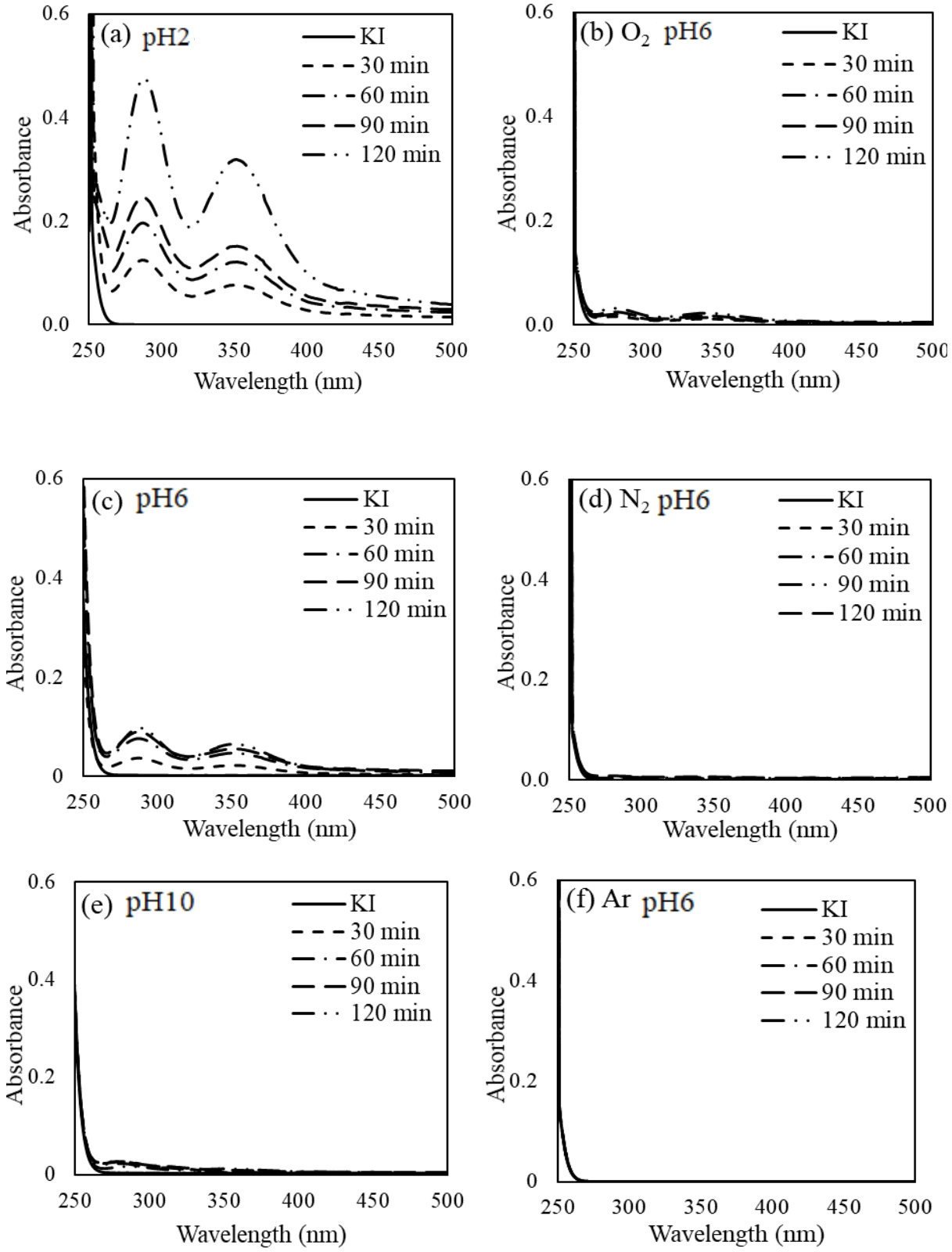

Figure 2.8: UV-vis spectra of KI after exposing 28 kHz with 1200 W at different conditions (a) pH2 (b) pH6 (c) pH10 (d) pH6 O_2 (e) pH6 N_2 and (f) pH6 Ar bubbling for 12 hours.

In a 0.1 M KI solution, oxidizing specie was confirmed to be generated with a 28 kHz low frequency US under different conditions. The absorption spectrum of this solution shown in figure 2.8 after US exposure was dominated by two maxima peaks at 288 nm and 352 nm due to the presence of triiodide I_3^- anion. During the evaluation an acidic (pH 2), neutral (pH 6) and basic (pH 10) medium were considered. The absorption of I_3^- anion increased steadily under acidic and neutral conditions with an increase US exposure time. On the other hand, the basic solution showed no classical I_3^- absorption even after 120 min with the max 1200 W US exposure.

Prior to US exposure, the solution was bubbled with various gases (O_2, N_2, or Ar), but no I_3^- absorption was seen especially in the cases of N_2 and Ar. The absorption peak intensity of the outcome was plotted against US exposure time in figure 2.9, and the absorbance was seen to increase with US power from 200 to 1200 W.

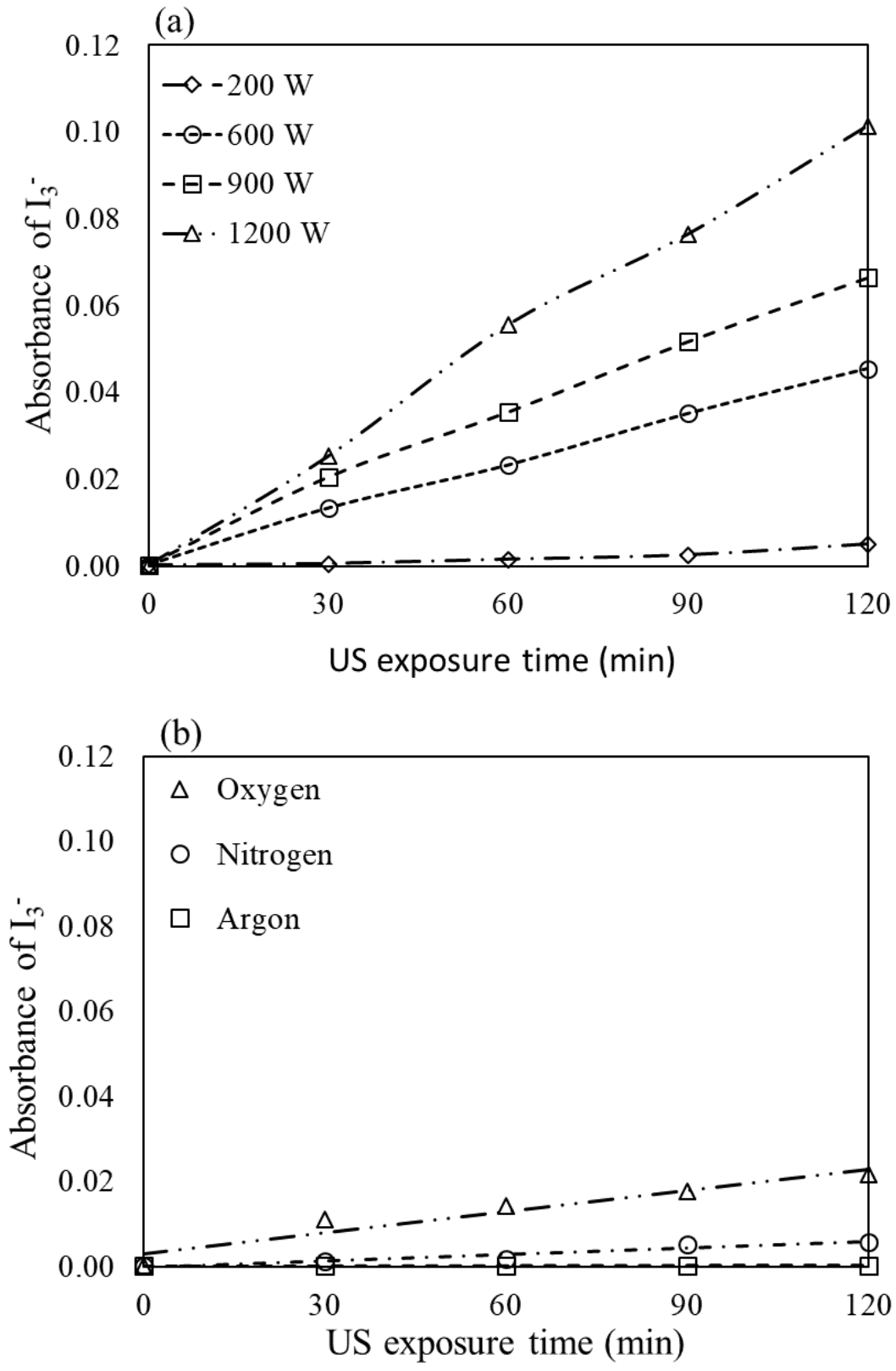

Figure 2.9: (a) Absorption of I_3^- after 28 kHz US exposure at different power for 120 min. (b) Absorption of I_3^- after 28 kHz 1200 W US exposure under O_2, N_2 and Ar atmosphere

Under O_2 atmospheres in Figure 2.9(b), the presence of the 352 nm peak was a clear indication of oxidants like oxygen radicals in the US medium. The absorbance of I_3^- increased with increasing US exposure (Figure 2.9(b)). However, in the case of N_2 and Ar, the absorbance of I_3^- was less intense which indicated that dissoluble O_2 from atmospheric air was lacking for the formation of the chemical species.

2.4. Conclusion

Using ultrapure water exposed to 23, 28, and 43 kHz US, the highest concentration of NO_2^-, NO_3^- and oxidant radicals were generated under 28 kHz low frequency with a maximum 1200 W high power US. In the presence of Ar, N_2, and O_2 gasses, the generation of these chemical species was less considerable compared to air atmosphere after 120 min. At 1200 W US exposure, oxidizing species generated by US oxidized I^- ions to I_3^- in acidic and neutral conditions. The absorption spectrum of the triiodide I_3^- anion showed maxima peaks at 288 nm and 352 nm. Contrary to N_2 and Ar conditions, in the O_2 atmospheres, the slight appearance of the 352 nm peak for I_3^- was an indication of oxidants.

Reference

1. T.J. Mason, J.P. Lorimer, Sonochemistry; Theory, Applications and uses of ultrasound in chemistry, Ellis Horwood, New York, 1989.
2. T.J. Mason, Advances in sonochemistry, vol. 1, JAI press, 1990.
3. K.S. Suslick, synthetic applications of ultrasound, *modern synth. Methods*, 4(1986) 1-60.
4. T.Y. Wu, N. Guo, C.Y. The, J.X.W. Hay. Advanced ultrasound technology for environmental remediation, 120 (2013) 11.

5. E. L. Mead, R. G. Sutherland, R. E. Verral, The effect of ultrasound on water in the presence of dissolved gases, *Can. J. chem*, 54 (1974) 1114.
6. M.Y. Li, C.Q. Wang, H.S. Bang, Y.P. Kim, Development of a flux-less soldering method by ultrasonic modulated laser, *J. Mater. Technol*. 168 (2005) 303-307.
7. Supeno, P. Kruus Sonochemical formation of nitrate and nitrite in water, *Ultrason. Sonochem*, 7 (2000) 109–113.
8. J.B. Heywood, Internal Combustion Engine Fundamentals, McGraw-Hill, New York, 1988.
9. T.F. Yen, Environmental Chemistry: Essentials of Chemistry for Engineering Practice, Vol. 4A, Prentice-Hall, Upper Saddle River, NJ, 1999.
10. A.I. Virtanen, N. Ellfolk, *J. Am. Chem. Soc*. 72 (1950) 104
11. H. Schultes, H. Gohr, *Angew. Chem*. 49 (1936) 420.
12. R. Kissner, W. Koppenol, qualitative andquantitative determination of nitrite and nitrate with ion chromatography, *meth. in Enzym. J*. 392 (2005) 61-68.
13. P. Damiani, G. Burini, fluorometric determination of nitrite, *talanta* 8 (1986) 649-52.
14. B. Narayana, K. Sunil, a spectrophotometric method for the determination of nitrite and nitrate, *Eurasian J anal. Chem*, 2(2009)204-214.
15. M. N. Moshoeshoe, V. Obuseng, Simultaneous determination of nitrate, nitrite and phosphate in environmental samples by high performance liquid chromatography with UV detector, *S. Afr. J. chem*. 2018, 71.
16. K.I. Kawabata, S.I. Umemura, J. Phys. Chem. 100 (1996) 18784-18789.
17. Y. lida, K. Yasui, T. Tuziuti, M. Sivakumar, *Microchem*. J. 80 (2005) 159-164.
18. A. Tiehm, in: A. Tiehm, U. Nies (Eds.), Ultrasound in Environmental Engineering, Technical University of Hamburg – Hamburg Reports on *Sanitary Eng*, 25 (1999) 167–180.

19. M.H. Entazari, P. Kruus, effect of frequency on sonochemical reactions ii: temperature and intensity effects, *ultraso sonochem,* 3 (1996) 19-24.
20. T.J. Mason, practical Sonochemistry; user's guide to applications in chemistry and chemical engineering, Ellis Horwood ltd, New York, 1992.
21. H.M. Hung, M.R. Hoffmann., *J. phys. Chem*. 103(1999)2734.
22. M. Lim, Y. Kim, S. kim, J. khim, *ultrason. Sonochem* 14(2007)93.
23. K.S. Suslick, Ultrasound: Applications of materials chemistry, in: R.W. Cahn (Ed.), Encyclopedia of materials science and engineering paragon, oxford, 3 (1992)2093.
24. J. Berlan, T.J. Mason, in: T.J. Mason (Ed.), *Adv. Sonochemistry*, 4(1996)1.
25. S. Koda, T. Kimura, T. Kondo, H. Mitome, A standard method to calibrate sonochemical efficiency of an individual reaction system, *Ultrason. Sonochem*. 10 (2003) 149-156.
26. Kwedi-Nsah L.M, Kobayashi.T, ultrasonic degradation of diaminobenzidine in aqueous medium, *ultrason sonochem* 52(2019) 69-76.
27. A. Abu-Dayeh, determination of nitrite and nitrate content in several vegetables in tulkam district, 1(2006)95.
28. K. Hirano, T. Kobayashi, Quantitative chemo-fluorometry diagnostic to nitrite ion in ultrasound aqueous medium, *ultrason. sonochem* 26 (2015) 345-350.
29. K. Hirano, T. Kobayashi, Coumarin fluorometry detectable OH radicals in ultrasound aqueous medium, *ultrason. Sonochem*, 30 (2016) 18-27.
30. K.R. Morison and C.A. Hutchinson. Limitations of the Weissler reaction as model reaction for measuring the efficiency of hydrodynamic cavitation. *Ultrason. Sonochem*, 16(2009)176.

CHAPTER: 3.

ULTRASONIC DEGRADATION OF DIAMINOBENZIDINE IN AQUEOUS MEDIUM

Abstract: The fluorescence of 1H,1'H-5,5'-Bibenzotriazole (BBT) was monitored when 3,3'- diaminobenzidine (DAB) aqueous solution was exposed to ultrasound (US) at 500 kHz with 0 -100 W power. Three different frequencies were used (43, 141, and 500 kHz) during this experiment. At 500 kHz ultrasound exposure, a significant broad-band was identified in the fluorescent spectra at 478 nm due to BBT formation after 90 min. The formation of BBT from DAB in an aqueous medium under US exposure was confirmed using an absorption spectrometer, fluorescent spectrometer, Fourier transformation (FT-IR) spectroscopy and NMR spectroscopy.

3.1. Introduction

Diaminobenzidine (DAB) is one of the analogs of benzidine, and it is known to be both carcinogenic and mutagenic [1-2]. DAB and its derivatives are used as raw materials for resistant polymers at high temperatures and are frequently encountered as useful reagents in industries. Due to its mutagenic property, DAB is sometimes combined with tissue components thus used as an immune-histochemical for staining nucleic acids and proteins during diagnosis processes [3]. Since DAB is unsafe for humans and the environment, several unsuccessful attempts have been made for its waste treatment. One of the most prominent is using sodium hypochlorite [4]. In this process, the chlorine bleach is ineffective to remove the mutagenic DAB molecule, but instead, the chlorine residue reacts with the DAB molecule

and forms a new mutagenic chemical. Since the chromogen to form antibody-antigen complex is toxic in nature [5], an elimination technique is therefore important.

Similarly, Azo dyes (synthetic organic colorants used for research purposes and in the textile, hair dyeing, paper making and food industries usually present in industrial wastewater are known to pose threats to public health. They are digested when they come in contact with intestinal or environmental microorganisms forming DAB [6-7].

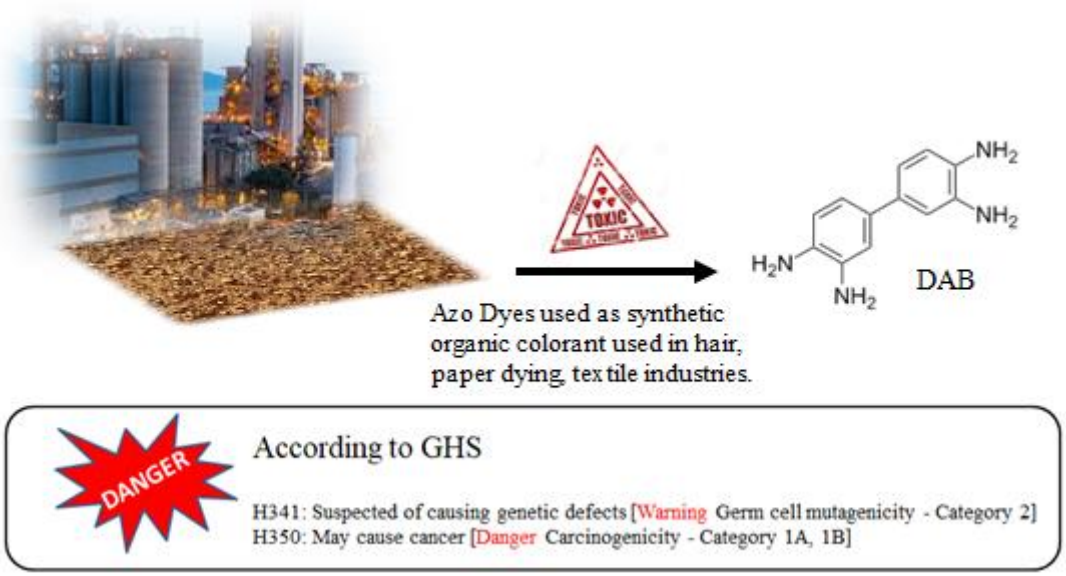

In sonochemistry, ultrasound (US) is known to induce a wide range of physical and chemical effects on compounds due to the phenomenon of acoustic cavitation [8]. During this cavitation process in an aqueous medium, formed bubbles collapse and make a local hot spot which becomes a source for reactive chemical species like nitrite oxides, hydroxyl radicals, and hydrogen peroxide [9-10]. When US are exposed in water under air atmosphere, nitrite species are formed from nitrogen in the air [11-12], this gives US the potential to produce new compounds and materials [13]. Schultes et al. reported that due to the presence of O_2 and N_2 gas in the US medium, NO_2^- and NO_3^- ions are formed under the effect of 900 kHz frequency [14]. For the formation of the NO, the Oxygen molecule dissociates, and the reactive oxygen react with nitrogen molecule [15]. In air atmosphere H_2O_2 and NO_2^- are the

primary products of water sonolyses. The NO_2^- ion is then oxidized by H_2O_2 to generate NO_3^- ion [14]. NO production is supported by Zeldovich mechanism as shown below [16].

$O_2 -))) \rightarrow 2O^\circ$

$N_2 + O^\circ \rightarrow NO + N^\circ$

$N^\circ + O_2 \rightarrow NO + O^\circ$

$N^\circ + OH^\circ \rightarrow NO + H^\circ$

The symbol "**)))**" indicates ultrasound irradiation. Further oxidation takes place induced by oxygen molecules or by OH radicals generated in US medium.

$H_2O -))) \rightarrow H^\circ + OH^\circ$

$NO + OH^\circ \rightarrow HNO_2$

$2NO + O_2 \rightarrow 2NO_2$

$NO_2 + OH^\circ \rightarrow HNO_3$

These new species formed under US medium can be detected in the fluorescence of the product. At high sonic frequencies (MHz), the production of cavitation bubbles becomes more difficult than at low sonic frequencies (kHz). For physical or chemical effect under US, the frequency is to be considered. At lower frequencies, the cycle speed is low, and the gaseous molecules are released outside of the bubbles thus, chemical species cannot be generated. On the other hand, at high frequency the speed is higher causing the gaseous molecules to remain in the bubbles [17]. These species decomposed from water are released in the US medium when bubbles collapse. Hence act as a reactive site for chemical synthesis.

This paper presents results showing how US is used to convert DAB into a new compound. The fluorometric and absorption titrations are implemented for chemical species detection. Considering our previous research on the sonochemical titration of reactant diaminoanthracene, and the product triazole moiety under US exposure [17-18], there is a

possibility to convert DAB to triazole. So far, there is no report on DAB sonochemical treatment. This technique is simple and viable with less complication in device operation.

3.2. Materials and Method

Solvents and reagents used for the experiment were used without further purification. Diaminobenzidine (DAB) was purchased from Wako Pure Chemical Industries. Ltd. Water used for the sample preparation was distilled and purified using an ion exchange column. 0.1mM DAB solution was prepared, and the acidity was adjusted to pH2 at room temperature. The sample solution was exposed to US under controlled temperature and monitored every 30 minutes for a period of 2 hrs.

The ultrasonic system consisted of a sonoreactor device HSR-305R (Honda Electronic Co. Ltd, Japan) and HAS-4012 (Honda Electronics Co. Ltd, Japan) for (43 and 141) kHz and 500 kHz respectively. For (43 and 141) kHz, an 8.5 x 8.5 x 13 (cm) stainless-steel water bath with a 3 cm transducer was used [19-20], meanwhile a 15.5 x 15.5 x 26 (cm) with an 11 cm transducer was used in the case of 500 kHz [9]. The power generated was controlled by a wave factor (WF1943B multifunction synthesizer). Absorption spectrometer (JASCO V-570) and fluorescent spectrometer (SHIMADZU, Tokyo, RF-5300PC) were used to analyze the concentration of DAB every 30 min time interval, while Fourier Transform infrared (FT-IR) spectroscopy as well as NMR spectroscopy were used to analyze the final product formed after 120 min of US exposure time.

3.3. Results and Discussion

3.3.1. *Absorption and Fluorescence titration under US exposure to DAB solution*

DAB aqueous solution was exposed to US for 120 min at a steady frequency and varied power 10 W – 100 W. The temperature of the surrounding water was controlled to avoid temperature increase. The absorbance and fluorescence spectroscopy were measured to determine the effect of US on DAB in the solutions at every given time. Figure 3.2 shows the absorption spectra of the DAB solutions for (a) 43 kHz (b) 141 kHz, and (c) – (d) 500 kHz. The US output power for (a)-(c) was 75 W and (d) 100 W. A change in absorbance was noticed with solution (b), (c) and (d). For 43 kHz no change in the absorbance was recorded even after 120 min of US exposure. A similar result to (a) was seen when low power 500 kHz was used, but when the power was raised to 100 W, a spectra change occurred in the broad range of 350 nm - 500 nm. The broad absorbance band increased with an increase in US exposure time. This proves the occurrence of a reaction in the ultrasonic aqueous medium at high frequency. An increase in the exposure time influenced the shoulder band at 475 nm, while the 280 nm band decreased. The 280 nm band was attributed to the π-π^* transition of the phenyl group in the benzidine ring. This means that the chemical structure of the benzidine conjugation remained unchanged. To analyze the reactant and product of the aqueous solution, a larger scale reaction was performed. Here, the reactant DAB (4.28g) was dissolved in acidic aqueous solution and then ultrasound was exposed as shown in the illustration below. The transparent aqueous solution changed to a red-brown solution after US was exposed as seen in figure 3.3.

Figure 3.4(a) and 3.4(b) presents plots of the absorbance at 475 nm and 280 nm respectively, for each US exposure case.

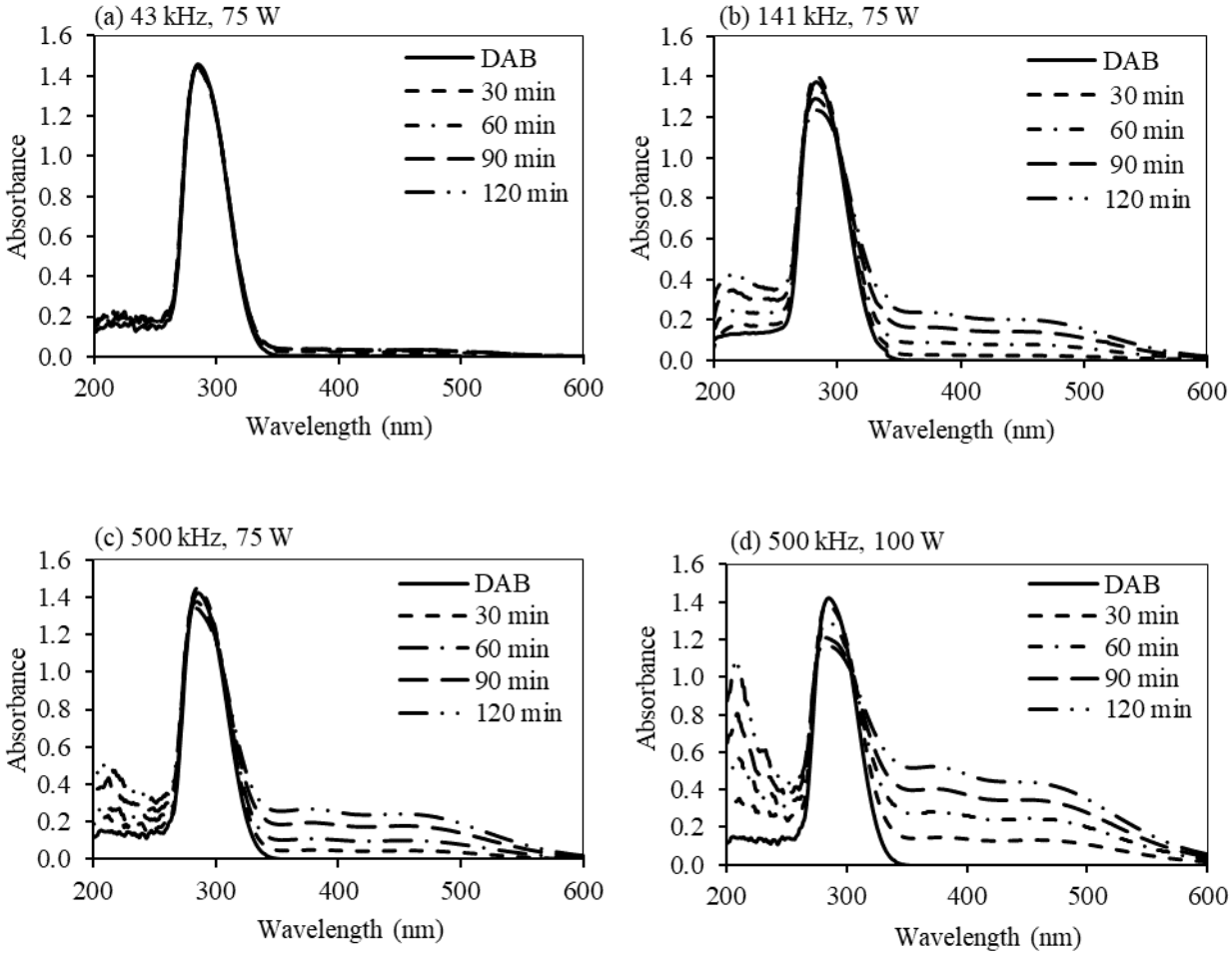

Figure 3.2: UV-Visible spectra of diaminobenzidine after exposing US with (a) 43 kHz 75 W (b) 141 kHz 75 W and 500 kHz (c) 75W and (d) 100W for 2hrs.

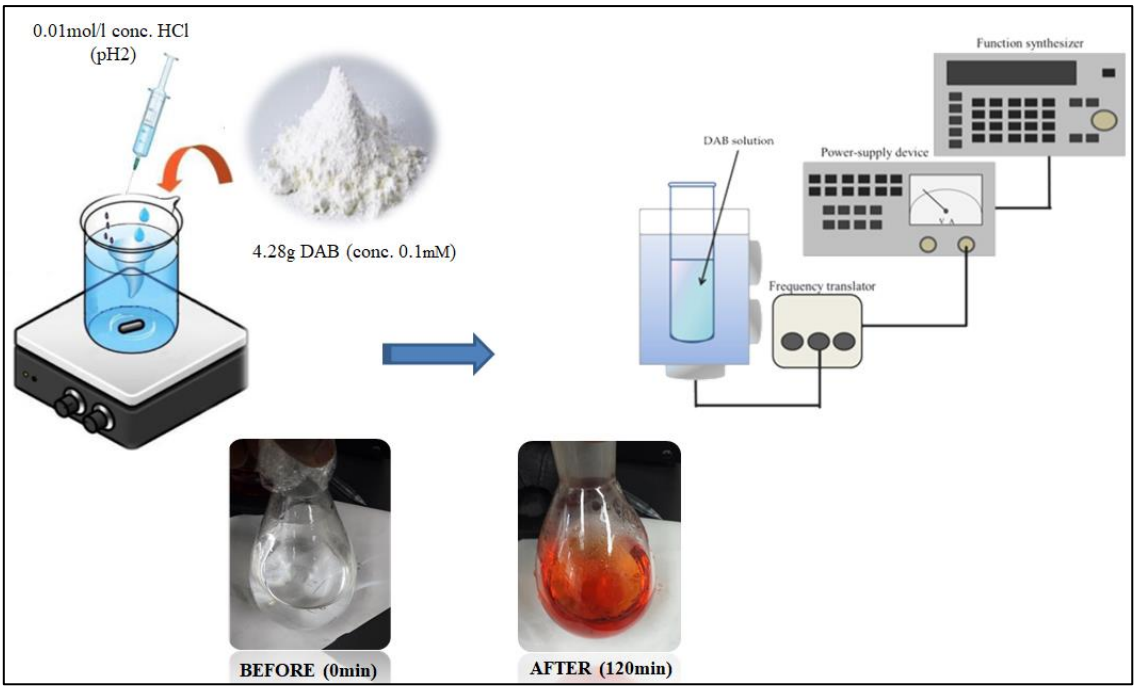

Figure 3.3

FT-IR and ^{1}H-NMR were measured as shown in Figure 3.5. A solution of 0.3 M DAB D_2O was prepared for NMR analyses. In Figure 3.5(a) the NMR spectrum of DAB shows the biphenyl protons at 6.89 ppm, 7.01 ppm, and 7.07 ppm. The lower magnetic field peak split to 7.01 ppm and 7.07 ppm due to the presence of NH_2 group. The lower chemical shift in the phenyl protons is an indication for the conversion of DAB to a higher electron density in the phenyl rings.

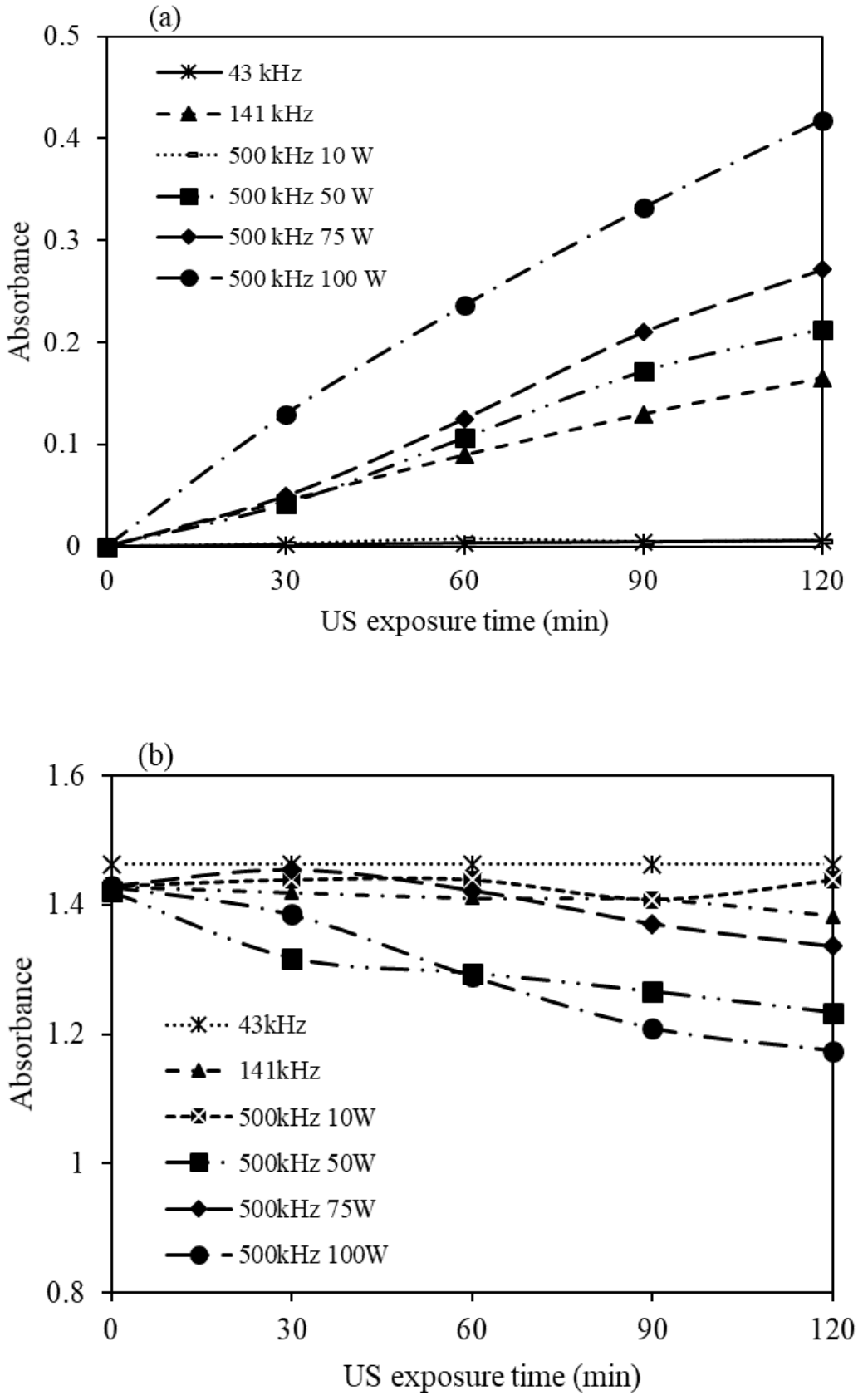

Figure 3.4: Plots of 478 nm absorbance against US exposure time exposed at 500 kHz 100 W for 120 mins and Relation of absorbance at 280 nm with US exposure time at each power.

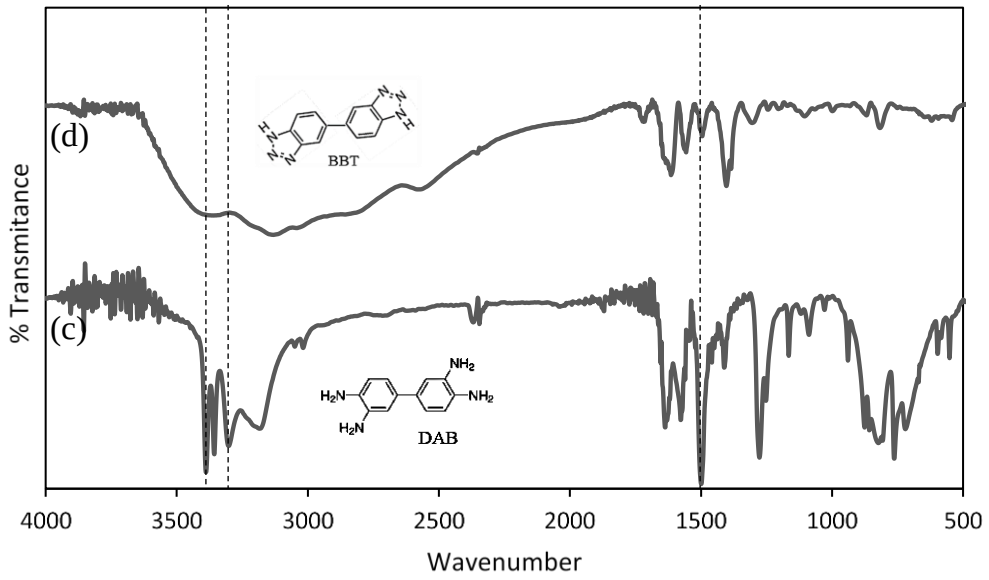

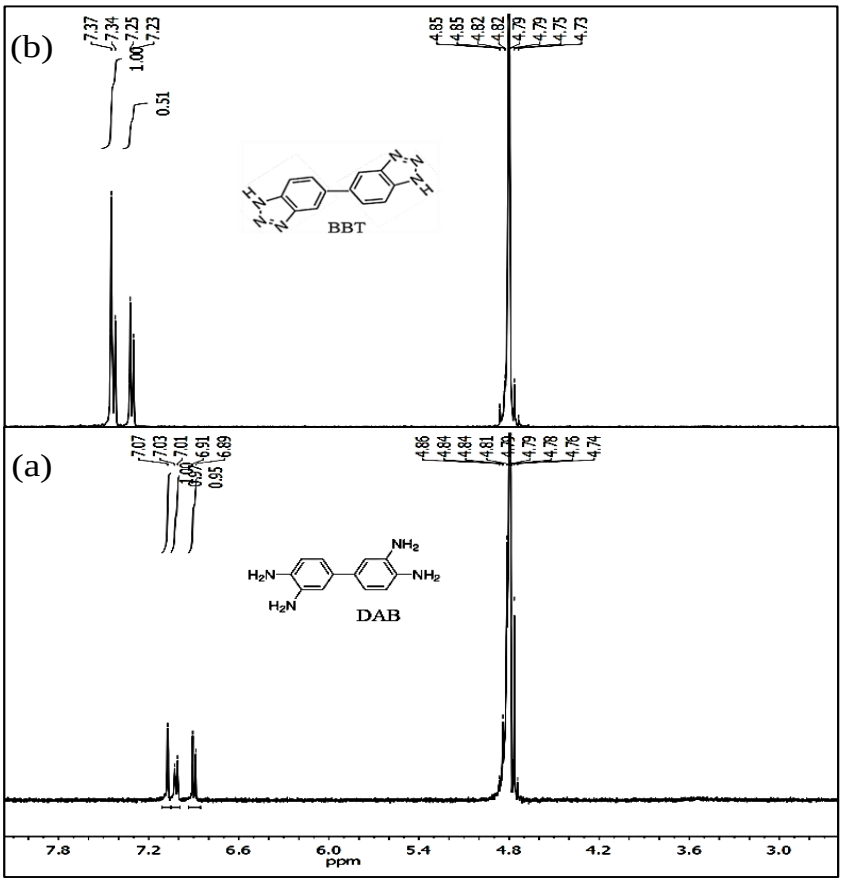

Figure 3.5: FTIR and ^{1}H NMR of DAB before and after the US exposure 120 min in D_2O solvent.

This also indicates that after 120 min of US, NH_2 proton is converted to a triazine ring as shown in scheme 3.1. The ring proton peaks of the product (Figure 3.5(b)) at 7.23 ppm and 7.37 ppm has a 1:2 intensity ratio, where as in 3.5(a) such observation of the proton peak is not seen. NH_2 stretching at 3400 cm^{-1} in the reactant disappears after the 500 kHz US exposure for 120 min (Figure 3.5(d)). Having NH group at 1500 cm^{-1} is an indication that the NH_2 groups were converted to another group of triazine, bibenzotriazole (BBT).

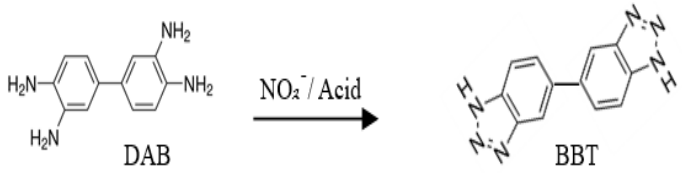

Scheme 3.1: Reaction of Diaminobenzidine with NO_2^- ion generating Bibenzotriazole in an acidic medium.

3.3.2. Effect of US on fluorometry of DAB.

For each DAB solution used for the absorption spectrometry, the fluorescence of the DAB aqueous solution was measured. Figure 3.6 shows the fluorescence spectra of the aqueous solutions at different conditions. At low frequency 43 kHz, no change in the fluorescence was registered. A similar effect was seen with 500 kHz at 10 W. When higher US power (50, 75, and 100 W) was used a broad fluorescence peak appeared at 478 nm whose intensity increased with US exposure time. Due to triazole fluorescence enhancement, the fluorescence band at 422 nm was absorbed. The change in DAB framework to BBT was clearly seen after a 120 min exposure, especially at higher power 75 W and 100 W as shown in Figure 3.6(e) and 3.6(f) respectively. The intensity of the biphenyl band at 422 nm decreased while the 478 nm increased. A comparison was made between the fluorescence band intensity of each case

as shown in Figure 3.7. We can see that US power is proportional to BBT production when exposed at 500 kHz.

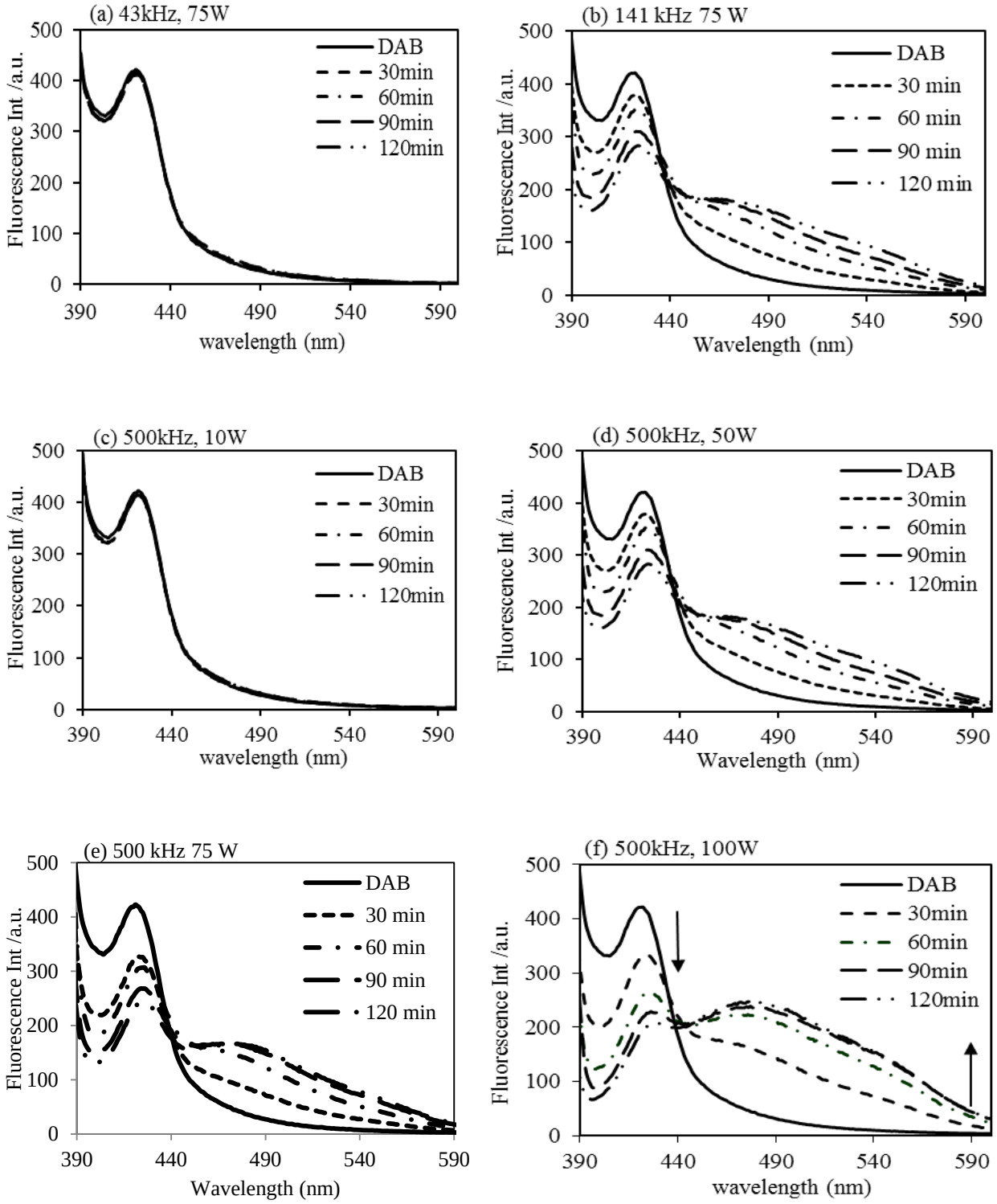

Figure 3.6: Fluorescence spectra of DAB after exposing (a) 43 kHz US 75 W, (b) 141 kHz 75 W and 500 kHz with (c) 10 W (d) 50 W (e) 75 W (f) 100 W for 120 min.

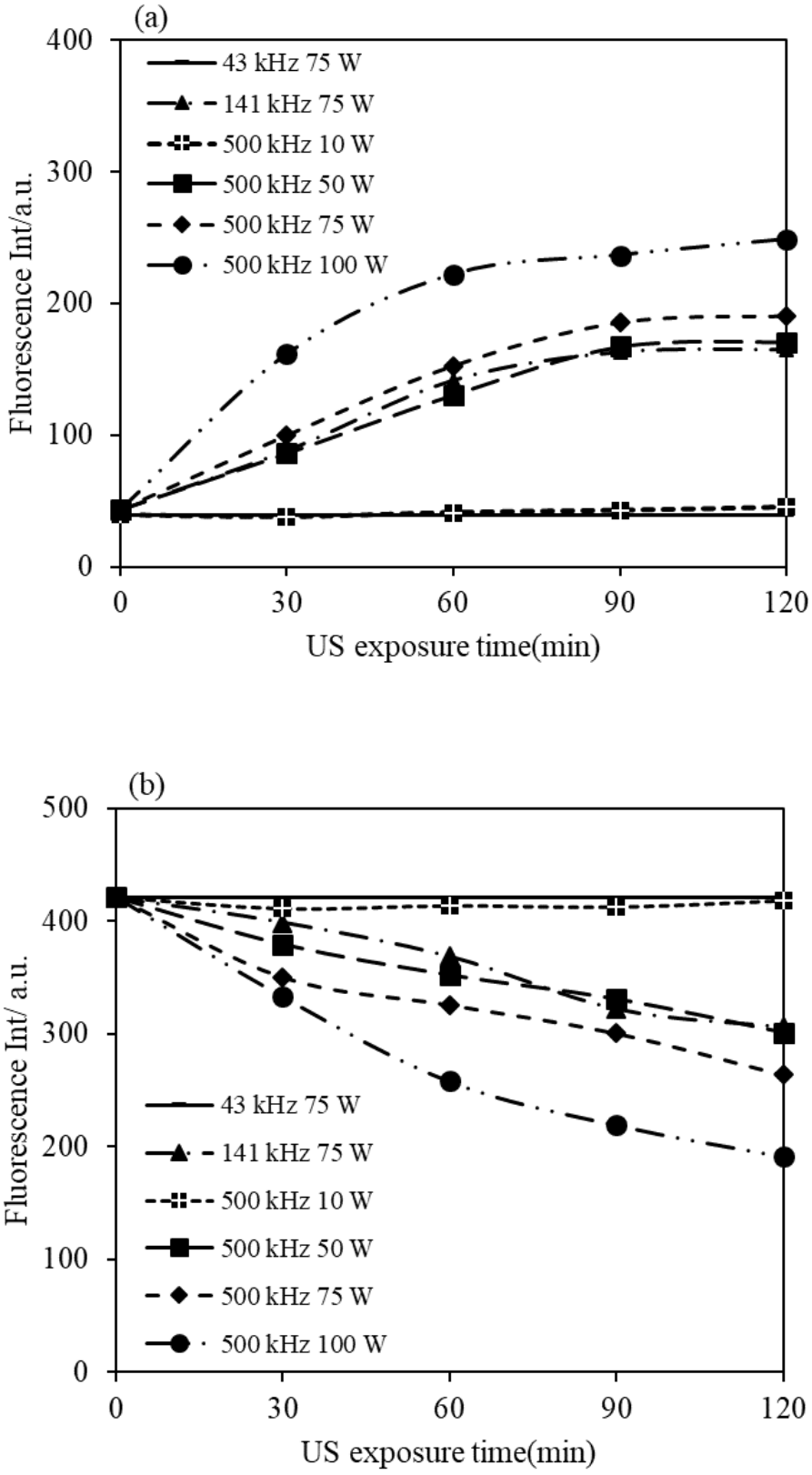

Figure 3.7: Relation of Fluorescent intensity at (a) 478 nm and (b) 422 nm with exposure time at each power.

As investigated at 500 kHz for diaminonaphthalene diagnosis [11], nitrite was formed, and a change in pH was noticed. This is because during sonochemical process, bubbles collapse and create a local hot spot for reactive chemical species. When 141 and 500 kHz US were used, nitrite ion and nitric acid was formed in the solution [16-17], which led to the production of acidic species such as HNO_2 and HNO_3 [21] hence causing the aqueous pH to shift towards the acid side. In the present work, the acidity of the exposed solution was monitored, and a change in pH was witnessed. Figure 3.8 shows that the pH shifts towards the acidic pH 1 at 500 kHz. Since air was bubbled into DAB solution for 2 hours before US exposure, we can conclude that air N_2 was the source for the formation of the nitric ion in the US aqueous solution.

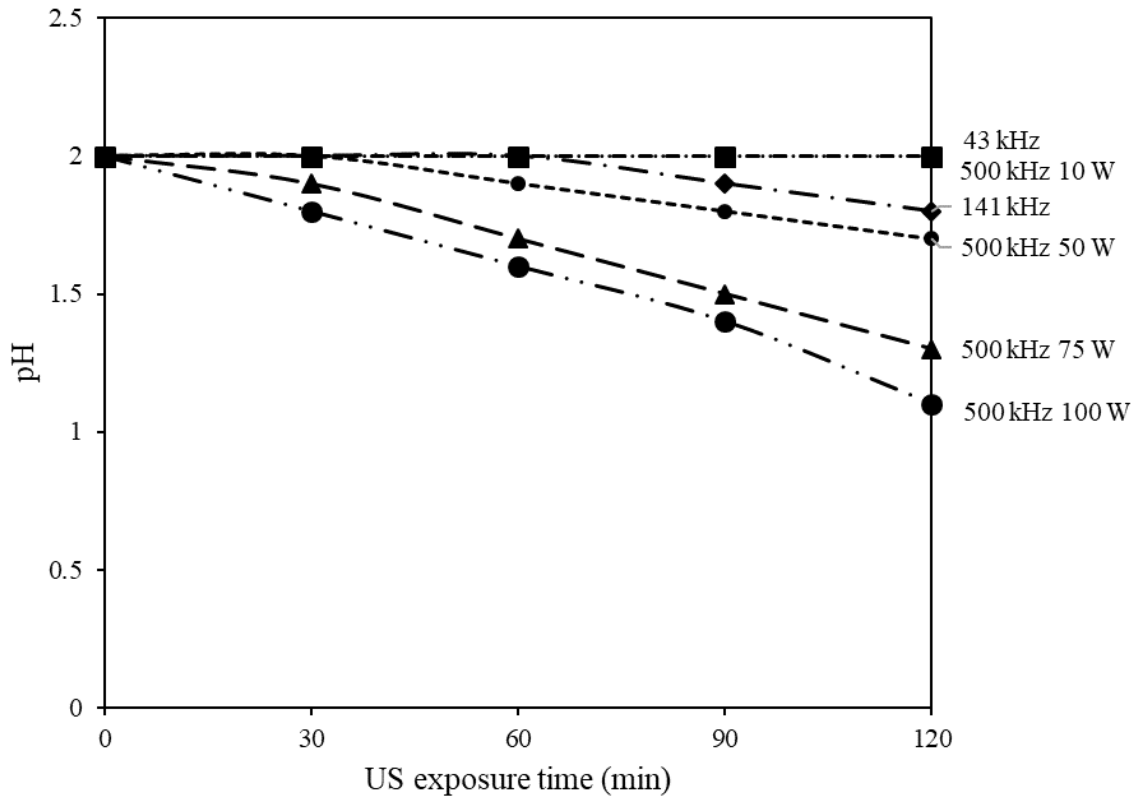

Figure 3.8: pH effect at 475 nm exposed at different frequency.

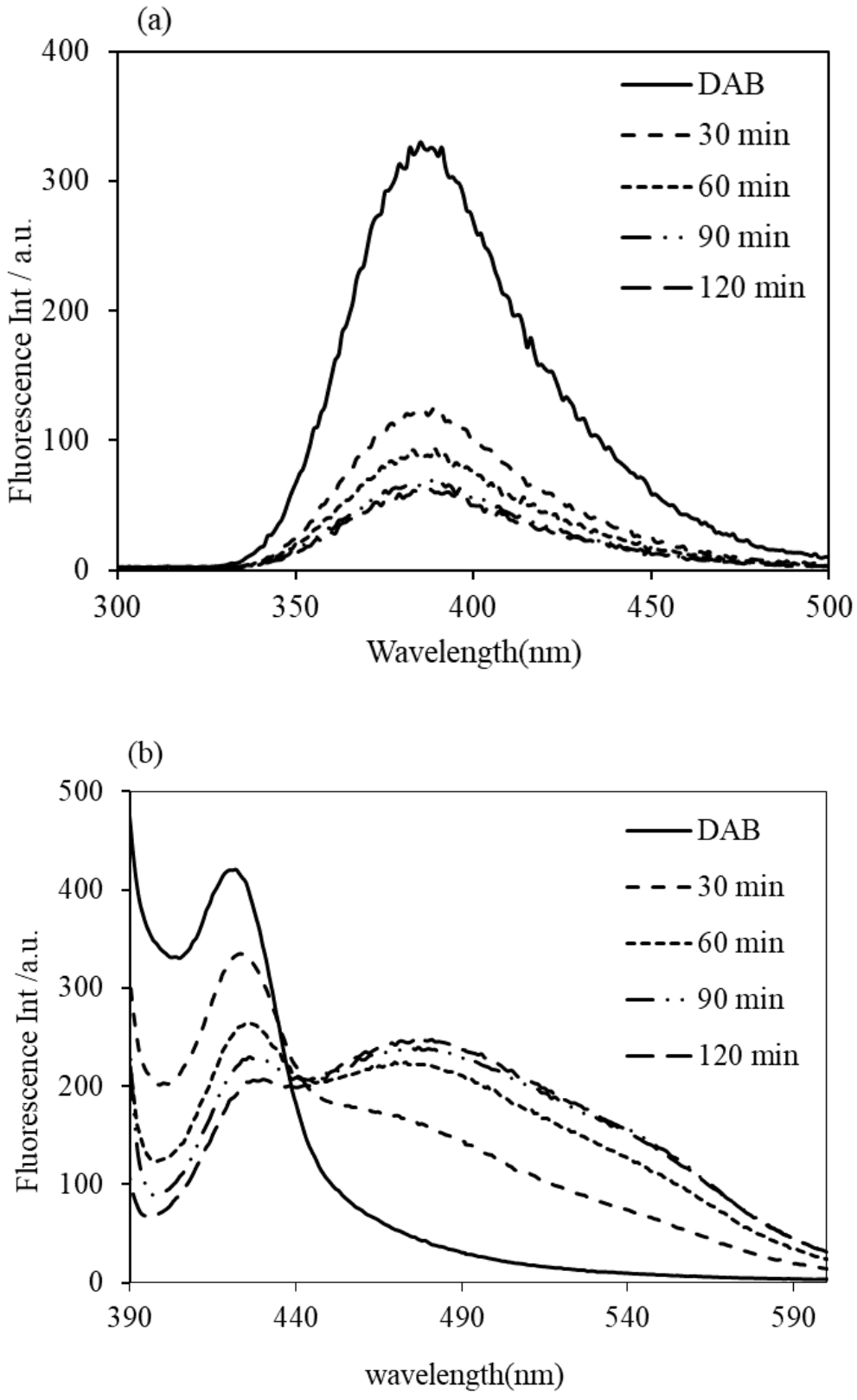

Figure 3.8**:** Fluorescence spectra of DAB air bubbled at (a) 280 nm and (b) 370 nm excitation wavelength.

The excitation wavelength of 280 nm and 370 nm was used to measure the fluorescence for DAB and BBT respectively (Figure 3.9). For quantitative information on the effect of US, experiments were carried out to determine DAB and NO_2^- rate kinetics. A calibration curve was made from standards prepared with different DAB concentrations. The curve was used to deduce the concentration of DAB from each US exposure case. The sonochemical degradation of DAB at 500 kHz fits well a second-order model as shown in figure 3.10.

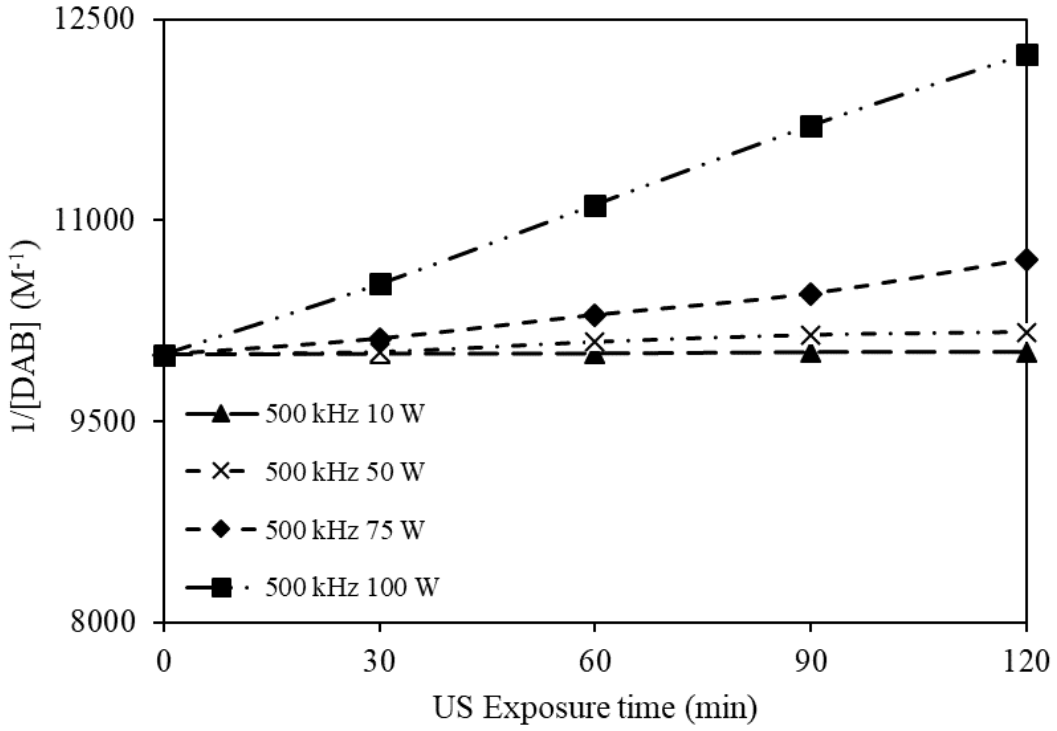

Figure 3.10: Decomposition of DAB under 500 kHz US.

At low power, no major change in DAB degradation occurred, meanwhile when the sample was exposed at 100 W; 3 times the concentration of 75 W degraded after 120 min.

Kinetic involved in nitrite formation during sonolysis of water is a vital part of DAB degradation under ultrasound for this reason nitrite was examined according to reference papers [22-25].

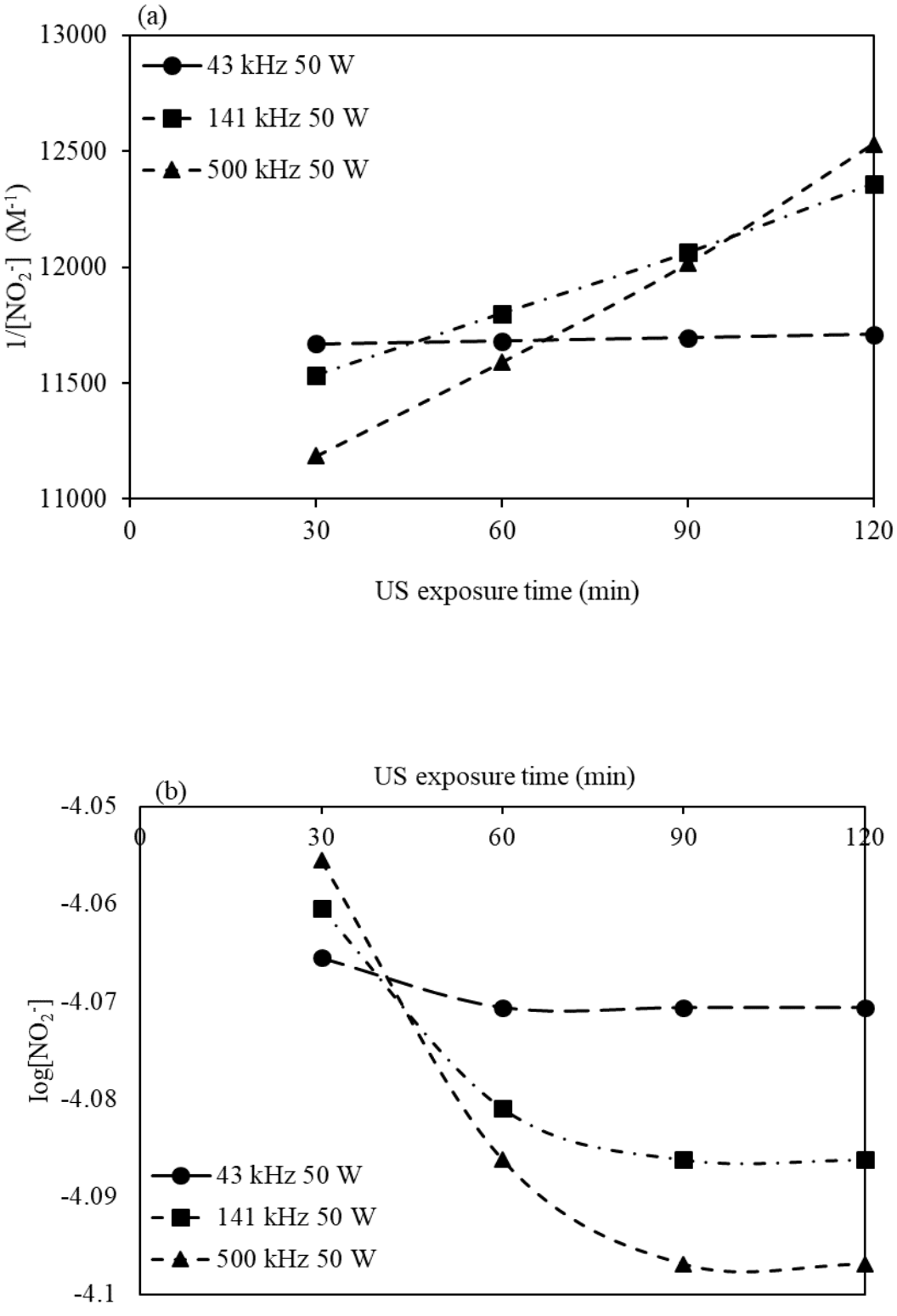

Figure 3.11: Kinetics of Nitrite (a) First order and (b) second order plots.

Ultraviolet spectrophotometry method was used, and a calibration curve was constructed following Beer's law. Samples with the same reaction geometry, same power (50 W) etc. were used to determine the reaction rate. The nitrate formation fits well with a second order plot but not with a first order as shown in figure 3.11(a). The reaction rate doubled as the nitrite ions were produced, due to a high rate of dissociation of the chemical specie and free radicals formed in the surrounding water. The reaction was fastest with 1.77×10^{-7} mol dm^{-3}/min (Table 3.1) at 500 kHz.

Table: 3.1. Reaction rate of Nitrate under same experimental condition with different ultrasonic frequency.

Frequency (kHz)	**Reaction rate ($moldm^{-3}$/min)**
43	3.33×10^{-9}
141	4.33×10^{-8}
500	1.77×10^{-7}

3.4. Conclusion

At lower frequencies, gaseous molecules are released outside the bubbles, thus chemical species are not generated, but at high frequency the gaseous molecules remain in the bubbles and facilitate chemical synthesis. 500 kHz US forms nitrite species in the aqueous solution and causes a change in the diaminobenzidine group to triazole species. In the absence of ultrasound, no reaction occurs in the DAB solution. But when DAB is mixed with a nitrite compound, a change in the DAB spectra is observed with a much slower reaction rate. Thus, 500 kHz US is effective for generating BBT with a triazole ring from DAB.

References

1. K.T. Chung, S.E. Stevens, C.E. Cerniglia, The reduction of azo dyes by the intestinal microflora. Crit. Rev. Microbiol. 18 (1992) 175–190.
2. K.T. Chung, S.E. Stevens, Degradation azo dyes by environmental microorganisms and helminths. Environ. Toxicol. Chem. 12 (1993) 2121–2132.
3. T. Nakata, N. Suzuki, Chromogen-based Immunohistochemical Method for Elucidation of the Coexpression of Two Antigens Using Antibodies from the Same Species. J. Histochem. Cytochem. 60 (2012) 611–619.
4. G. Lunn, E.B. Sansone, The safe disposal of diaminobenzidine. Appl. Occup. Environ. Hyg. 6 (1991) 49-53.
5. K. Ishizaka, T. Ishizaka, D. H. Campbell. The Biologic activity of soluble antigen-antibody complexes. J. Exp. Med. 109(1959) 127-143.
6. K, T.Chung, C.E.Cerniglia, Mutagenecitu of azo dyes: structure activity relationship. Mutation. research, 277(1992)201-220.
7. K, T. Chung, E. Steven (Jr), Degradation azo dyes by environmental microorganisms and helminthes, Environmental Toxicology and Chemistry, 12(2009)2121-2132.
8. K.S. Suslick, Gareth J. Price, Applications of ultrasound to material chemistry. Annu. Rev. Mater. Sci. 29 (1999) 295–326.
9. M.Y. Li, C.Q. Wang, H.S. Bang, Y.P. Kim, Development of a flux-less soldering method by ultrasonic modulated laser. J. Mater. Technol. 168 (2005) 303-307.
10. K.S. Suslick, L.A. Crum, In Encyclopedia of Acoustics. Ed. MJ Crocker. 1 (1997) 271–82.
11. K. Hirano, T. Kobayashi, Coumarin fluorometry to quantitatively detectable OH radicals in ultrasound aqueous medium. Ultrason. Sonochem. 30 (2016) 18-27.
12. I.I. Stepero, R.I. Adamchuk, V.I. Stepero. Biophysics. 49 (2004) 705-712.

13. K.S. Suslick, P.F. Schubert, S. W. Goodale. J. AM. Chem. Soc. 103 (1981) 7343.
14. H. Schultes, H. Gohr, Uber chemische Wirkungen der Ultraschallwellen, Angew. Chem., 49 (1936) 420-423.
15. C. A. Wakeford, R. Blackburn, P. D. Lickiss, Effect of ionic strength of the acoustic generation of nitrite, nitrate and hydrogen peroxide, Ultrason. Sonochem., 6 (1996) 141-148.
16. Y. Zeldovich, D. Frank-Kamenetskii, P. Sadovnikov, oxidation of nitrogen in conbustion; Publishing House of the Academy of sciences of USSR: Moscow (1947).
17. K. Hirano, T. Kobayashi, Quantitatively chemo-fluorometry diagnostic to nitrite ion in ultrasound aqueous medium containing 2, 3-diaminonaphthalene. Ultrason. Sonochem. 26 (2015) 345-350.
18. M. Sato, H. Itoh, T. Fujii, Frequency dependence of H2O2 generation from distilled water. Ultrason. 38 (2000) 312.
19. K. Li, T. Kobayashi, Ultrasound response of aqueous poly(ionic liquid) solution. Ultrason. Sonochem. 30 (2016) 52-60.
20. J. A. Venegas-Sánchez, M. Tagaya, T. Kobayashi. Ultrason. Sonochem. 21 (2014) 295-309.
21. M. Sato, H. Itoh, T. Fujii, Frequency dependence of H2O2 generation from distilled water Ultrasonics, 38 (2000) 312-315.
22. R. C. Hoather, R. F. Rackham. Oxidised nitrogen in waters and sewage effluents observed by ultra-violet spectrophotometry. Anal.84 (1959) 549.
23. E. Goldman, R. Jacobs. Determination of nitrates by ultraviolet absorbtion. J. Amer. Water Works Assoc. 53 (1961) 187.
24. F. A. J. Armstrong, Determination of nitrate in water by ultraviolet spectrometry. Anal. Chem. 35 (1963) 1292.

25. P.K. Tarafder, P.S. Rathore, Spectrophotometric determination of nitrite in water. Analyst,113(1988)1073-1076.

CHAPTER: 4.

SOIL RECYCLING GEOPOLYMERS FABRICATED FROM HIGH POWER ULTRASOUND TREATED SOIL SLURRY IN THE PRESENCE OF AMMONIA

Abstract: Soil slurry was recycled to prepare a geopolymer after treatment with high power ultrasound (US) in the presence of NH_3, HCl and NaOH. Under 28 kHz US, 0.1 M NH3 additives effectively decarbonized the slurry, eliminating 72.2 % of Carbon (C) content from the original soil. The US treated soils were used as raw materials for geopolymer as they contained Si and Al components in the range of 25-30 and 8-10 wt. %, respectively. The geopolymer was prepared with Na_2SiO_4/NaOH aqueous solution at a ¼ weight ratio at 80^oC for 24 hours. The resultant geopolymers showed best compressive strength, with low C content, when NH_3 was used as an additive as opposed to HCl and NaOH under 1200 US exposure.

4.1. Introduction

Geopolymer is a ceramic material which can be prepared at low temperature in the presence of an alkaline activator [1]. Considering the advantage that ceramic blocks can be prepared at low temperature, attractive research is focused on sustainable materials for reuse of fly ash and other inorganics [2]. Since the interest towards sustainability is an attractive point in the construction sector [3], there is an alarming growth of geopolymer researches recently. Pioneering research on geopolymer shows highly promising results relating to durability and fire resistance [4-5].

It is interesting to note that soil contains minerals, water, air, gases, organic matter, and microorganisms [6-8]. Among which the mineral part is the largest component with sand, silt and clay making approximately 45 – 50 % of the total soil. Thus, this implies that soil is made up of SiO_2, Al_2O_3, Fe_2O_3 and CaO constituents. The organic matter in the soil is derived mainly from dead plants and animals, while at low percentage concentration, the carbon parts are decomposed by microorganisms [9]. Generally, when soil has to be recycled, the soil must be sintered at high temperature to remove such organic components [10-14]. So, because high temperature facilitates the elimination, soil recycling into concrete for-example becomes a reality. As organic carbon parts are known to decrease the strength and stability of inorganic ceramic materials, less Carbon content in soil is therefore an important factor to consider during soil recycling for the application of inorganic concrete and geopolymers [15].

So far, the ideal elimination method of soil carbon remains to be discovered. But, the most prominent method is shaking the soil in water for several hours [16]. Usually, water or aqueous chemicals such as acids, bases, surfactants, and chelating agents are vital for the conventional washing method [17]. This technology is recognized as a very important method for the elimination of hazardous contaminants and for washing heavy-metal contaminated soils [18]. But, the drawback of this soil washing technique with the addition of reagents in sequential washing steps [19], is that the washing process can remove pollutants or unwanted compounds only from the surface of the soil particle [20-21].

Ultrasound (US) which is the vibration of sound waves above audible frequency causes remarkable mechanical soil dispersion. This is because bubbles generated by US inside the reaction vessel oscillates/increases in size, and then explodes with a violent power generating extreme sonochemical and sonophysical effects in aqueous soil [22, 23]. It is known that, both effects are applied in some technologies for surface cleaning, extraction, and micromixing [24-27]. For US soil washing, in addition to other factors, the effect of

sonication power has been reported in several papers [24-26]. Sonication power is known to accelerate sequential extraction by US washing. Also, US waves can break down the particle size of soil and aggressively agitate the slurry solution.

Although excavated soil is used as a renewable material in the construction industry, however, the recycling rate seems very low [28]. This is because these soils are usually categorized as waste [29]. From a financial perspective, soil displacement is about 5-16% of the capital cost of every project [30]. In South Korea [31, 32], Canada [33], and Italy [34] for example, programs have been created to encourage the re-use of excavated soil. In Japan as well, due to the limitation of available natural resources and land space for landfills, the re-use in the field of construction is greatly encouraged [35]. Because these waste soils are being converted into other useful products, it is quite meaningful to study soil reuses.

As earlier mentioned, soil clay is generally rich in Al_2O_3 and SiO_2 components, giving the possibility for soil to be re-used as inorganic materials. Although the researches are limited**,** one of the major possibilities of soil re-use is for the fabrication of a geopolymer. An attempt has been made by Singhi et al. investigating soil–geopolymer incorporated with slag, fly ash, and a mixture of slag and fly ash [36-37]. The addition of nanoparticles of layered mineral silicates led to the flocculation of clay particles which improved the rheological properties of geopolymer nanocomposites, suitable to be used in 3D printing applications [38-39]. In the present study, high power US soil washing is performed and the treated soil is used as geopolymer source material.

4.2. Materials and Methods

Waste soil sampled from Niigata (Japan) was used for this study without further treatment. The soil sample which classified as sludge (ρ = 1.3 g/cm^3) was air-dried, ground, and passed through a 1.18 mm sieve before treatment. The experiment was carried out in a stainless-steel bath (10 cm length x 60 cm width x 50 cm depth) with a submersible stainless-steel rectangular container housing seven transducers (42 x 30 x 10 cm^3). The US was generated with a resonance frequency of 28 kHz by a Honda electronic device (Dynashock WD 1200-28) and 300 -1200 W output power. For US washing of the excavated soil, the ratio of soil and washing liquid was set at 1:10 and the sample vessel was placed 5 cm from the transducer heads. The slurry sample was exposed to different ultrasonic intensities 0-1200 W for a period of 60 min.

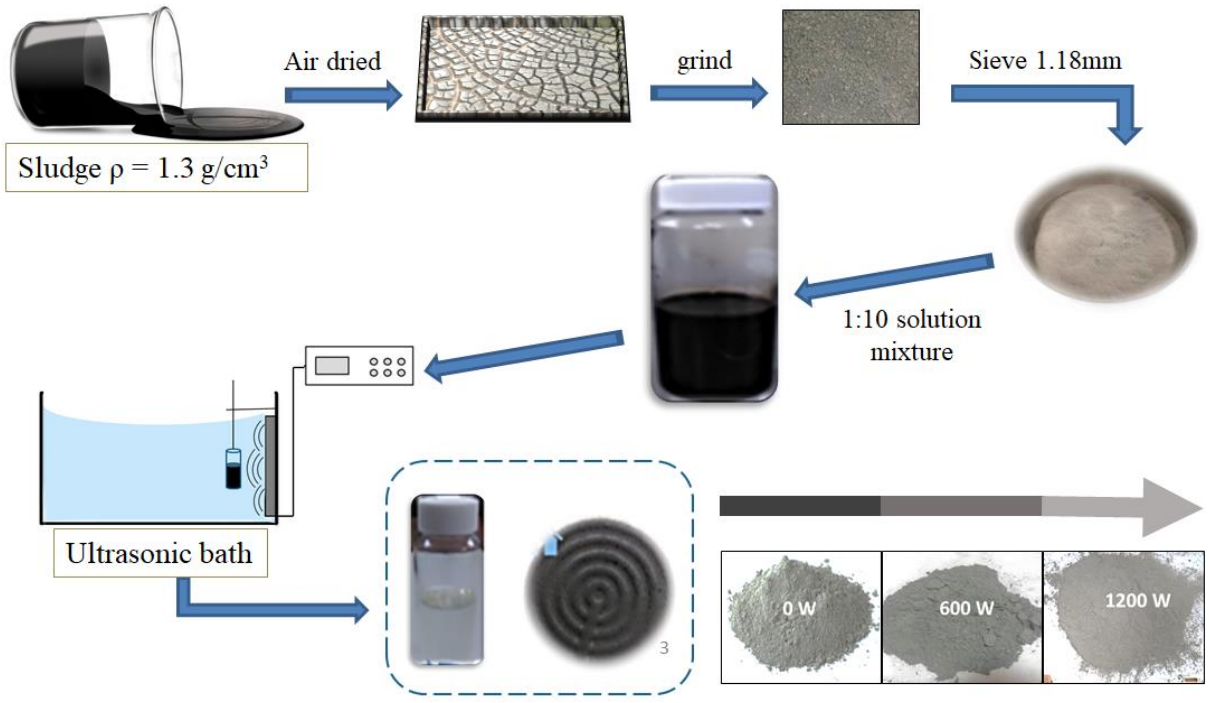

Figure 4.1

The resultant solution was filter pressed to efficiently separate the liquid from the solid. Then the powder was dried at ≤ 35˚C to avoid any chemical loss. The powder was seen to have a

different color especially at higher power which looked whiter and very similar to Portland cement. During this study, 0.01-1 M aqueous solutions of HCl (acid), NaOH (strong base), and NH_3 (weak base) were prepared and used as treatment additives. The upper view of the US setup used for treatment was as shown in Figure 4.2.

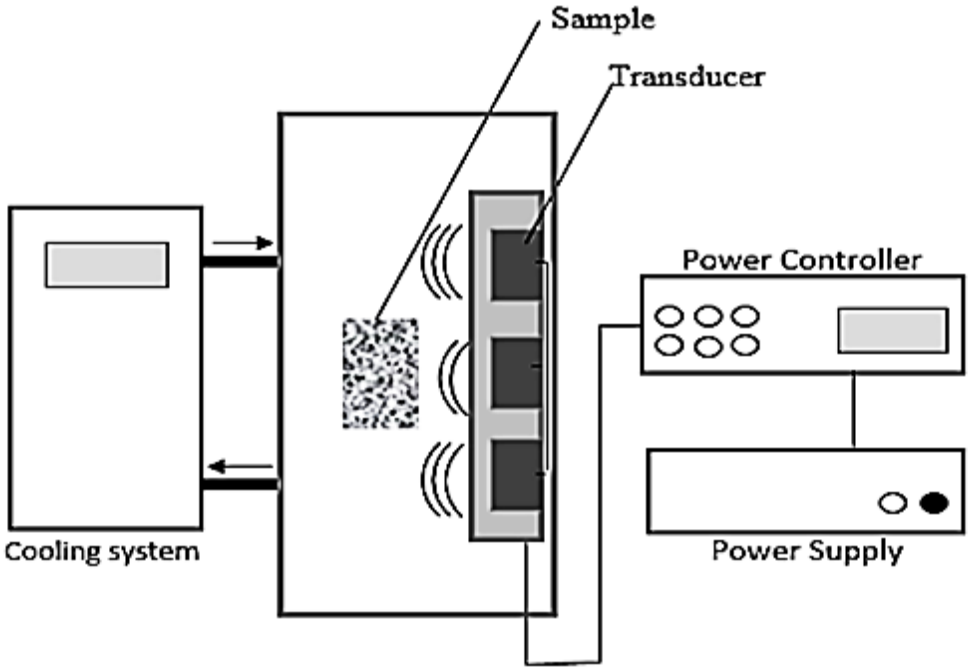

FIGURE 4.2: Upper view of ultrasound experimental setup

At the end of each US treatment, the slurry mixture was filter-pressed (Nihon Roka Sochi filter press, Japan) with filter cloth ($0.3cm^3/cm^2sec$) for effective separation of the solid and liquid content. For the determination of soil components, the soil extracts were dried at 40˚C for 24 hours. The dried extracts were then fused in pellets and the mineral content of the soil was analyzed by XRF (Rigaku ZSX Primus II; Rigaku Corp. Japan), Table 1 shows the effect of US on the soils chemical constituent when different additives were used for soil washing.

TABLE 4.1: Chemical composition (mass %) of raw sample (soil), before treatment and after 1200 W US treatment with different concentration of additive.

US treatment	Soil	No additive	HCl 0.01M	HCl 0.1M	HCl 1M	NH_3 0.01M	NH_3 0.1M	NH_3 1M	NaOH 0.01M	NaOH 0.1M	NaOH 1 M
C	3.6	2.4	2.4	2.4	2.1	2.3	1.0	1.9	1.9	1.1	2.0
Na_2O	1.3	1.4	2.0	1.84	2.2	2.1	2.1	2.0	2.2	2.8	5.0
SiO_2	50.4	55.3	63.6	62.8	63.9	64.8	65.2	63.5	64.2	63.3	62.6
Al_2O_3	18.8	17.1	15.8	15.4	14.7	15.7	16.2	16	16	16.1	15.3
Fe_2O_3	4.1	4.0	3.9	3.2	2.9	3.9	4.1	4.2	4.1	3.9	3.4

To evaluate the percentage efficiency of US to Carbon in soil (CIS) extraction, the following formula was used;

$$\text{CIS} = \frac{XRF\ value\ before\ US - XRF\ value\ after\ US}{XRF\ value\ before\ US} \times 100.$$

After XRF analysis, the remaining solid extract was crushed and passed through a 0.25 mm sieve and fine soil powder was obtained. Considering the numerous generic information available on geopolymers, a rigorous trial-and-error method was adopted to fabricate soil-based geopolymer concrete similar to the technology currently used to manufacture fly ash-based geopolymer concrete.

An alkalis activator was prepared using 1 M aqueous Na_2SiO_3 with 10 M NaOH at a ratio of 1:4, meanwhile the weight ratio of soil (S) and the alkali activator solution (AAS) was fixed at 1:1. The US treated soil powder was mixed with the AAS and then stirred for 60 seconds forming a paste. The paste was poured into a plastic-mold (30 x 30 x 30 mm^3) and cured in an oven (Avo 200NS, ASONE-Japan) at 80°C for 24 hr. After curing, the samples were crushed for further characterization. The X-ray Diffractometer (XRD) (Rigaku smart lab 3kW) was used with Cu Kα radiation at 40kV and 30mA. And the sample was measured on a

glass plate after crushing, with scanning angle 10-60 degrees, and scanning speed was fixed at 2˚/min. X-ray fluorescence analyzer (Rigaku ZSX primus) was used to analyze the composition of geopolymer samples. For this measurement, 10 mm diameter pellets were made using an aluminium ring and a high pressing machine. To investigate the chemical bonding inside the geopolymer, the geopolymer powder after crushing was mixed with KBr at a concentration of 1.0-5.0 wt% after which a disk of the mixture was formed by a high press machine. FTIR (FT-IR-4100, JASCO) spectra were obtained with 20 scans from 400 to 4000 cm^{-1} at a resolution of 2.0 cm^{-1} in transparent mode. SEM (Desktop Scanning Electron Microscope, Hitachi TM3030 Plus) was used to see the microstructure in geopolymer. For this analysis, all the geopolymer samples were coated with a thin layer of gold on their surfaces after drying with a vacuum pump for 24 hours. The compressive strength of geopolymer samples was measured with a testing machine (UH-F50A, SHIMAZU) and the ratio of compression was fixed to 0.5 mm/min.

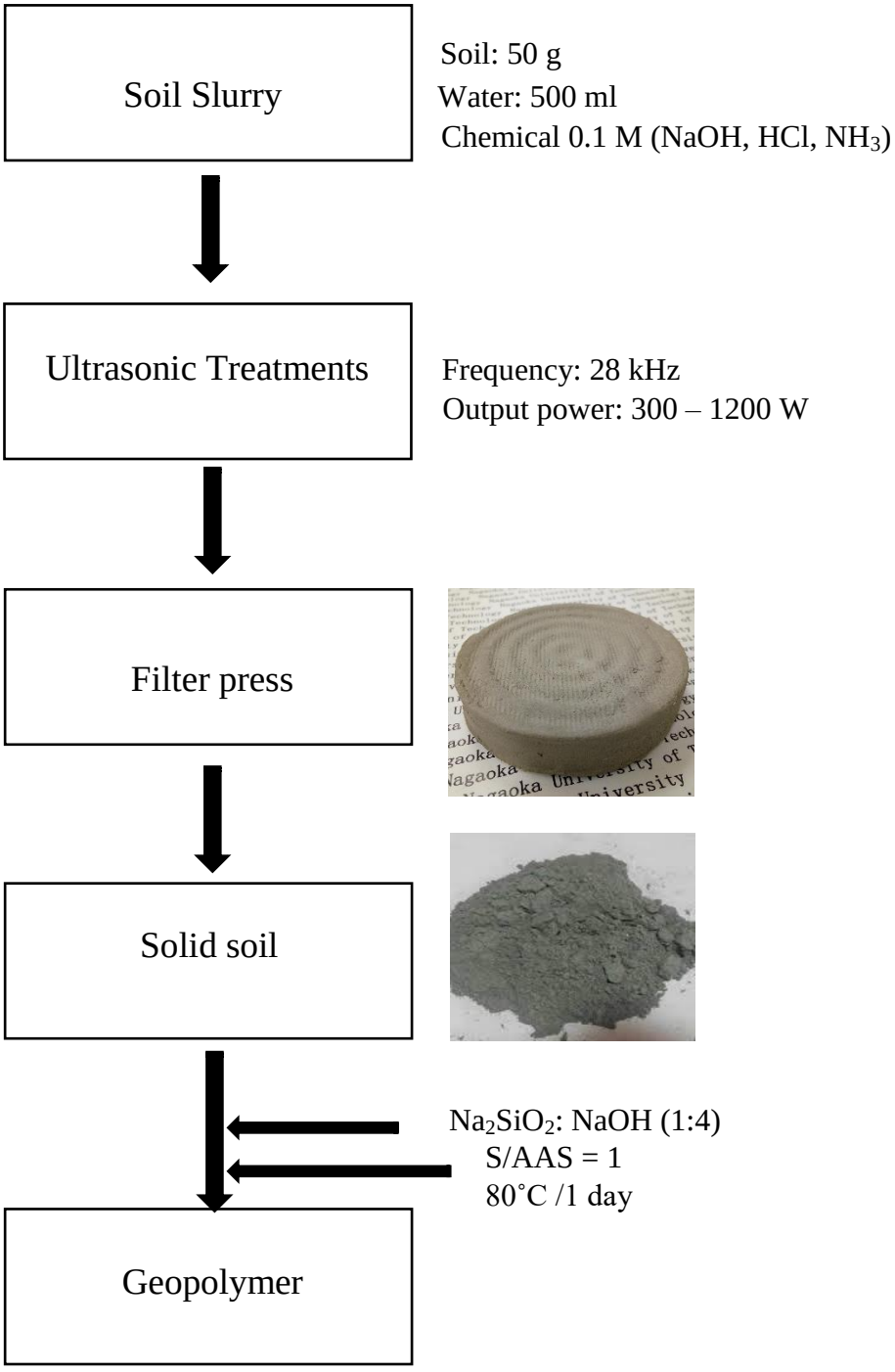

FIGURE 4.3: Protocol for US soil washing and geopolymer fabrication.

4.3. Results and discussion

4.3.1. US soil washing in the presence of acid or base.

After US soil washing, the soil obtained after filter-press was dried and analysed by XRD to determine the effect of sonication on the soil components. Figure 4.4 shows the XRD diffractograms of the US treated soil with different additives exposed to 1200W US.

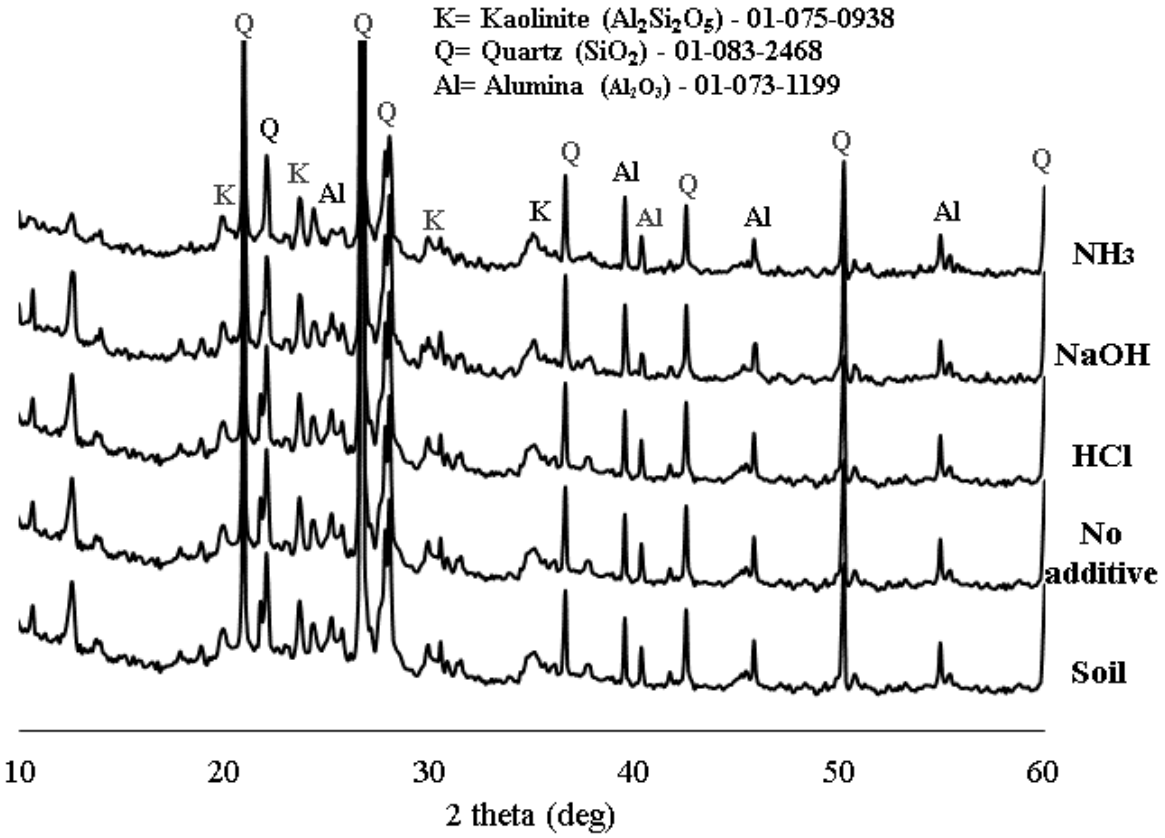

FIGURE 4.4: XRD of soil before and after US treatment.

The X-ray powder diffraction pattern of soil treated with HCl, NaOH and NH_3 were compared with that of non-treated soil. The particle mineralogy of XRD pattern was compared, but no significant difference was observed between the samples. All the diffractograms consisted of Quartz (Q), Kaolinite (K) and alumina (Al), dominated by quartz peaks around 21 and 27°Θ. When the soil was treated with additives, especially when NH3

was used, the peak intensity at 25°Θ decreased. This indicated the dissolution of alumina. As little or no change was observed in the XRD data before and after treatment, therefore XRD analysis is not sufficient for carbon extraction determination. On the other hand, when the mineralogical content of the soil was analysed by XRF, results showed that US influenced the extraction of about 22% of soil carbon, and altered the concentration of silica as well as alumina as shown in Table 4.1. The concentration of carbon extracted was deduced from the XRF data when different concentrations (0.01-1 M) of chemical additive (HCl, NH_3 and NaOH) were used for treatment. The result obtained was plotted as shown in Figure 4.5, and it was noticed that US treatment for carbon extraction (%) depended on the concentration of the washing solvent as well as the US washing time. In the case of NH_3, for example in Fig 4.5(a), when 0.01-1 M NH_3 was used, 72.2% carbon was extracted when 0.1M concentration was used for 60 min. Meanwhile other concentrations of 0.01 M and 1 M were not seen to be effective.

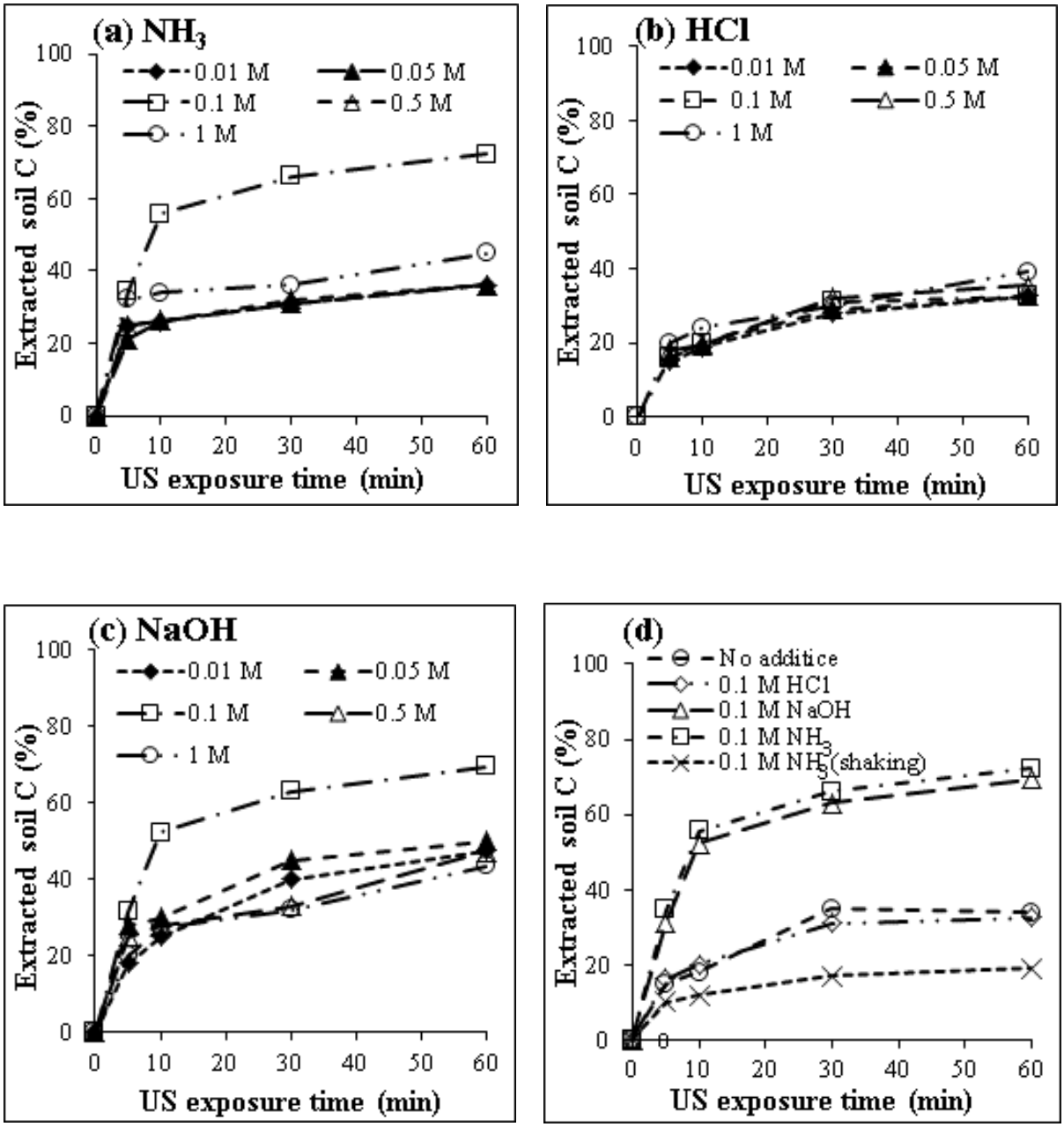

FIGURE 4.5: Calculated percentage of carbon extracted under 1200 W US exposure with 0.01M – 1 M concentration of (a) NH_3 and (b) HCl (c) NaOH and (d) shows a comparison of US with no additive and 0.1 M concentration of various additives.

HCl on its part had no influence regardless of the concentration, even after 60 min US exposure as seen in Fig. 4.5(b). As another base, the effect of 0.001-1M NaOH was investigated as shown in figure 4.5(c). Here, the carbon extraction trend was very similar to that of NH_3. 69.4% of carbon content was extracted when 0.1 M NaOH was used, a value which was slightly lesser than when NH_3 was used. Overall this figure is dominated by NH_3 and NaOH, revealing the effectiveness of base additives for carbon extraction from soil under US at 1200W. The possible reason why more Carbon was extracted when 0.1 M NH_3 additive was used is that, weaker base tends to suspend organic matter [20].

It was noted that, the amount of carbon extracted with 0.1 M HCl was similar to the amount of carbon extracted when no additive was used for treatment. Interestingly, when 0.1 M concentration of NH_3 was used without US, only 19 % of carbon was extracted. This means that the carbon extraction was influenced by US irradiation, and not entirely the additives effect. To confirm this, different US conditions were considered and the plot of the effect of US power from 300 – 1200 W is shown in figure 4.6 below.

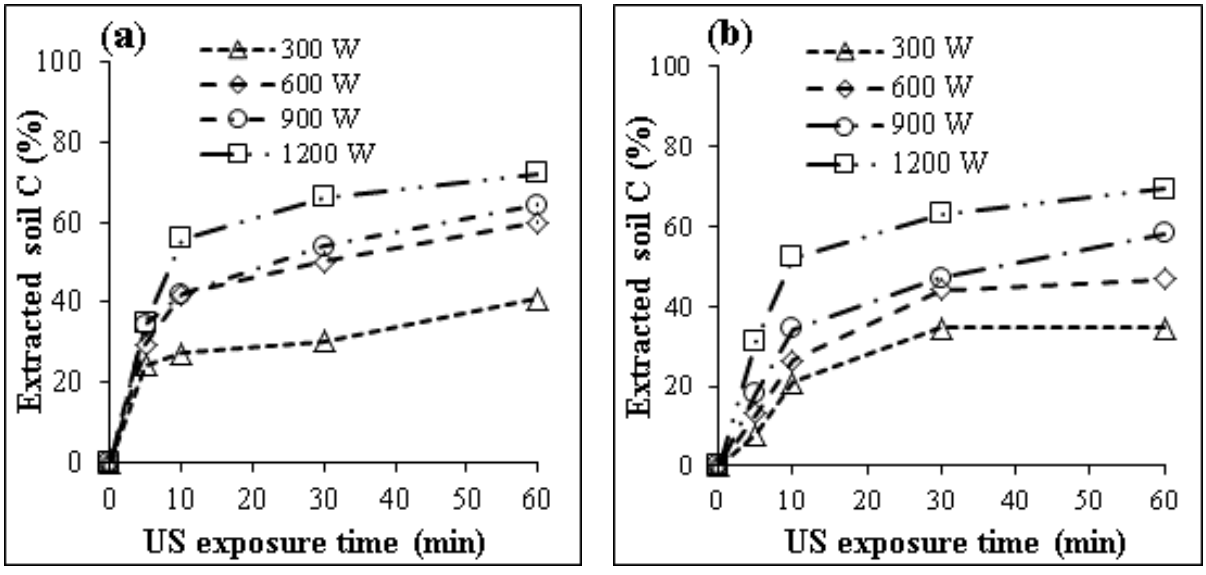

FIGURE 4.6: Calculated percentage of organic carbon extracted after 1200 W US exposure at different US power for 0.1 M (a) NH_3 and (b) NaOH additives

With both solvents, the amount of carbon extracted increased with US exposure time. In figure 4.6 (a), a slightly steady increase was seen under all the US conditions, but when NaOH was used, after 30 min of US exposure under 300 and 600 W, saturation was seen. It is apparent that the amount of extracted C (%) was proportional to the intensity when US was exposed for 60 min. For a better understanding of the effect of US in relation to carbon extraction, the soil fraction was analysed using a particle size analyser after various US conditions. As known, US dispersion is essential during US treatment by reducing sample particles [19, 24], and figure 4.7 (a)-(f) shows us the particle size distribution obtained after exposure. The particle distribution shifted towards 5.5μm and 0.29μm for 600 W and 1200 W, respectively. Particle size decreased more when basic additives were used for treatment (d) and (f).

After US treatment, the slurry was observed to be more viscous than it was before exposure, which could be linked to particle breakage. The apparent viscosity of the slurry was measured at $1s^{-1}$ shear rate as a function of additive concentration in Fig 4.8(a) and different shear rate in Fig 4.8(b) with 0.1 M concentration of each additive. As seen in Fig 4.8(b), the viscosity decreased when the shear rate increased from 1 to $1000s^{-1}$, suggesting that the samples followed pseudo plastic flow behaviour. The viscosity curve of NH_3 and NaOH treated soils showed thixotropic shear rate especially for NaOH cases. This might be because strong alkali like NaOH produced metal colloids for $Si(OH)_4$ or $Al(OH)_3$, meaning that hydrogen interaction influenced the viscosity and the thixotropic behaviour [37] in the base cases.

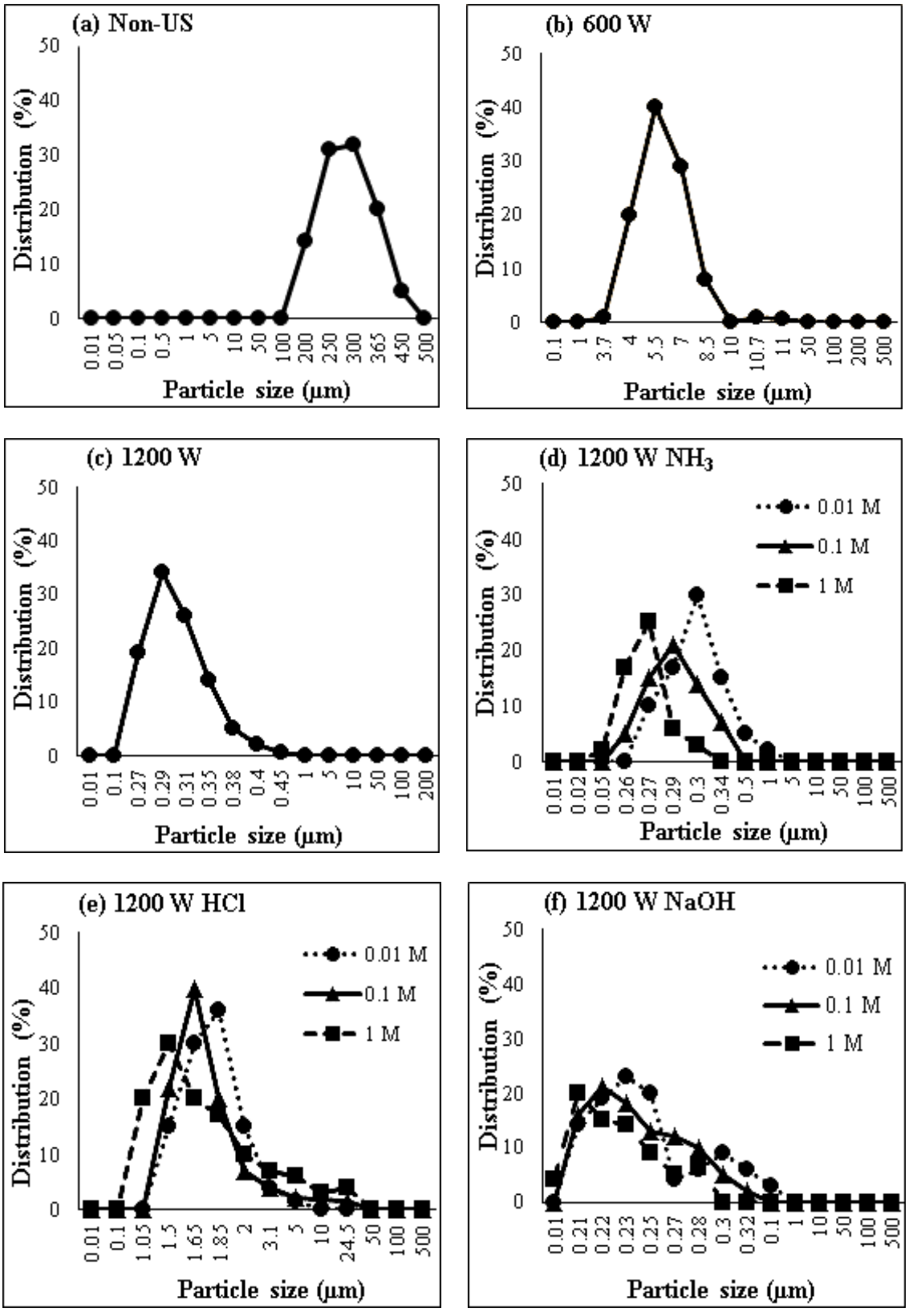

FIGURE 4.7: Particle size distribution analyses of soil sample exposed with no additive at (a) 0 W (b) 600 W and (c) 1200 W and with (0.01-1 M) additive under 1200 W with (d) NH3 (e) HCl (f) NaOH.

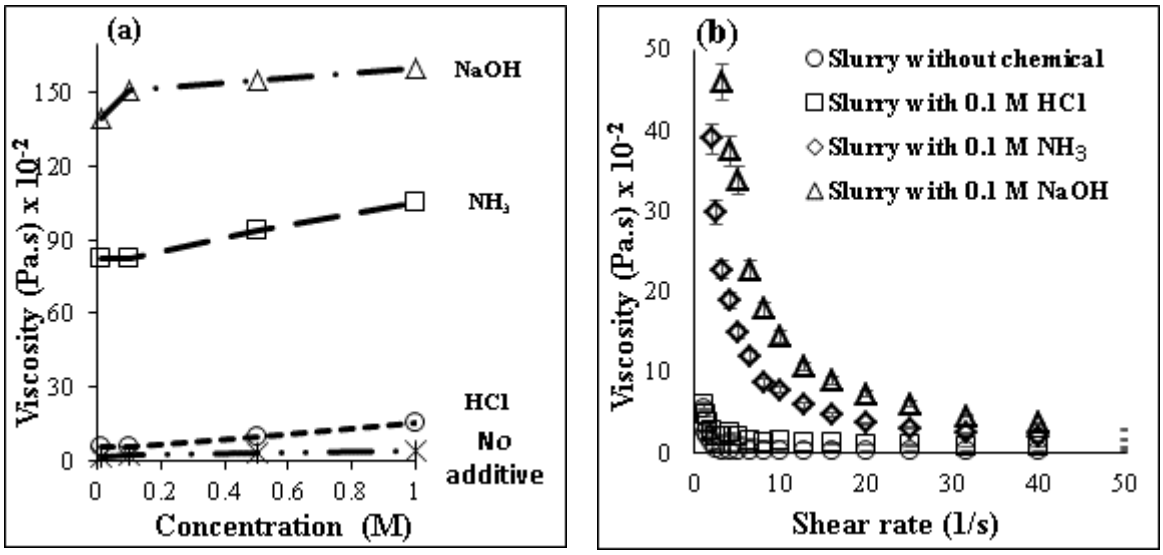

FIGURE 4.8: Viscosity changes for 60 min treatment soil slurries with additives (a) with different additive concentration and (b) shear rate of 0.1M additive concentration.

4.3.2. Fabrication and properties of soil geopolymers

Before US treatment from table 1 we can see that the original soil used for the experiment had 3.6% organic carbon content, 50.4% SiO_2 and 18.8% AL_2O_3 content. But after US treatment, NaOH like NH3 washing extracted $^1/_3$ the carbon content, while an increase in SiO_2 from 65.2-63.3% was noticed Al_2O_3 contents decreased from 16.2-16.1%. For geopolymer, three samples were considered; the original soil without US treatment (US-0), soil washed with 0.1 M NH_3 additive under 600 W US (US600), and soil washed with 0.1 M NH_3 additive under 1200 W US (US1200). When the soils were mixed with the alkaline activator, the workability of the paste was best with the soil treated with 1200 W (US1200). After forming the geopolymer matrix, the morphology of the geopolymers were analysed and the SEM images are shown in Figure 4.9. The geopolymer formed from untreated soil in Figure 4.9 (a) shows a clear boundary between the particles and the alkalis activator in the geopolymers. This result explains that the layer has a less compact structure which can clearly be seen with a high focus of 10μm in Fig 4.9(c). However, in the case of US1200 for

Figs 4.9(g)-(i), it can be seen that the effect of the high power US created fine powder. The geopolymer interface shows a more discrete matrix indicated by the globular unit and a few unreacted particles (layered structure). This means that the soil particles and the alkaline activator in the geopolymers formed a dense matrix with fewer gaps at the interfaces, signifying that US was effective in the soil slurry dispersion in the aqueous medium.

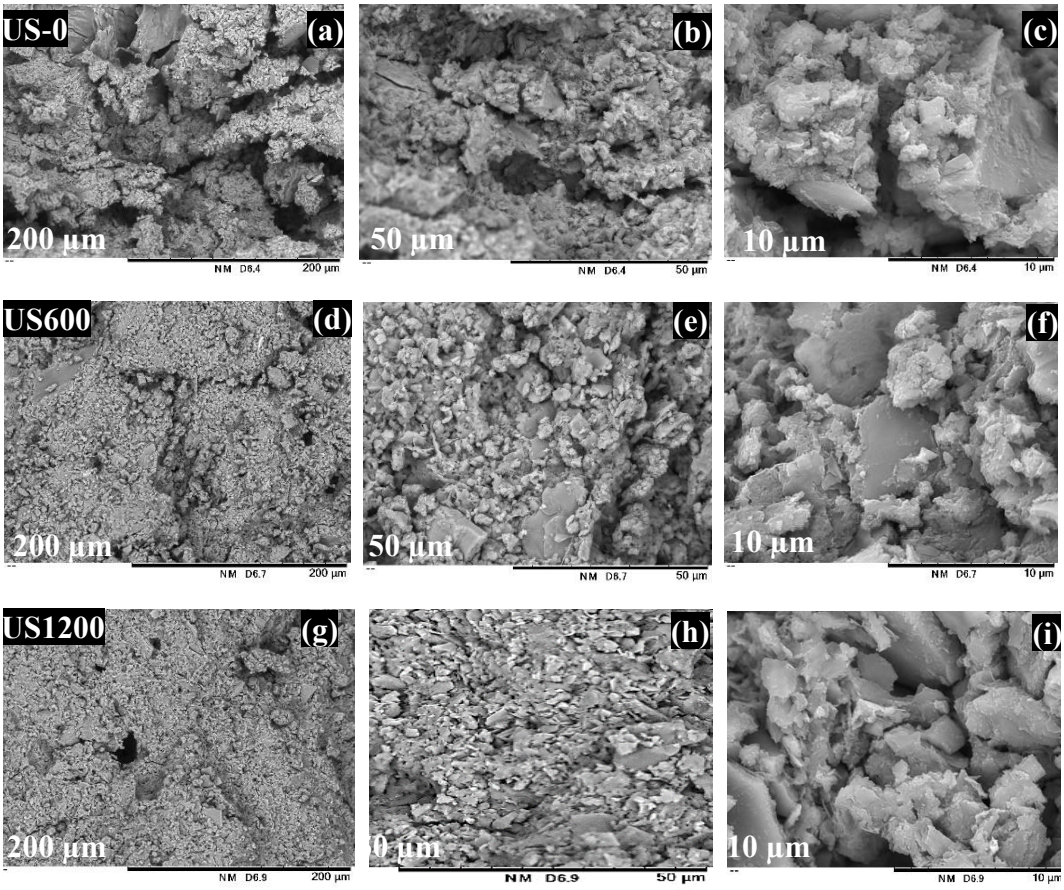

FIGURE 4.9: Microstructure of geopolymer sample before and after ultrasonic treatment at different intensities (0 W, 600 W and 1200 W) of NH_3.

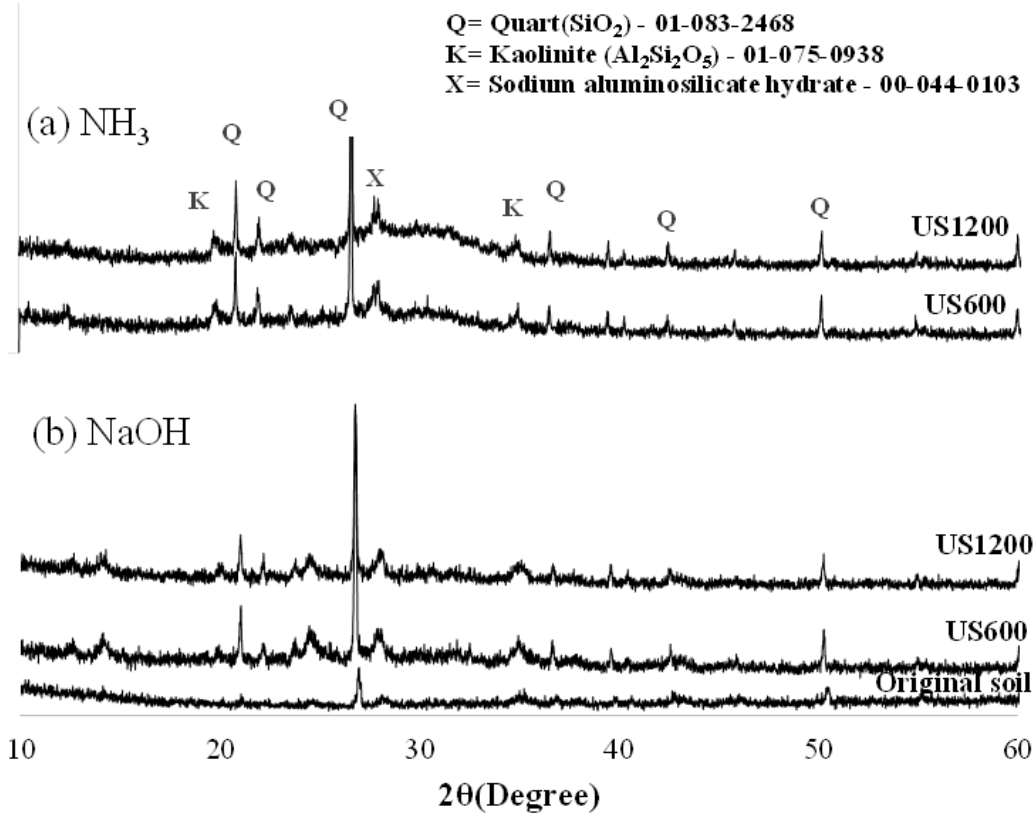

FIGURE 4.10: XRD patterns of original soil and soil after geopolymerization under different ultrasound power

The XRD of the geopolymers formed from NH_3 above was analysed and just for clarification it was compared with geopolymer formed from soil treated with NaOH and soil treated with no additive. The geopolymers consisted mainly of amorphous alumino-silicate products with similar amount or slight increase of SiO_2 and $Al_2Si_2O_5$ crystals relative to original sample as shown in Figure 4.10. The synthesized geopolymers diffractogram showed the presence of residual peaks relating to SiO_2 (21.11˚ and 26.8˚). One major difference between the XRD patterns of the geopolymer from NaOH treated soil and NH_3 soil was the occurrence of a broad diffuse hump between 25˚ and 35˚ 2Θ in Figure 4.10(a) when the soil was washed with NH_3. This amorphous peak corresponded to the alumino-silicates which were formed at the binder phase in geopolymer matrix. The component analyses of the

geopolymer in Table 2 shows an increase in SiO_2 component and Al_2O_3 component which is apparent, for NH_3.

TABLE: 4.2. XRF of geopolymer.

Mass %			
No additive		NH_3	NaOH
CO_2	21.5	11.6	12.4
Na_2O	20.9	17.1	18
Al_2O_3	11	13.9	12.7
SiO_2	40.4	48.9	48.8
Fe_2O_3	2.41	3.45	3.17

To confirm the formation of geopolymer alumino-silicate, FT-IR spectra for the US treated soil and geopolymer samples were analysed as shown in Figure 4.11. The FT-IR data of the additives were seen to have numerous transmission bands around 900 cm^{-1}, 1100 cm^{-1} and 3200-3500 cm^{-1} for Al-O, Si-O and Si-OH groups, respectively [36]. In Figure 4.11(a), 0W indicates no US treatment, while 600 W and 1200 W indicate their respective US powers without additive.

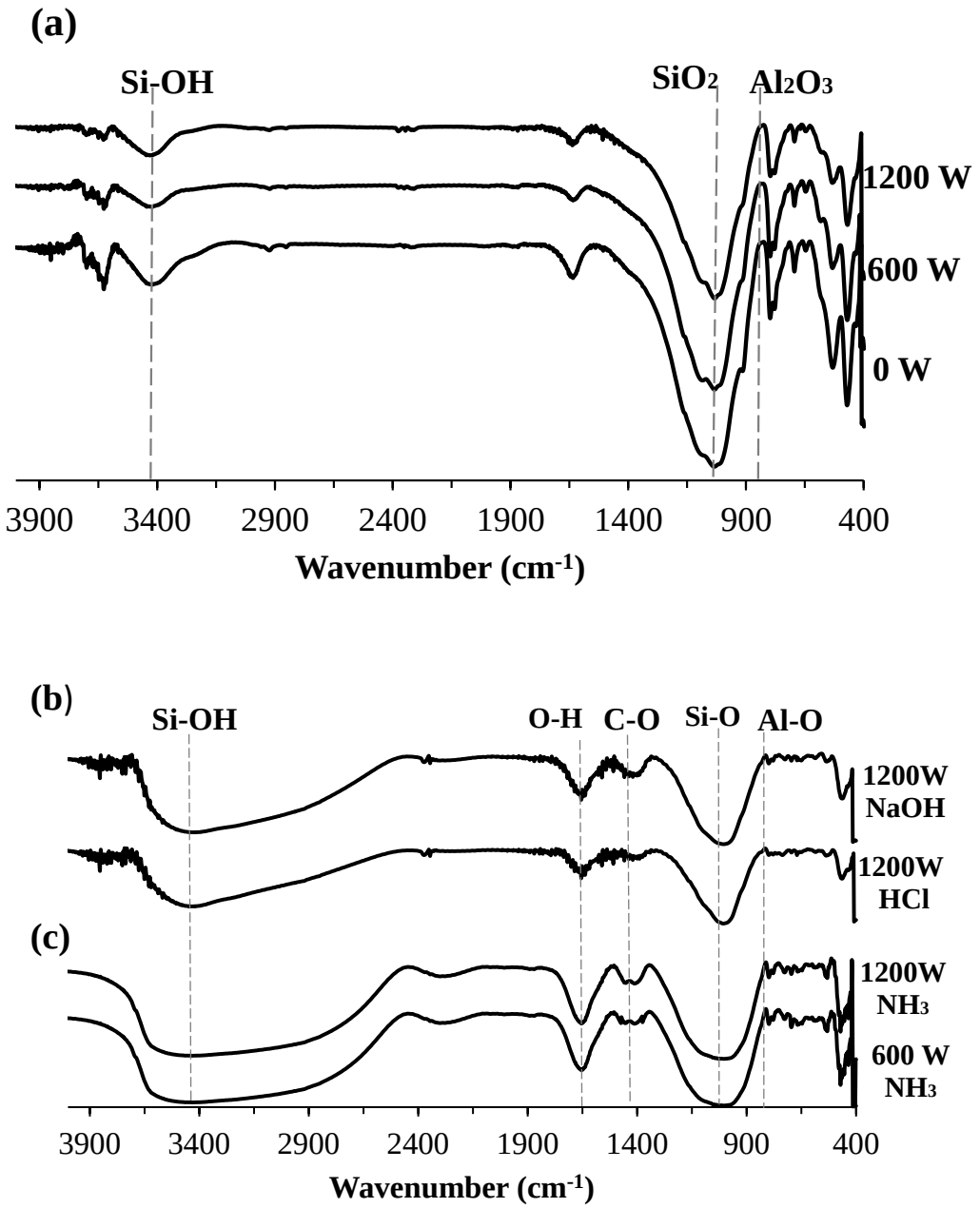

FIGURE 4.11: FT-IR analysis after geopolymerization of 1200 W US (a) treated soil with no additive (b) treated with 0.1 M NaOH (top) and 0.1 M HCl (bottom)) and (c) treated with 0.1 M NH_3.

From the FT-IR, the main feature of the spectra of the US treated powder is the appearance of the central band between 1107 and 1040 cm^{-1} characterized by the asymmetric stretching of Si-O-Si. The characteristic stretching vibration of Al-O was observed in the geopolymers formed from non-additive treated soil as shown in Fig 4.11(a). In figure 4.11(b), the Si-O

stretching band at about 1100 cm^{-1} of the geopolymer formed from treated soil slightly shifted towards the lower wavenumber region, indicating that condensation occurred in the soil between SiO_2 and the sodium silicate. At 1490- 1650cm^{-1}, the characteristic carbonate band appeared. This band from sodium carbonate was formed during the absorption of CO_2 gas from the atmosphere by the sodium silicate.

As strength one of the major characteristics of a geopolymer, the mechanical strength of the geopolymer matrix was analysed and plotted in Figure 4.12. Two plots were made, the compressive strength of the geopolymer formed from the soil which was washed with 0.1M NH_3 additive under different US power (0-1200W) (Fig.4.12(a)), and the geopolymer from made from soil washed with 0.1 HCl and NaOH (Fig.4.12(b)) as shown below.

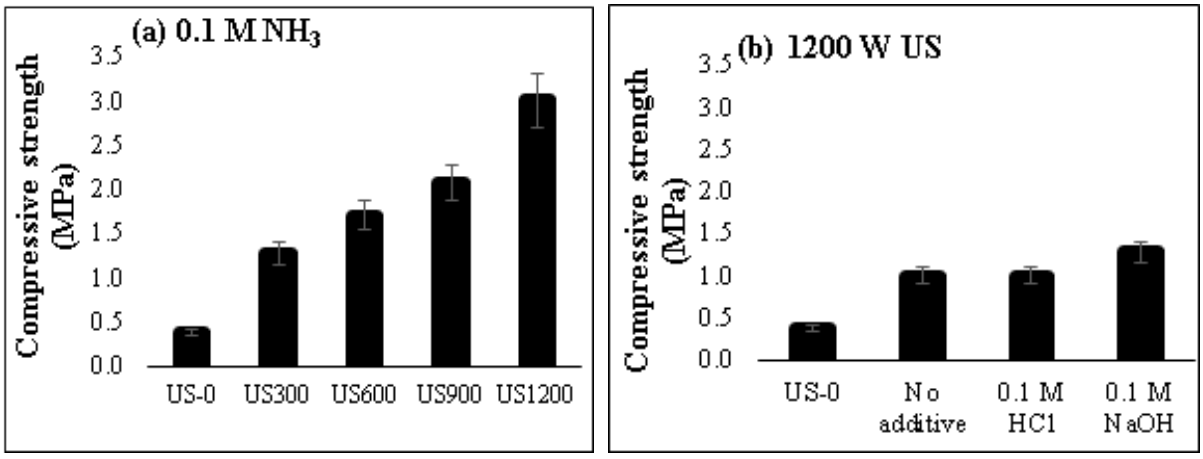

FIGURE 4.12: Compressive strength of (a) geopolymer from 0.1 M NH_3 US treated soil at different power (b) geopolymer from US treated soil with different additive.

In figure 4.12(a), 0.1M NH_3, an increase in US power led to an increase in the compressive strength, from 0.4 MPa to 3.0 MPa when 1200 W US (US1200) treated soil was used. This result was mainly related to the morphological structure of the geopolymer, as higher US power of 1200 W created finer particles which required less geopolimerization reaction time

as compared to larger soil particles in the case of lower powers [40]. When similar US conditions of 1200 W were applied to soils with other additives like HCl and NaOH, although their particle size was assumed to be the same, their compressive strengths were far lesser than that of NH_3 mentioned earlier. The main reason for this could be attributed to the carbon content in the material [15]. The particle size influenced the strength when no additive, 0.1M HCl and 0.1M NaOH was used as seen in Figure 4.12(b).

4.4. Conclusion

Soil slurry which was considered as waste was recycled to prepare geopolymer after being treated with high power ultrasound (US). Due to the limitation of land fields for waste soil disposal, soil decarbonation is a necessity for soil recycling. Under 28 kHz US exposure, 60 min was sufficient to extract 72.2 % of organic carbon from excavated soil with 0.1M NH_3 solution as washing solvent. Geopolymer formed from the resultant soil showed a remarkable compressive strength after curing at 80°C for 24hr due to the low proportion of carbon content after treatment. Although the compressive strength acquired with 0.1M NH_3, is thought to be negligible it is significant when compared to geopolymers formed with soils treated with a similar concentration of HCl and NaOH. Since the compressive strength depends on the particle size and carbon content in the soil, more research is required to develop a geopolymer with better strength by altering the concentration of alkalis activator and other ultrasonic parameters.

References

1. J. Davidovits, Geopolymer chemistry and applications, 4th edition; Institute geopolymere; France, 2015; pp.4-5.
2. T.Y Huang, P.T. Chuieh, Life cycle assessment of reusing fly ash from municipal waste incineration. Proceedia eng. 2015, 11, 984-991.
3. B. S Nakshatra. Ffly ash based geopolymer binder: a construction material. Mineral 2018, 8,299.
4. N. Johansson, J. Krook, M. Eklund, B. Berglund, An Integrated Review of Concepts and Initiatives for Mining the technosphere towards a new taxonomy. J. Cleaner Prod 2013, 55, 35-44.
5. Residential and Civil Construction Alliance of Ontario (RCCAO) Best Management Practices for Handling Excess Construction Soils in Ontario. http://www.rccao.com/news/files/RCCAO_NOV2012.pdf (10.7.2019).
6. R.L. Wilpiszeski, J.A. Aufrecht, S.T. Retterer, M.B. Sullivan, D.E. Graham, Soil Aggregate Microbial Communities: Towards Understanding Microbiome Interactions at Biologically Relevant Scales, Appl. Environ Microbiol 2019, 85.
7. T. DeGomez, P. Kolb, S. Kleinman, Basic Soil Components https://climate-woodlands.extension.org/basic-soil-components/ (2019).
8. K. Mohammadi, G. Heidari, S. Khalesro, Y. Sohrabi, Soil management, microorganisms and organic matter interactions: A review, Afr. J. Biotechnol. 10 (2011), 19840-19849
9. G.P. Robertson, E.A. Paul, R.R. Harwood, Greenhouse gases in intensive agriculture: contributions of individual gases to the radiative forcing of the atmosphere. Science 2000, 289, 1922-1925.

10. M.U.F. Kirschbaum, The temperature dependence of soil organic matter 587 decomposition and the effect of global warming on soil organic carbon storage. Soil Biol. Biochem 1995, 27, 753–760.
11. E. A. Davidson, I. A. Janssens, Temperature sensitivity of soil carbon decomposition and feedbacks to climate change. Nature 2006, 440, 165-173.
12. D. M. Linn, J. W. Doran, Effect of water-filled pore-space on carbon-dioxide and nitrous-oxide production in tilled and non-tilled soils. Soil Sci. Soc. Am. J 1984, 48, 1267-1272.
13. J. Skopp, M. D. Jawson, J. W. Doran, Steady-state aerobic microbial activity as a function of soil-water content. Soil Sci. Soc. Am. J. 1990, 54, 1619-1625.
14. Barnwell low level radioactive waste disposal facility. http://www.atlanticcompact.org/pdf_file/29f3737663937c53aebb326b1a87c628.ACC_Conceptual_Design_Report_071004.pdf (10.72019).
15. M. P. C. M. Gunasekara, D.W. Law, S. Setunge, Effect of composition of fly ash on compressive strength of fly ash based geopolymer morta, ACMSM 2014, 113-118.
16. M. Kaiser, A. A. Berhe, M. Sommer, M. Kleber, Application of ultrasound to disperse soil aggregates of high mechanical stability. J. Plant Nutr. Soil Sci. 2012, 4, 521–526.
17. M. L. Jackson, N. N. Helman, X-ray diffraction procedure for positive differentiation of montmorillonite from hydrous mica; Soil Science Society of America Proceedings, America.
18. R. A. Griffiths, Soil-washing technology and practice. J. Hazard. Mater 1995, 40, 175–189.
19. G. Dermont, M. Bergeron, G. Mercier, Soil washing for metal removal: A review of physical/chemical technologies and field applications. J. Hard. Mat 2008, 152, 1-31.

20. Schmidt, M.W.I; Rumpel, C; Kögel-Knabner, I. Evaluation of an ultrasonic dispersion procedure to isolate primary organo-mineral complexes from soils. Eur. J. Soil Sci. 1996, 50, 87–94.
21. Schmidt, M.W.I; Rumpel, C; Kögel-Knabner, I. Particle size fractionation of soil containing coal and combusted particle. Eur. J. Soil Sci. 1996, 50, 515–522.
22. Levesque, M; Schnitzer, M. Effect of NaOH concentration on the extraction of organic matter and of major inorganic constituents from a soil. Can. J. soil Sci. 1996, 46, 7-12.
23. Kulhawy, F. H; Jie-Ru, C. Identification and description of soils containing very coarse fractions. J. geo. eng, 2009,135.
24. Gregorich, E. G; Kachanoski, R. G; voroney, R. P. Ultrasonic dispersion of aggregates: distribution of organic matter in size fractions. Can. J. Soil Sci. 1998, 68, 395-403.
25. Raine, S. R; So, H. B. Ultrasonic dispersion of soil water: the effect of suspension properties on energy dissipation and soil dispersion. Aust. J. Soil Res. 1994, 32, 1157-1174.
26. Roscoe, R; Buurman, P; Velthorst, E. J. Disruption of soil aggregates by varied amount of ultrasound energy in fractionation of organic matter of a clay latosol: carbon, nitrogen and delta 13C distribution in particle size fractions. Eur. J. Soil Sci. 2000, 51, 445-454.
27. Bray, R, H. The significance of particle-size within the clay fraction. Journal of the American Ceramic Society 1937, 20, 257- 261.
28. Feng, D; Aldrich, C. Sonochemical treatment of simulated soil contaminated with diesel. Adv. Environ. Res. 2000, 4, 103–112.
29. Freeman. H.M; E. F. Harris. Hazardous Waste Remediation: Innovative Treatment Technologies, Tehnomic Publishing Co., Inc., Lancaster, UK, 1995, 103-112.

30. Torres, R. A.; P_etrier, C.; Combet, E.; Carrier, M.; Pulgarin, C. Ultrasonic cavitation applied to the treatment of bisphenol A. Effect of sonochemical parameters and analysis of BPA by-products. Ultrason. Sonochem. 2008, 15, 605–611.
31. Inoue, M.; Masuda, Y.; Okada, F.; Sakurai, A.; Ichiro, T.; Sakakibara, M. Degradation of bisphenol-A using sonochemical reactions. Water Res. 2008, 42, 1379–1386.
32. Teo, B. M.; Chen, F.; Hatton, T. A.; Grieser, F.; Ashokkumar, M. Novel one-pot synthesis of magnetite latex nanoparticles by ultrasound irradiation. Langmuir 2009, 29, 2593–2595.
33. Teo, B. M.; Prescott, S. W.; Ashokkumar, M.; Grieser, F. Ultrasound initiated miniemulsion polymerization of methacrylate monomers. Ultrason. Sonochem. 2008, 15, 89–94.
34. Farmer, A. D.; Collings, A. F.; Jameson, G. J; The application of power ultrasound to the durface cleaning of silica and heavy mineral sands; Ultrason. Sonochem. 2000, 7, 243–247.
35. Balachandran, S.; Kentish, S. E.; Mawson, R.; Ashokkumar, M. Ultrasonics enhancement of the supercritical extraction from ginger. Ultrason. Sonochem. 2006, 13, 471–479.
36. Rovnavik P. Effect of curing temperature on the development of hard structure of metakaoline based geopolymer. Contr Build Mater 2012, 24, 1176-83.
37. Singhi, B., Laskar, A. I., Ahmed, M. A.;. Investigation on soil–geopolymer with slag, fly ash and their blending. Arabian Journal for Science and Engineering, 2016, 41, 393-400.
38. M.A. Rao; Flow and functional models for rheological properties of fluid foods, Rheology of Fluid, Semisolid, and Solid Foods; Food Engineering Series, Science and Business Media, New York, 2014, 21–67.

39. B. Panda, C. Unluer, M.J. Tan, Extrusion and rheology characterization of geopolymer nanocomposites used in 3D printing. Composites Part B: Engineering, 2019. 176, 107290.

40. I. Christine, C. Grant. Lukey, Hua Xu, Jannie S.J. van; The Effect of Aggregate Particle Size on Formation of Geopolymeric Gel; Advanced Materials for Construction of Bridges, Buildings, and Other Structures III, Art. 2003, 9, 1-10.

CHAPTER: 5.

SUMMARY

The term “ultrasound” means vibrations which are similar to sound waves, but with frequencies too high to be detected by the human ear. The application of sound waves to chemical systems has been known since the early 20th century. From that time until now the application of US has gained importance especially in the field of chemistry and more recently in sono-processing. All these developments lead to environmental friendly processes and compounds.

This thesis describes the contribution of ultrasound technology to a sustainable green environment in line with the United Nations sustainable development goals (SDGs). The present work elaborated on the studies and effect of ultrasound to organic pollutants in aqueous mediums and also elaborates on the possibility of soil recycling.

Chapter 1 of this thesis briefly introduces the environment and its waste affecting livelihood. In this chapter, sonoprocessing considered as a solution was also introduced and factors influencing its application for a sustainable environment are highlighted.

Chapter 2 revealed the generation of Sonochemical species such as nitrite (NO_2^-) and nitrate (NO_3^-) in an ultrapure aqueous medium when it was exposed to 23, 28, and 43 kHz frequency ultrasound (US). The formation generation of other oxidizing agents such as OH^- was also considered due to the transformation of iodide to triiodide. Air containing a mixture of nitrogen and oxygen greatly influenced the results obtained.

In Chapter 3, when a higher frequency of 500 kHz was used, the concentration of NO_2^- and NO_3^- species increased. This condition was sufficient to decompose diaminobenzidene while forming Bibenzotriazole due to the presence of the NO_2^- ion in the medium.

In Chapter 4, the application of sonoprocesses was extended to soil washing were 72.2 % of Carbon content was eliminated from waste soil. For this, 28 kHz with a high power of 1200W was determined to be the appropriate frequency for such an application. For sustainability, the soil was recycled to fabricate a geopolymer.

As a general conclusion, ultrasound and sonoprocesses successfully created chemical species for pollutant chemical decomposition by insertion of Nitrogen. It was also seen that soil treated with high power US was a suitable resource for geopolymer.

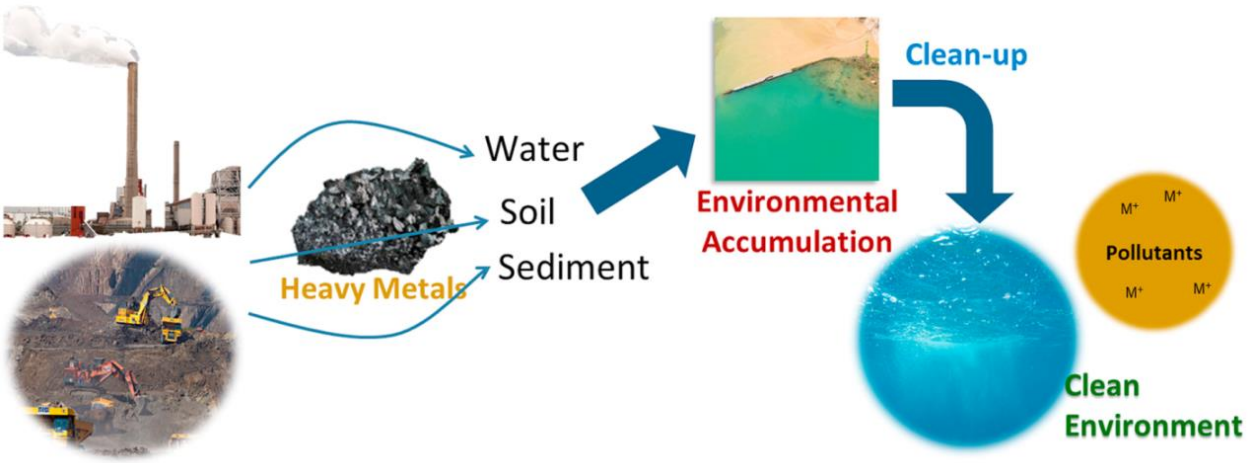

List of Achievements

Publications

1. Sonochemical nitrogen fixation for the generation of NO_2^- and NO_3^- ions under high-powered ultrasound in aqueous medium.
   Louis-Marly Kwedi Nsah, Takaomi Kobayashi
   Ultrasonics Sonochemistry, 66(2020) 105051

2. Ultrasonic degradation of diaminobenzidine in aqueous medium
   Louis-Marly Kwedi-Nsah, Takaomi Kobayashi
   Ultrasonics Sonochemistry, 52(2019)69-76

3. Soil Recycling Geopolymers Fabricated from High Power Ultrasound Treated Soil Slurry in the Presence of Ammonia
   Louis-Marly Kwedi-Nsah, Yuta Watanabe, Takaomi Kobayashi
   Materials, 12(2019)3804

International and National Conferences

1. **The 25th Annual Meeting of the Japan Society of Sonochemistry in Toyama, Japan.**

Fluorometric analysis proving with Ultrasounded Diaminobenzidine in aqueous medium

Kwedi Nsah Louis-Marly, Takaomi Kobayashi (October 2016)

2. **The 1st International Symposium on Local Innovative Activation by Food and Energy (ISLife 2017), Nagashima, Kagoshima, Japan**

Ultrasonic wastewater treatment for sustainable fish farming

Kwedi Nsah Louis-Marly and Takaomi Kobayashi, (March 2017)

3. **The 9th International Conference on Waste Management (ICWM'17) in Dubai, U.A.E**

Ultrasound Treatment of 3, 3-Diaminobenzidine in Industrial waste

Kwedi Nsah Louis-Marly, Takaomi Kobayashi (May 2017)